

1 **Title:** Crabs Grab Strongly Depending on Mechanical Advantages of Pinching and
2 Disarticulation of Chela

3

4 **Authors:** Shin-ichi Fujiwara¹ and Hiroki Kawai¹

5

6 **Affiliation:** ¹*Nagoya University Museum, Furocho, Chikusa-ku, Nagoya, 466-8601,*
7 *JAPAN.*

8

9 **Short title:** FUNCTIONAL MORPHOLOGY OF DECAPOD CHELA

10

11 ***Correspondence to:** Shin-ichi Fujiwara, Nagoya University Museum, Furocho,
12 Chikusa-ku, Nagoya, 466-8601, JAPAN. E-mail: sifjwr@num.nagoya-u.ac.jp

13

14

15 *ABSTRACT* A small morphological variation of an organ can cause a great diversity of
16 its function in animal evolution. A decapod chela has a great functional variation among
17 taxa, between sex, and even within the individual, but also retains a simple mechanism
18 of motion. Therefore, the decapod chela is one of the best structures to study the
19 evolutionary process of functional diversifications, though the relationship between
20 form and function is yet inadequately understood. We estimated the mechanical
21 advantages of pinching and passive disarticulation resistance, and chela size relative to
22 the carapace in 317 chelae of 168 decapod specimens, and compared these indices with
23 the functions of each chela. Our study revealed that both mechanical advantages of
24 pinching efficiency and passive disarticulation resistance were greatest in shell-crushing
25 chelae, followed by gripping and pinching chelae, whereas the chela size relative to the
26 carapace was not related to differences among these functions. We also found that the
27 chelae are designed to retain the ratio between depth and width of the proximal dactylus.
28 In the evolutionary process of decapods, the diversifications of chela functions were
29 accompanied by the diversifications of the mechanical advantages, and played an
30 essential role in their ecological diversification.

31

32 **KEY WORDS:** Brachyura; durophagous; moment arm; functional morphology.

33

34 **INTRODUCTION**

35 Chelae are pincer-like grasping organs derived from the distal two segments (the
36 dactylus and the propodus) of the crustacean pereopod, and the pereopod bearing the
37 chela is called the cheliped (Fig. 1A, B). Among the arthropods, grasping abilities,
38 associated with the chelipeds, were independently acquired in several lineages of
39 crustaceans, insecta, and cheliceratans (e.g., Boxshall, 2004; Regier et al., 2010;
40 Weirauch et al., 2011; Meusemann et al., 2014). Decapods (Crustacea) are one of the
41 most successful groups among these in terms of diversity. Decapod chelae are greatly
42 diversified in their form and function. The forms vary not only among species (e.g.,
43 Hughes, 1989; Rosenberg, 2002), but also between sexes (e.g., Valiela et al., 1974),
44 between right and left sides (e.g., Palmer, 2004), and between before and after the
45 post-autotomy recovery (e.g., Pynn, 1998). There is also a great variety in pinching
46 abilities of chelae (Taylor and Schram, 1999; Mariappan, et al., 2000). Many decapods
47 have a pair of chela asymmetric in size, shape, and function (e.g., Warner, 1977; Palmer,
48 2004). Crushing and chipping abilities (C) are employed in some durophagous decapod
49 major chela to crush/chip hard tissues of the prey (e.g., bivalve and crustacean shells:
50 Table S1: Zipser and Vermeij, 1978; Lau, 1987; Hughes, 1989; Schweitzer and
51 Feldmann, 2009). Gripping ability (G) is employed by many decapods to hold

52 struggling prey by using the teeth on the pinching surface of the chela (Table S1).
53 Soft-pinching ability (P) is employed by detritus feeders to scoop particles or to pick up
54 a tiny benthos using the distal-end of chela (Table S1). The major chela of the male
55 fiddler crab (U: Ucinae, Ocypodidae) is known to be used for grasping the females or
56 for grappling with the other males, as well as for waving to attract females, though the
57 grasp does little damage to the other individuals (Table S1: Crane, 1966; Lau, 1987;
58 Field, 1990; Levinton and Judge, 1993; Dennenmoser and Christy, 2013). Such
59 diversification in decapod chelae function may have played an essential role in their
60 diversification, especially in feeding behavior (Anker et al., 2006).

61 Though the forms and functions are diverse among decapods, their chelae employ a
62 relatively simple structure and mechanism of motion. The lateral and medial facets on
63 the distal articular surface of the propodus (the proximal segment of chela) occupy the
64 lateral and medial fulcra on the articular surface of the proximal side of the dactylus (the
65 distal segment), respectively (see points *b* and *c* in Figs. 1 and 2). The margins of the
66 distal side of the propodus and the proximal side of the dactylus are connected to each
67 other by an articular membrane (Fig. 1C, D). Due to the biarticular connections at the
68 lateral and medial fulcra, the propodus-dactylus (P-D) joint forms a hinge joint (see axis
69 *X* in Fig. 1B–D)—the structure of which can be comparable to the biarticular hinges in
70 temporomandibular and costovertebral joints of vertebrates (e.g., Moore and Dalley,
71 2006), though the construction of the musculoskeletal system is different in decapods
72 and vertebrates. The opening and closing motions of the chela at the P-D joint are
73 controlled by the opener muscle, which insert to the dorsal margin of the proximal
74 dactylus via the opener apodeme, and the closer muscle, which insert to the ventral
75 margin of the proximal dactylus via the closer apodeme, respectively (Fig. 1B–D).
76 These simple motion mechanisms of the joint are shared widespread among
77 inter-segmental joints in malacostracan crustacean pereopods (Manton, 1968; Shultz,
78 1989), though non-biarticular joints are employed in some arthropods (e.g., screw joint
79 in *Trigonopterus*, Coleoptera, Insecta [Van de Kamp et al., 2011]; and scissor-like joints
80 in *Psalidopus*, Caridea, Decapoda [Chace and Holthuis, 1978]). Given their simple
81 motion mechanism and their great diversity in forms and functions, the decapod
82 (Malacostraca, Crustacea) chelae are one of the best examples to study the functional
83 morphologies and the process of diversification within the group.

84 A number of studies have been conducted on the functional morphologies of
85 crustacean and cheliceratan chelae—for example, the relationship between the pinching
86 force and the height, width, cross-sectional area of the propodus, strength of chela, and
87 volume, pennation angle, and sarcomere length of the closing muscle of chela have been
88 studied in several taxa (e.g., Vermeij, 1977; Warner et al., 1982; Levinton and Judge,

89 1993; Backwell, 2000; Van der Meijden et al., 2010; Taylor et al., 2009; Van der
90 Meijden et al., 2012; Payne and Kraemer, 2013). Some of these studies used the
91 mechanical advantage of pinching efficiency (the ratio between the in-lever and
92 out-lever of the chela) as a morphological indicator of the pinching abilities of
93 arthropod chelae (Warner and Jones, 1976; Vermeij, 1977; Brown et al., 1979; Elnor and
94 Campbell, 1981; Govind and Blundon, 1985; Levinton and Judge, 1993; Labadie and
95 Palmer, 1996; Yamada and Boulding, 1998; Palmer et al., 1999). However, the
96 mechanical advantage of pinching efficiency has been compared among a limited
97 number of taxa, up to six genera (Vermeij, 1977), because most of studies have focused
98 on the variation in pinching efficiency among a few genera, or among a population
99 within a single species whose chelae are referred to as sexually dimorphic or laterally
100 asymmetric (e.g., Labadie and Palmer, 1996). The relationship between form and
101 function would become clearer if data was obtained from a larger number of samples.

102 Strong pinching can be performed by having a joint with an adequate mechanical
103 strength, which is relatively difficult to disarticulate by the reaction force from the
104 object, in addition to having a relatively high mechanical advantage for pinching
105 efficiency. The relationship between form and function could be further elucidated with
106 data from multiple mechanical indices (e.g., moment arms of the extensor, flexor, and
107 adductor muscles in the tetrapod elbow joint for deducing their forelimb postures
108 [Fujiwara et al., 2011; Fujiwara and Hutchinson, 2012]). The additional mechanical
109 index for ability to resist disarticulation of the chela would be useful for a further
110 understanding of the relationship between the form and function of arthropod chela. If
111 these indices were directly reflected in chelae morphology, it would give new insight on
112 the basic design and the pinching ability of arthropod chela.

113 Here we combine indices measuring mechanical advantages of pinching and
114 resistance to mediolateral failure of the P-D joint to test the difference among the
115 decapod chelae with different functions (C, crushing/chipping; G, gripping; P, pinching;
116 U, grasping function employed by male ucine chela) by using a wide range of decapod
117 species.

118

119 **Mechanical Condition of Pinching**

120 Figure 2B shows a decapod chela pinching an object at the distal end. The closer
121 apodeme is pulled proximally by a certain contractive force (F_{C1}) of the closer muscle to
122 adduct the dactylus about the P-D joint axis (axis X) in Figure 2B. The distance from the
123 axis to the closer muscle contraction force vector is the moment arm of the force. The
124 moment arm is maximized at an angle where the force applied by the closing muscle
125 contraction (F_{C1}) and the line connecting the axis X and the muscle insertion (point d)

126 are perpendicular with each other (Fig. 2B). Therefore, the distance between the axis X
 127 and the point d can be defined as a possible maximum moment arm of the closer muscle
 128 (C_1). At the same time, the pinched object applies a reaction force (F_{C_2}) to the distal end
 129 of the chela to abduct the dactylus, and the moment arm of the force (C_2) is the distance
 130 from the distal end of chela to the axis (Fig. 2B). We assumed that the chela is held in an
 131 angle where the force vector of the closing muscle contraction (F_{C_1}) is perpendicular to
 132 the in-lever (the line segment connecting between axis X and point d in Fig. 2A, B). In
 133 this joint angle, adduction ($F_{C_1} \times C_1$) and abduction ($F_{C_2} \times C_2$) torques of the dactylus
 134 about the axis X are balanced in following equation:

$$135 \quad F_{C_1} \times C_1 = F_{C_2} \times C_2 \quad (1).$$

136 The equation can be developed as follows:

$$137 \quad F_{C_2} = (C_1/C_2) \times F_{C_1} \quad (2),$$

138 where C_1/C_2 can be defined as a mechanical advantage of “pinching efficiency” (Waner
 139 and Jones, 1976; Vermeij, 1977; Yamada and Boulding, 1998; Labadie and Palmer,
 140 1996). Decapods with relatively high pinching efficiency (C_1/C_2) have advantages in
 141 durophagous (shell-breaking) predation.

142

143 **Mechanical Condition of Passive Chela Disarticulation**

144 We also assumed a mechanical condition in which the distal end of the dactylus is
 145 subjected to a lateral or medial out-force (Fig. 2C, D), such as the medio-lateral
 146 component of the reaction force from an object pinched by the chela, or a medio-lateral
 147 reaction force from the object when the crab is prying on the object (Fig. 2C). Such
 148 lateral and medial out-forces function to rotate the dactylus about an axis through the
 149 lateral and medial facets of P-D joint, respectively (see axes Y and Y' in Figs. 1 and 2).

150 The lateral-ward torque about the axis Y in Figure 2C is defined as the product of
 151 the lateral force ($F_{M_{2L}}$) and the possible maximum moment arm (M_{2L} : the distance
 152 between points a and b in Figs. 1 and 2). The disarticulation of the medial facet (point c)
 153 is assumed to be prevented by the medial-ward torque generated by the product of
 154 reaction force of the articular membrane ($F_{M_{1L}}$: Fig. 2C) and the possible maximum
 155 moment arm about the axis Y (M_1 : the distance between points b and c in Figs. 1 and 2).
 156 The condition of the rotational equilibrium about the axis Y is described in following
 157 equation:

$$158 \quad F_{M_{1L}} \times M_1 = F_{M_{2L}} \times M_{2L} \quad (3).$$

159 The equation can be developed as follows:

$$160 \quad F_{M_{1L}} = F_{M_{2L}} / (M_1/M_{2L}) \quad (4).$$

161 Likewise, the medial-ward torque about the axis Y' in Figure 2E is defined as the
 162 product of the medial reaction force ($F_{M_{2M}}$) and the possible maximum moment arm

163 (M_{2M} : the distance between points *a* and *c* in Figs. 1 and 2). The disarticulation of the
 164 lateral facet (point *b*) is prevented by the lateral-ward torque generated by the product of
 165 reaction force of the articular membrane (F_{M1M} : Fig. 2E) and the possible maximum
 166 moment arm about the axis Y' (M_1). The condition of the rotational equilibrium about
 167 the axis Y' is described in following equation:

$$168 \quad F_{M1M} \times M_1 = F_{M2M} \times M_{2M} \quad (5).$$

169 The equation can be developed as follows:

$$170 \quad F_{M1M} = F_{M2M} / (M_1/M_{2M}) \quad (6).$$

171 F_{M1L} and F_{M1M} are the tensile force on the medial and lateral articular membrane,
 172 respectively. Therefore M_1/M_{2L} and M_1/M_{2M} can be defined as mechanical advantages
 173 of “passive disarticulation resistance” against lateral- and medial reaction forces on the
 174 distal end of the chela, respectively.

175 In this study, we defined M_1/M_{2L} or M_1/M_{2M} whichever is smaller (M_1/M_2) as an
 176 index of the passive disarticulation resistance at the P-D joint. The passive
 177 disarticulation resistance (M_1/M_2) can be used as a safety factor—the cabs with
 178 relatively large M_1/M_2 have lower risks of the P-D joint disarticulation when they pinch
 179 hard tissues or pry on bivalves. In addition to the reaction forces applied by the articular
 180 membranes at the lateral and medial facets, respectively, forces applied proximally by
 181 opener and closer muscles at the points *e* and *d*, respectively (Figs. 1 and 2), may also
 182 contribute to actively provide resistant torques against the disarticulations. However, to
 183 simplify the model, we focused on the passive disarticulation resistance provided by the
 184 articular membrane for this study, but left considering the effect of the active
 185 disarticulation resistance for the future studies.

186 Crushing chelae (C) are expected to provide a relatively high mechanical advantage
 187 in both pinching efficiency (C_1/C_2) and passive disarticulation resistance (M_1/M_2).
 188 C_1/C_2 and M_1/M_2 in gripping chelae (G) are expected to be lower than those in crushing
 189 chelae, but larger than those in other chelae. The softly-pinching chelae (P), which are
 190 used for feeding on detritus, are expected to require a relatively low mechanical
 191 advantage in both C_1/C_2 and M_1/M_2 . The male ucine (Ucinae) major chelae (U) are used
 192 for pinching objects, but are not for gripping them strongly as in the cases of C and G
 193 (e.g., Levinton and Judge, 1993), or for feeding on detritus like P (Crane, 1966).
 194 Therefore, high mechanical advantages are not necessary in the male ucine major chelae
 195 (U). In this study, we tested the following hypotheses; that the mechanical advantages of
 196 both C_1/C_2 and M_1/M_2 are greater in C and G, but are lesser in P and U.

197 The moment arms C_2 , M_{2L} , and M_{2M} indirectly reflect the length of the dactylus
 198 (Fig. 2A). Therefore, if the pinching efficiency (C_1/C_2) and the passive disarticulation
 199 resistance (M_1/M_2) were correlated with each other, the aspect ratio between M_1 (the

200 width of the proximal dactylus) and C_1 (the depth of the proximal dactylus from the P-D
201 joint to the insertion of the closer muscle) may also be correlated with each other.

202

203 MATERIALS AND METHODS

204 Materials and Functional Categorization of Chelae

205 To test the above-mentioned hypotheses, we used 317 chelae of 168 brachyuran and
206 11 outgroup decapod (Anomura, Astacea, and Axiidea) specimens, for total of 34
207 families, 63 genera, and 92 species (Table S1). We followed Ng et al. (2008) for the
208 classification of the species. The study specimens are from the collections in the
209 Kanagawa Prefectural Museum of Natural History (Odawara, Japan), Toyohashi
210 Museum of Natural History (Toyohashi, Japan), National Museum of Nature and
211 Science (Tsukuba, Japan), and in the personal collections of the authors (Nagoya
212 University Museum, Nagoya, Japan). The personal collections were sampled by the
213 authors at Iriomote and Ishigaki islands (Okinawa, Japan), Fujimae Tidal Flat (Aichi,
214 Japan), and Yahagi River (Aichi, Japan); by S. Nawa (Tsuda Fishing Port, Tokushima,
215 Japan) at Seto Inland Sea (Japan); by Seike K. (The University of Tokyo, Kashiwa,
216 Japan) at Suncheon Tidal Flats (Suncheon, South Korea); and by Koizumi T. (Kyoto
217 University, Wakayama, Japan) at Kino River estuary (Wakayama, Japan). The study
218 specimens varied in taxa, body mass (0.930–3,070 g), and functions of their chelae
219 (Table S1).

220 The chela which is larger and smaller in size within a pair of chelipeds was
221 respectively defined as major and minor chelae. Both the major and minor chelae in the
222 studied taxa were categorized into four different functions in terms of pinching abilities
223 based on the available literature: C, crushing chelae; G, gripping chelae; P, pinching
224 chelae; U, male ucine major chelae; and X, the chelae whose abilities for pinching are
225 unknown (Table S1). Chelae, that are mainly used to pick up tiny particles at their tips,
226 were defined as P. In this way, the chelae of the studied taxa who rely on detritus were
227 included in this category. The major chelae of male fiddler crab (*Uca*) were defined as
228 U—their chelae are used for less destructive pinching, but are not used for feeding on
229 detritus like chelae categorized as “P” (e.g., Levinton and Judge, 1993). Chelae, that are
230 used to grab relatively large objects by using denticles on their chela, were categorized
231 as G. The major chelae of the studied taxa who crush or chip the molluscan shells were
232 categorized as C. The minor chelae of these taxa (the contralateral chela of C) were
233 categorized as group G if they were used to grip and hold relatively large objects, or
234 were categorized as P if they were mainly used to feed on detritus. The contralateral
235 chelae of C were not categorized as C in this study because it was uncertain from the
236 literature whether both chelae were used to crush molluscan shells. Functions of the

237 other chelae were categorized as unknown (X).

238

239 **Measurements**

240 Measurements were taken by a caliper (0.00–200.00 mm; Mitsutoyo Co., Ltd.) to
 241 the nearest 0.01 mm and a Martin-type anthropometer (200–1950 mm; Takei Scientific
 242 Instruments Co., Ltd.) to the nearest 1 mm for the length, and an electronic analytical
 243 scale to the nearest 0.001 g (0.000–620.000 g; Shinko Denshi Co., Ltd.), a weighing
 244 scale (620–2,000 g; Tanita Co., Ltd.) to the nearest 100 g, and a spring scale (2,000–
 245 8,000 g; Sanko Seikohjo Co., Ltd.) to the nearest 100 g for the mass. We also referred
 246 the body mass data, if available, which have been taken for the specimens in the
 247 museum collections.

248 The size of the chela in relation to the size of the carapace was estimated for each
 249 chela. To simplify the chelae and body sizes, we approximated the carapace, propodus,
 250 and dactylus using rectangles and triangles. The product of the width and length (area of
 251 the rectangle: Fig. 1A) was defined as carapace size (CS [mm²]) (Fig. 1A, Table S1).
 252 The propodus (PS [mm²]) and dactylus (DS [mm²]) sizes were defined as the area of
 253 triangle formed by the distal end of the element and two fulcra at the proximal end,
 254 respectively. PS is an area of triangle formed by points *f*, *g*, and *h* in Figure 1; and DS is
 255 an area of triangle formed by points *a*, *b*, and *c* in Figure 1 (Table S1). Areas of the
 256 triangles were calculated from lengths of the three sides by using following equation
 257 (Heron's formula: see Dunham, 1990):

$$258 \quad T = ((\alpha + \beta + \gamma) \times (-\alpha + \beta + \gamma) \times (\alpha - \beta + \gamma) \times (\alpha + \beta - \gamma))^{0.5} / 4 \quad (7)$$

259 where *T* is an area, and α , β , and γ are the lengths of three sides of the triangle. The sum
 260 of PS and DS was defined as the chela size. The relative size of the chela to the
 261 carapace (RC), which can be calculated as “(PS+DS)/CS,” was estimated for each chela
 262 of the study specimens (Table S1).

263 We assumed that the pinching occurs at the distal-most point of the chela. The
 264 mechanical advantage of pinching efficiency (C_1/C_2) is calculated as the ratio of
 265 moment arms of the closer muscle (C_1) and the tip of the chela (C_2) (Fig. 2A, B). C_1 is
 266 defined as the distance (line segment *d-d'* or *d-X*) between the insertion of the closing
 267 muscle (point *d*) and an intersection (point *d'*) between the P-D joint axis (line *X*) and a
 268 perpendicular line to the line *X* through the point *d* (Fig. 2A, B). C_2 is defined as the
 269 distance (line segment *a-a'* or *a-X*) between the distal end of the dactylus (point *a*) and a
 270 foot on the P-D joint axis of a perpendicular line through the point *a* (point *a'*: Fig. 2A,
 271 B). Thus, there are no landmarks of points *a'* and *d'* to take measurements on the
 272 specimen (Fig. 2A). We therefore calculated the distance from the point *a* (or *d*) to the
 273 feet *a'* (or *d'*) on the P-D joint axis (*X*) as a height of triangle formed by the vertices *a*

274 (or d), and medial and lateral fulcra of the P-D joint (points b and c : Fig. 2A). Areas of
275 triangles formed by vertices a , b , and c , and vertices d , b , and c , respectively, were
276 calculated by measurements on lengths of the three sides and Heron's formula. Finally,
277 the heights of these triangles (moment arms C_1 and C_2) were calculated by dividing the
278 length of the base (distance between points b and c) from twice the amount of the
279 triangle area.

280 The mechanical advantage of passive disarticulation resistance (M_1/M_2) is defined
281 as the ratio of M_1 and M_{2L} or the ratio of M_1 and M_{2M} whichever is smaller, where M_1 ,
282 M_{2L} , and M_{2M} are moment arms of the closer muscle, the lateral and medial out-forces
283 applied at the distal-end of the chela, respectively (Fig. 2A, C–F). M_1 is defined as the
284 distance (line segment $c-b$) between the medial (point c) and the lateral (point b) fulcra
285 (Fig. 2A, C, D). M_{2L} is defined as the distance (line segment $a-b$) between the distal end
286 of dactylus (point a) and the lateral fulcrum (point b : Fig. 2A, C, D). M_{2M} is defined as
287 the distance (line segment $a-c$) between the distal end of dactylus (point a) and the
288 medial fulcrum (point c : Fig. 2A, E, F). M_1 , M_{2L} , and M_{2M} can be obtained using simple
289 measurements on the specimen.

290

291 **Comparison of Indices among Functional Categories**

292 We used statistical software R 3.1.0 (R Core Team, 2014) for our statistical analyses.
293 To test differences in distributions between pairs of three different indices among the
294 functional categories, we conducted a pair-wise non-parametric comparison
295 (Steel-Dwass test) for the mechanical advantages of pinching efficiency (C_1/C_2) and
296 passive disarticulation resistance (M_1/M_2), and relative size of chela (RC) among
297 functional categories (C, G, P, and U). This was done using a free source code released
298 for Steel-Dwass test (Aoki, 2004a) on R 3.1.0. The distributions of the two categories
299 are significantly different if the p -value did not exceed 0.05.

300 The relationships between C_1/C_2 and M_1/M_2 , RC and C_1/C_2 , and RC and M_1/M_2
301 were compared. Kernel density distributions of each functional category were drawn
302 using the package “ks” (Duong, 2007) in R 3.1.0. We also conducted Spearman's and
303 correlation tests for two-dimensional plots of whole chela, C, G, P, and U, to determine
304 whether the mechanical indices (C_1/C_2 , M_1/M_2 , and RC) were correlated with each other.
305 The null hypothesis was that there was no association between the two variables and it
306 is therefore rejected if the p -value did not exceed 0.05.

307 “ C_1/C_2 ” and “ M_1/M_2 ” could not be estimated in some chelae because their chelae
308 were too small to take measurements by caliper. “RC” could not be estimated in some
309 specimens that lacked a carapace. Therefore, we used 317 chelae in total (C, 34; G, 159;
310 P, 45; U, 21; X, 58) for the statistical analyses between the two mechanical advantages

311 (C_1/C_2 [%] and M_1/M_2 [%]), and 230 specimens (C, 24; G, 121; P, 33; U, 13; X, 39) for
312 the analyses between the relative size of chela (RC [%]) and the mechanical advantages
313 (See Table S1). The phylogenetic signals were estimated for these three indices to test
314 whether these indices are phylogenetically autocorrelated (Harvey and Pagel, 1991;
315 Abouheif, 1999; Blomberg and Garland, 2002; Münkemüller et al., 2012; Pavione and
316 Ricotta, 2012; Hallmann and Griebeler, 2015). We used six different phylogenetic trees
317 (Schubart et al., 2006; Ahyong et al., 2007; Tsang et al., 2008; Bracken et al., 2009;
318 Spiridonov et al., 2014; Tsang et al., 2014) for testing the phylogenetic signals (See
319 Appendix S1 for the detail).

320

321 **Basic Design of the Proximal Dactylus**

322 To test whether the proximal dactylus of decapods are designed to retain a definite
323 range of the aspect ratio between the depth (C_1) and the width (M_1) of the proximal
324 dactylus, Spearman's and correlation tests were used to determine the relationships
325 between the logarithmic values of C_1 and M_1 [mm] using R 3.1.3 (Fig. 2A). The tests
326 were conducted for all studied chelae ($n = 317$) and for those categorized as C ($n = 24$),
327 G ($n = 121$), P ($n = 33$), and U ($n = 39$).

328 To test the differences between the regression lines, we conducted a parallel line
329 analysis (PLA) and an analysis of covariance (ANCOVA) between pairs of regression
330 lines for each functional category (C, G, P, and U) using a free-source code released for
331 these statistical analyses (Aoki, 2004b) in R 3.1.0. PLA tests the null hypothesis that the
332 slopes of the regression lines between the categories are parallel. If the slopes were
333 found to be parallel to each other ($p \geq 0.05$), an ANCOVA was conducted to test the null
334 hypothesis that the adjusted means of the slopes were equal (Aoki, 2004b). Two
335 regression lines were considered to be equal if the null hypothesis in ANCOVA was not
336 rejected ($p \geq 0.05$).

337

338 **RESULTS**

339 **Variations of three variables: C_1/C_2 , M_1/M_2 , and RC**

340 In the bivariate distribution of pinching efficiency (C_1/C_2) and passive
341 disarticulation resistance (M_1/M_2), the distributions of categories C, P, and U were
342 separated from each other (Fig. 3). By comparing median values among the functional
343 categories (C, G, P, and U), both the mechanical advantages of pinching efficiency
344 (C_1/C_2) and passive disarticulation resistance (M_1/M_2) were greatest in the crushing
345 chelae (C), followed by gripping (G), then other chelae (U, male ucine major chelae;
346 and P, pinching chelae). Notably, the difference between the medians of categories P and
347 U were not pronounced (box plots in Fig. 3 and Appendix S2). According to the

348 Steel-Dwass test, the similarity of distributions among each pair of functional categories
349 was rejected between every pair (C and G; C and P; C and U; G and P; G and U) except
350 for a single pair (P and U), regardless of the sample size (Table 1; Fig. 3; Appendix S2).

351 The major and the minor chelae varied in the mechanical advantages (Table S1; Fig.
352 4; Appendix S3). Both mechanical advantages tended to be greater in the major chelae
353 compared with the minor in some decapod clades (e.g., coenobitid anomurans, carpiiids,
354 calappids, parthenopines, dorippids, oziids, ocypodines [Appendix S3]). In contrast, the
355 differences of the mechanical advantages were not clear in astacoids, dromiaceans,
356 raninids, majoids, potamids, cancrids, leucosiids, xanthids, grapsoids, macrophthalmids,
357 and ucines (Appendix S3). In most of the decapod taxa whose major chelae have
358 crushing ability (C), the two mechanical advantages were greater in major chelae (C)
359 whereas those were lessor in the minor chelae (G) (Table S1). Among the crabs with
360 crushing on the major chelae (C), mechanical advantages in both major and minor
361 chelae were relatively large in cancrids, and there were little differences of mechanical
362 advantages between their major- and minor chelae (Appendix S3). In ucines, the
363 differences of mechanical advantages were not pronounced between major and minor
364 chelae (Appendix S3).

365 Among the functional categories of chelae (C, G, P, and U), median value of
366 relative chela size (RC) was by far the largest in U, followed by C, P, and G (boxplots in
367 Appendix S2). However, the difference of the median values among categories C, G,
368 and P were not pronounced. The Steel-Dwass test on RC among the four different
369 functional categories showed that the similarity of distributions between U and the other
370 functional categories (C, G, and P) were rejected ($p < 0.05$), whereas those among C, G,
371 and P were not rejected (Appendix S2).

372

373 **Correlation between Variables for Each Functional Category**

374 The ranges of two mechanical advantages (C_1/C_2 and M_1/M_2) were widespread in
375 several decapod lineages (Fig. 4; Appendix S3: Calappidae [C_1/C_2 : 19–52%; M_1/M_2 :
376 21–46%]; Parthenopidae [C_1/C_2 : 23–55%; M_1/M_2 : 30–44%]; Cancridae + Dorippidae +
377 Leucosiidae clade [C_1/C_2 : 5–48%; M_1/M_2 : 8–39%]; Portunoidea [C_1/C_2 : 3–41%;
378 M_1/M_2 : 4–39%]). The ranges of both mechanical advantages (C_1/C_2 and M_1/M_2) within
379 the group were especially pronounced in lithodids (C_1/C_2 : 18–42%; M_1/M_2 : 25–45%),
380 calappids, parthenopines (C_1/C_2 : 23–46%; M_1/M_2 : 30–41%), dorippids (C_1/C_2 : 6–48%;
381 M_1/M_2 : 17–39%), portunines (C_1/C_2 : 3–41%; M_1/M_2 : 4–39%), and ocypodines (C_1/C_2 :
382 18–35%; M_1/M_2 : 14–34%) (Fig. 4; Appendix S3). The functional categories of chelae
383 varied (more than two categories) within these clades as well (Table S1). The value RC
384 was extremely high in the major chelae (U) of fiddler crabs (Ucinae: Table S1; Fig. 4;

385 Appendix S2). In the other studied taxa, the RC were somewhat large ($> 25\%$) in some
386 non-brachyuran taxa (e.g., major chelae in ghost shrimp [*Glypturus*], coconut crab
387 [*Birgus*]; and major and minor chelae in crayfish [*Pacifastacus*]), but were smaller than
388 25% in all the non-ucine brachyurans (Table S1; Appendix S2). Abouheif's test based
389 on a phylogenetic tree comprised of major lineages of brachyuran superfamilies
390 (Schubart et al., 2006; Ahyong et al., 2007; Spiridonov et al., 2014; Tsang et al., 2014)
391 found that the pinching efficiency (C_1/C_2), passive disarticulation resistance (M_1/M_2),
392 and relative size of chela (RC), were not phylogenetically autocorrelated ($p \geq 0.05$) in
393 the major (L), minor (S), and the average of major and minor (L+S) chelae (Appendix
394 S1).

395 According to Spearman's test for two of three variables (C_1/C_2 , M_1/M_2 , and RC) in
396 all chelae used for this study, positive correlation was supported between C_1/C_2 and
397 M_1/M_2 (Table 2; Fig. 3: total), while the correlation was not supported between RC and
398 C_1/C_2 and between RC and M_1/M_2 (Appendix S2: total). The coefficient of
399 determination (R^2) was high (> 0.6) in relationship between C_1/C_2 and M_1/M_2 (Table 2:
400 total), whereas those were extremely low (≈ 0) in relationships between RC and the
401 other two variables (Appendix S2: total).

402 According to the Spearman's and correlation tests used to find relationships
403 between C_1/C_2 and M_1/M_2 , positive correlations were supported in all functional
404 categories, though the correlation coefficients were moderate ($0.4 < R^2 < 0.7$) (Table 2;
405 Fig. 3: C, G, P, U). In chelae belonging to categories C, G, and P, the regression lines
406 were close to each other (Fig. 3). However, in chelae belonging to category U, the
407 pinching efficiency (C_1/C_2) tended to be greater than passive disarticulation resistance
408 (M_1/M_2) compared with the other categories (Fig. 3).

409 Correlations between RC and C_1/C_2 and between RC and M_1/M_2 were not
410 supported in categories C and P (Appendix S2). Correlations between RC and C_1/C_2 ,
411 and between RC and M_1/M_2 were supported in category G; however, the coefficients of
412 determination were weak ($R^2 < 0.2$) in both cases (Appendix S2). Correlation between
413 RC and M_1/M_2 were supported in category U, and the correlation coefficient was
414 moderate (≈ 0.5) (Appendix S2).

415

416 **Aspect Ratio at the Proximal Dactylus**

417 Significant correlations were found between the depth ($\log [C_1]$) and width (\log
418 [M_1]) of the proximal dactylus in all studied chela and every functional category (C, G,
419 P, and U: Fig. 5; Table 3). The coefficients of determination (R^2) were extremely high
420 ($0.85 < R^2$) in all functional categories and in all studied chelae (Table 3).

421 However, the aspect ratio between C_1 and M_1 (M_1/C_1) ranged from 0.636 to 2.91

422 (Fig. 5; Table S1). A relatively high aspect ratio indicates that the dactylus is flat in
423 depth (C_1), whereas a relatively low ratio indicates that the dactylus is narrow in width
424 (M_1). The aspect ratio (M_1/C_1) was highly concentrated at approximately 1.00; the
425 quartiles of the ratio in all studied chelae were as follows: first, 0.945; second (median),
426 1.061; third, 1.26 (Fig. 5).

427 The slopes of the regression lines were parallel between most pairs of functional
428 categories (pairs among C, G, and U, and between P and U: Table 4). However,
429 according to the covariance tests, none of the pairs were the same (Table 4). The aspect
430 ratio was relatively large in G and P, followed by C and U (in descending order, Fig. 5).
431 This result implies that the proximal dactyli in G and P were wider than deep ($M_1 > C_1$),
432 whereas those in U were deeper than wide ($C_1 > M_1$).

433

434 **DISCUSSION**

435 **Mechanical Advantages as Indices of Chela Function**

436 This study, to our knowledge, is the first study that compared mechanical
437 advantages of chela among a huge variety of decapod taxa (representing 63 genera:
438 Table S1). We also introduced a new indicator for passive disarticulation resistance
439 (M_1/M_2), in addition to an indicator for pinching efficiency (C_1/C_2) that has been used
440 by previous studies (e.g., Warner and Jones, 1976; Yamada and Boulding, 1998;
441 Labadie and Palmer, 1996; Schenk and Wainwright, 2001).

442 The most important outcome of our study is that mechanical advantages of both
443 pinching efficiency (C_1/C_2) and passive disarticulation resistance (M_1/M_2) on decapod
444 chelae were elucidated to be good indices for estimating the function among
445 crushing/chipping (C), gripping (G), pinching (P), or male ucine major (U) chelae.
446 Specifically, the separation of the distribution of the two mechanical advantages
447 between the crushing/chipping (C) chelae and pinching (P) chelae were apparent—the
448 former are used to open hard shells, and the latter are dedicated for pinching small
449 particles, such as detritus, at the chela-tip (Fig. 3). The results were also consistent with
450 our hypotheses that crushing/chipping chelae (C) are relatively large in the mechanical
451 advantages, whereas pinching chelae (P) and male ucine major chelae (U) are relatively
452 small in the mechanical advantages. Neither mechanical advantage (C_1/C_2 or M_1/M_2)
453 was phylogenetically autocorrelated in tests based on the phylogenetic trees of decapods
454 with more than two studied taxa within most of the brachyuran superfamilies (Schubart
455 et al., 2006; Ahyong et al., 2007; Tsang et al., 2008; Bracken et al., 2009; Spiridonov et
456 al., 2014; Tsang et al., 2014: Appendix S1; Fig. 4). Therefore, diversifications of these
457 indices among decapods are interpreted to be independent from the phylogeny.

458 Preston et al. (1996) found that some durophagous brachyuran (portunid and

459 cancrid) taxa have major crushing chelae (C) with a relatively high pinching force and
460 minor gripping chelae (G) with a relatively low pinching force. Most of the
461 durophagous taxa we used had relatively high mechanical advantages for C and low
462 mechanical advantages for G (Lithodidae, Carpiliidae, Tasmanian giant crab
463 [*Pseudocarcinus*], Calappidae, Parthenopinae, Carcininae, mangrove crab [*Scylla*],
464 Oziidae, and Ocypodinae: Table S1; Fig. 4; Appendix S3); therefore, our results are
465 consistent with results of Preston et al. (1996). However, reef crab (*Atergatis*:
466 Xanthidae) was somewhat unique among the durophagous taxa we used. The
467 mechanical advantages (C_1/C_2 and M_1/M_2) of both the major (C) and minor (G) chelae
468 were high and similar (Table S1; Fig. 4; Appendix S3). The reef crab (*Atergatis*) chelae
469 are described as isochelous (Schweitzer and Feldmann, 2010), so the minor chela may
470 also have a crushing ability (C).

471 In an index of pinching efficiency (C_1/C_2), the numerator C_1 is the distance between
472 the P-D joint axis and the insertion of the closer muscle, which may indirectly reflect a
473 dorso-ventral depth of the proximal edges of the dactylus (Fig. 2A, B). In the same way,
474 the dorso-ventral depth of the proximal dactylus reflects the dorso-ventral depth of the
475 propodus (Fig. 2B). The relationship between pinching force and the dorso-ventral
476 depth has been reported in several arthropod chelipeds (Van der Meijden et al., 2010;
477 Taylor et al., 2009), and our results are consistent with these studies.

478 Dissimilarly, the passive disarticulation resistance (M_1/M_2), is directly proportional
479 to the medio-lateral width (M_1) of the proximal dactylus (Fig. 2A, C). The mechanical
480 advantage (M_1/M_2) is relatively simple to estimate because both the denomination (M_2)
481 and the numerator (M_1) can be directly measured on the specimen, unlike the length of
482 moment arms C_1 and C_2 in the estimation of pinching efficiency (Fig. 2A).

483 The relative size of the chela to the carapace size (RC) was relatively large only in
484 ucine chelae (U); there was little difference in RC among the other categories of
485 pinching abilities (C, G, and P) (Appendix S2). Moreover, all the chelae categorized as
486 U in this study belonged to the major chelae of male fiddler crabs (*Uca*, Ucininae: Table
487 S1), and it remains unclear whether the relatively high value of RC in U, estimated for a
488 single genus (*Uca*), reflects the entire spectrum of ucine chelae among decapods. In
489 conclusion, the relative size of the chela (RC) may not be a good indicator for
490 determining the function of chelae at present.

491 The moment arms C_1 and M_1 showed a high correlation with each other, which
492 suggests a high correlation between the dorso-ventral depth and the medio-lateral width
493 of the proximal dactyli (Fig. 5). None of the dactylus in the studied chela were very
494 small in width ($M_1/C_1 < 0.635$) nor in depth ($2.92 < M_1/C_1$: Table S1). These results
495 indicate that the chelae are designed to retain the ratio between dorso-ventral depth and

496 medio-lateral width of the proximal dactylus. In other words, the pinching efficiency
497 and the resistance against passive disarticulation are strongly correlated with each other
498 in chelae with a pinching ability. This hypothesis can be validated if the mechanical
499 advantages of several types of pereopods (e.g., chelate, carpochelate, semichelate, and
500 the other non-chalate types) are comprehensively studied in the future (e.g., diversified
501 pereopod morphology in reduviid hemipterans, [Weirauch et al., 2011]; chelate major-
502 and semichelate minor chelae in callianassid axiideans [Hyžný and Gašparič, 2014]).

503

504 **Limitations**

505 There are some limitations in the methods used in this study. The first limitation is
506 in the difficulty in determination of chela functions (Table S1). It is difficult to
507 categorize the functions of chelae. There are numerous studies on diets of the studied
508 taxa; however, there are few reports on how they use their chelae during feeding, mating,
509 digging, or fighting. We simply assumed that the shell-crushing chelae (C) are expected
510 to have large mechanical advantages (C_1/C_2 and M_1/M_2) over the other functional
511 categories (G, P, and U). However, the strengths of molluscan shells vary by species and
512 growth stages (e.g., Preston et al., 1996); therefore, the relatively large pinching force
513 may not simply be correlated with the species' durophagy. Moreover, some
514 non-durophagous decapods may have strong pinching abilities for other purposes. For
515 example, among the non-durophagous taxa, coconut crabs (*Birgus*, Coenobitidae,
516 Anomura) are known to have strong pinching force (Muraoka and Odawara, 1995).
517 Mechanical advantages of their chelae were estimated as be as high as those for
518 crushing chelae (C) (Table S1; Fig. S2). The functional categories should ideally be
519 based on the differences of pinching force at the tip of chela (F_{out} ; Fig. 2B, C); the
520 functional categories based on difference in diets (C, G, P, and U) are not the most
521 appropriate method to compare mechanical advantages. However, studies on pinching
522 forces alone are still not sufficient to compare the mechanical advantages among
523 various taxa (e.g., Elnor, 1978; Govind and Blundon, 1985; Taylor et al., 2009; Van der
524 Meijden, 2012). This limitation remains an issue for future study.

525 The second limitation concerns the potential role of the opener and closer muscles
526 in resisting mediolateral disarticulations of the P-D joint. These muscles may function
527 to rotate the dactylus about the axes Y or Y' for resisting against the P-D joint
528 disarticulation (Fig. 1B). Therefore, the ratio between the moment arms of the dactylus
529 (M_2) and these muscles (the mediolateral distance from points d or e to the axes Y or Y' :
530 Fig. 1B) may also be used as an additional index for the disarticulation resistance, and it
531 is worth testing the validity of this index in the future studies.

532 The third limitation concerns the validity of the use of the triangular area (PS + DS)

533 for the proxy of chela size, because the value has not been widely used as the proxy in
534 previous studies. However, the correlation between the traditionally used proxy (the
535 propodus length) and our new proxy (PS + DS) was strongly supported (see Appendix
536 S4). Therefore, we consider that the use of the triangular area for the chela size is valid.

537 The fourth limitation concerns the points on the chelae that these taxa use to pinch
538 the object. Mechanical advantages employed in this study (C_1/C_2 and M_1/M_2) are based
539 on the assumption that the chelae pinch objects at the distal ends (Fig. 2B, C). However,
540 in many cases, objects are pinched at the teeth along the pinching surface of chela (Fig.
541 1C, D: e.g., Muraoka and Odawara, 1995). For example, many durophagous species are
542 known to have molariform or hooked teeth at the proximal portions of the pinching
543 surface on the chelae to crush or chip molluscan shells (Vermeij, 1977; Schweitzer and
544 Feldmann, 2010). Mechanical advantages of both pinching and passive disarticulation
545 resistance would be increased if the studied taxa pinched objects at these teeth, because
546 the distance between the rotational axis and the teeth is smaller than those between the
547 axis and the distal end of the dactylus (Fig. 2B, C). On the other hand, some detritus
548 feeders, such as mud crabs (*Macrophthalmus*: P) and fiddler crabs (*Uca*: P and U), have
549 few teeth, if any, at the distal portions of the pinching surfaces of the chelae (Table S1).
550 The mechanical advantages would not be increased dramatically if these studied taxa
551 pinched objects at these teeth. The concern on the points on the chelae to pinch the
552 object remains an issue for future study.

553

554 **Mechanical Advantages as Tools to Reconstruct Evolutionary Process of Chelae** 555 **Functions**

556 The mechanical advantages C_1/C_2 and M_1/M_2 can be calculated from simple
557 measurements on the chela. Therefore, these indices could be powerful tools to estimate
558 the functions of chelae in species whose ecologies are not well known (X, unidentified
559 chelae: Table S1). These indices could also be applied to estimate chelae function in
560 extinct species, whose functions have mainly been reconstructed by relying on the
561 morphological features of the chelae (e.g., Dietl and Vega, 2008; Schweitzer and
562 Feldmann, 2010). Further studies on the additional mechanical indices, such as the
563 cuticle strengths of the chela (Palmar et al., 1999; Van der Meijden et al., 2012) or the
564 ability of resistance against the torsion of the P-D joint, will provide us a deeper
565 knowledge on the relationship between the design and function of the chelae.

566 In the study specimens, the mechanical advantages of C_1/C_2 and M_1/M_2 were
567 diversified within the ranges of 0–60% in each lineage of decapods (Table S1; Fig. 4;
568 Appendix S3), and these indices were not phylogenetically autocorrelated at least in the
569 Abouheif's test based on the trees which comprise many taxa within each superfamily

570 (Appendix S1). These results indicate that the diversification of chela functions and
571 diets was accompanied by the diversifications of these mechanical advantages. Hence,
572 varying the mechanical advantages of pinching efficiency and passive disarticulation
573 resistance played significant role in ecological diversification of decapods, though these
574 variables were well correlated with each other.

575

576 **CONCLUSIONS**

577 In comparing the major and minor chelae of 93 decapod species of 63 genera, the
578 mechanical advantages of both pinching efficiency and passive disarticulation resistance
579 were demonstrated to be good indices for the evaluation of pinching abilities. Both
580 mechanical advantages were greater in the abilities of the shell-crushing/chipping chelae,
581 followed by the grasping, and the pinching/male ucine major chelae. On the other hand,
582 the relative size of the chelae to the carapace size was not related to differences among
583 the crushing/chipping, gripping, or pinching functions.

584

585 **AUTHOR CONTRIBUTIONS**

586 S.-i. Fujiwara: study conception, design, and shaping manuscript; H. Kawai:
587 sampling and measurements; S.-i. Fujiwara and H. Kawai: data analyses. The authors
588 declare that there are no conflicts of interest.

589

590 **ACKNOWLEDGEMENTS**

591 We thank Sato T. (Kanagawa Prefectural Museum, Odawara, Japan), Komatsu H.
592 (National Science Museum of Nature and Science, Tsukuba, Japan), and Nishi H.
593 (Toyohashi Museum of Natural History, Toyohashi, Japan) for the permissions to
594 observe the specimens; Ando Y. and Karasawa H. (Mizunami Fossil Museum,
595 Mizunami, Japan), Seike K. (The University of Tokyo, Kashiwa, Japan), Nawa S.
596 (Tsuda Fishing Port, Sanuki, Japan), and Koizumi T. (Seto Marine Biological
597 Laboratory, Kyoto University, Wakayama, Japan) for providing the specimens; Oji T.
598 (Nagoya University Museum, Nagoya, Japan), Mochizuki T. (Iwate Prefectural Museum,
599 Morioka, Japan), and Matsumoto R. (Kanagawa Prefectural Museum, Odawara, Japan)
600 for helping the samplings; Seike K. (The University of Tokyo, Kashiwa, Japan) and
601 Nishida S. (Nagoya University Museum, Nagoya, Japan) for helpful advice on
602 statistical analysis; Suto I. and Hayashi S. (Nagoya University, Nagoya, Japan) for
603 improving the manuscript; and Kato H. (Natural History Museum and Institute, Chiba,
604 Japan) for the helpful advice. The authors are extremely grateful for the two anonymous
605 reviewers and the editor who greatly improved our manuscript.

606

607 **LITERATURE CITED**

- 608 Abouheif E. 1999. A method for testing the assumption of phylogenetic independence in
609 comparative data. *Evol Ecol Res* 1:895–909.
- 610 Ahyong ST, Lai JCY, Sharkey D, Colgan DJ, Ng PKL. 2007. Phylogenetics of the
611 brachyuran crabs (Crustacea: Decapoda): the status of Podotremata based on small
612 subunit nuclear ribosomal RNA. *Mol Phylogenet Evol* 45:576–586.
- 613 Anker A, Ahyong ST, Noël PY, Palmer AR. 2006. Morphological phylogeny of alpheid
614 shrimps: parallel preadaptation and the origin of a key morphological innovation,
615 the snapping claw. *Evolution* 60:2507–2528.
- 616 Aoki S. 2004a. Multiple comparison based on Steel-Dwass test by using R.
617 <http://aoki2.si.gunma-u.ac.jp/R/Steel-Dwass.html>.
- 618 Aoki S. 2004b. Covariance test by using R.
619 <http://aoki2.si.gunma-u.ac.jp/R/covar-test.html>.
- 620 Backwell RY. 2000. Dishonest signaling in a fiddler crab. *Proc R Soc B-Biol Sci*
621 267:719–724.
- 622 Blomberg SP, Garland T. 2002. Tempo and mode in evolution: phylogenetic inertia,
623 adaptation and comparative methods. *J Evol Biol* 15:899–910.
- 624 Boxshall GA. 2004. The evolution of arthropod limbs. *Biol Rev* 79:253–300.
- 625 Bracken HD, Toon A, Felder DL, Martin JW, Finley M, Rasmussen J, Palero F, Crandall
626 KA. 2009. The decapod tree of life: compiling the data and moving toward a
627 consensus of decapod evolution. *Arthropod Syst Phyl* 67:99–116.
- 628 Brown SC, Cassuto SR, Loos RW. 1979. Biomechanics of chelipeds in some decapod
629 crustaceans. *J Zool, Lond* 188:143–159.
- 630 Chace FA, Holthuis LB. 1978. *Psalidopus*: the scissor-foot shrimps (Crustacea:
631 Decapoda: Caridea). *Smithson Contr Zool* 277:1–22.
- 632 Crane J. 1966. Combat, display and ritualization in fiddler crabs (Ocypodidae, Genus
633 *Uca*). *Philos T R Soc B, Biol Sci* 251:459–472.
- 634 Dennenmoser S, Christy JH. 2013. The design of a beautiful weapon: compensation for
635 opposing sexual selection on a trait with two functions. *Evolution* 67:1181–1188.
- 636 Dietl GP, Vega FJ. 2008. Specialized shell-breaking crab claws in Cretaceous seas. *Biol*
637 *Lett* 4:290–293.
- 638 Dunham W. 1990. *Journey through Genius: The Great Theorems of Mathematics*. New
639 York: Wiley. 287p.
- 640 Duong T. 2007. ks: Kernel density estimation and kernel discriminant analysis for
641 multivariate data in R. *J Stat Softw* 21:1–16.
- 642 Elner RW. 1978. The mechanics of predation by the shore crab, *Carcinus maenas* (L.),
643 on the edible mussel, *Mytilus edulis* L. *Oecologia* 36:333–344.

- 644 Elner RW, Campbell A. 1981. Force, function, and mechanical advantage in the claw of
645 the American lobster *Homarus americanus* (Decapoda: Crustacea). *J Zool, Lond*
646 173:395–406.
- 647 Field LH. 1990. Aberrant defense displays of the big-handed crab, *Heterozius*
648 *rotundifrons* (Brachyura: Belliidae). *New Zeal J Mar Fresh* 24:211–220.
- 649 Fujiwara S, Endo H, Hutchinson JR. 2011. Topsy-turvy locomotion: biomechanical
650 specializations of the elbow in suspended quadrupeds reflect inverted gravitational
651 constraints. *J Anat* 219:176–191.
- 652 Fujiwara S, Hutchinson JR. 2012. Elbow joint adductor moment arm as an indicator of
653 forelimb posture in extinct quadrupedal tetrapods. *Proc Roy Soc B, Biol Ser*
654 279:2561–2570.
- 655 Govind CK, Blundon JA. 1985. Form and function of the asymmetric chelae in blue
656 crabs with normal and reversed handedness. *Biol Bull-US* 168:321–331.
- 657 Hallmann K, Griebeler EM. 2015. Eggshell types and their evolutionary correlation
658 with life-history strategies in squamates. *PLoS ONE* 10:e0138785.
- 659 Harvey PH, Pagel MD. 1991. *The Comparative Method in Evolutionary Biology*.
660 Oxford: Oxford University Press. 239p.
- 661 Hughes RN. 1989. Foraging behaviour of a tropical crab: *Ozius verreauxii*. *Proc R Soc*
662 *B-Biol Sci* 237:201–212.
- 663 Hyžný M, Gašparič R. 2014. Ghost shrimp *Calliax* de Saint Laurent, 1973 (Decapoda:
664 Axiidea: Callianassidae) in the fossil record: systematics, palaeoecology and
665 palaeobiogeography. *Zootaxa* 3821:37–57.
- 666 Labadie LV, Palmer AR. 1996. Pronounced heterochely in the ghost shrimp, *Neotrypaea*
667 *californiensis* (Decapoda: Thalassinidea: Callianassidae): allometry, inferred
668 function and development. *J Zool, Lond* 240:659–675.
- 669 Lau CJ. 1987. Feeding behavior of the Hawaiian slipper lobster *Scyllarides*
670 *squammosus*, with a review of decapod crustacean feeding tactics on molluscan
671 prey. *Bull Mar Sci* 41:378–391.
- 672 Levinton JS, Judge ML. 1993. The relationship of closing force to body size for the
673 major claw of *Uca pugnax* (Decapoda: Ocypodidae). *Funct Ecol* 7:339–345.
- 674 Manton SM. 1968. Terrestrial Arthropoda (II). In: Gray J, editor. *Animal Locomotion*.
675 New York: W. W. Norton & Company, Inc. p 333–376.
- 676 Mariappan P, Balasundaram C, Schmitz B. 2000. Decapod crustacean chelipeds: an
677 overview. *J Biosci* 25:301–313.
- 678 Meusemann K, Reumont BM, Simon S, Roeding F, Strauss S, Kück P, Ebersberger I,
679 Walzl M, Pass G, Breuers S, Achter V, von Haeseler A, Burmester T, Hadrys H,
680 Wägele J-W, Misof B. 2014. A phylogenomic approach to resolve the arthropod

- 681 tree of life. *Mol Biol Evol* 27:2451–2464.
- 682 Moore KL, Dalley AF. 2006. *Clinically Oriented Anatomy, Fifth Edition*. Baltimore:
683 Lippincott Williams and Wilkins. 1209p.
- 684 Münkemüller T, Lavergne S, Bzeznik B, Dray S, Jombart T, Schiffers K, Thuiller W.
685 2012. How to measure and test phylogenetic signal. *Methods Ecol Evol* 3:743–756.
- 686 Muraoka K, Odawara T. 1995. *The Visual Guide to Crabs*. Tokyo: Seibido. 159p [In
687 Japanese].
- 688 Ng PKL, Guinot DG, Davie PJF. 2008. *Systema brachyorum: Part I. An annotated*
689 *checklist of extant brachyuran crabs of the world*. *Raffles Bull Zool* 17:1–286.
- 690 Palmer AR. 2004. Symmetry breaking and the evolution of development. *Science*
691 306:828–833.
- 692 Palmer AR, Taylor GM, Barton A. 1999. Cuticle strength and the size-dependence of
693 safety factors in *Cancer* crab claws. *Biol Bull* 196:281–294.
- 694 Pavione S, Ricotta C. 2012. Testing for phylogenetic signal in biological traits: the
695 ubiquity of cross-product statistics. *Evolution* 67:828–840.
- 696 Payne A, Kraemer GP. 2013. Morphometry and claw strength of the non-native Asian
697 shore crab, *Hemigrapsus sanguineus*. *Northeast Nat* 20:478–492.
- 698 Preston SJ, Revie IC, Orr JF, Roberts D. 1996. A comparison of the strength of
699 gastropod shells with forces generated by potential crab predators. *J Zool, Lond*
700 238:181–193.
- 701 Pynn HJ. 1998. Chela dimorphism and handedness in the shore crab *Carcinus maenas*.
702 *Field Stud* 9:343–353.
- 703 R Core Team. 2014. *R: A Language and Environment for Statistical Computing*. Vienna:
704 R Foundation for Statistical Computing. URL <http://www.R-project.org/>.
- 705 Regier JC, Shultz JW, Zwick A, Hussey A, Ball B, Wetzler R, Martin JW, Cunningham
706 C. 2010. Arthropod relationships revealed by phylogenomic analysis of nuclear
707 protein-coding sequences. *Nature* 463:1079–1083.
- 708 Rosenberg MS. 2002. Fiddler crab claw shape variation: a geometric morphometric
709 analysis across the genus *Uca* (Crustacea: Brachyura: Ocypodidae). *Biol J Linn Soc*
710 75:147–162.
- 711 Schenk SC, Wainwright PC. 2001. Dimorphism and the functional basis of claw
712 strength in six brachyuran crabs. *J Zool, Lond* 255:105–109.
- 713 Schubart CD, Cannicci S, Vannini M, Fratini S. 2006. Molecular phylogeny of grapsoid
714 crabs (Decapoda, Brachyura) and allies based on two mitochondrial genes and a
715 proposal for refraining from current superfamily classification. *J Zool Syst Evol*
716 *Res* 44:193–199.
- 717 Schweitzer CE, Feldmann RM. 2010. The Decapoda (Crustacea) as predators on

- 718 mollusca through geologic time. *Palaios* 25:167–182.
- 719 Shultz JW. 1989. Morphology of locomotor appendages in Arachnida: evolutionary
720 trends and phylogenetic implications. *Zool J Linn Soc* 97:1–56.
- 721 Spiridonov VA, Neretina TV, Schepetov D. 2014. Morphological characterization and
722 molecular phylogeny of Portunoidea Rafinesque, 1815 (Crustacea Brachyura):
723 implications for understanding evolution of swimming capacity and revision of the
724 family-level classification. *Zool Anz* 253:404–429.
- 725 Taylor GM, Keyghobadi N, Schmidt PS. 2009. The geography of crushing: Variation in
726 claw performance of the invasive crab, *Carcinus maenus*. *J Exp Mar Biol Ecol*
727 377:48–53.
- 728 Taylor RS, Schram FR. 1999. Meiura (anomalan and brachyuran crabs). In: Savazzi E,
729 editor. *Functional Morphology of the Invertebrate Skeleton*. Chichester: John Wiley.
730 p 517–528.
- 731 Tsang LM, Ma KY, Ahyong ST, Chan T-Y, Chu KH. 2008. Phylogeny of Decapoda
732 using two nuclear protein-coding genes: origin and evolution of the Reptantia.
733 *Mol Phylogenet Evol* 48:359–368.
- 734 Tsang LM, Schubart CD, Ahyong ST, Lai JCY, Au E, Chan T-Y, Ng PKL, Chu KH.
735 2014. Evolutionary history of true crabs (Crustacea: Decapoda: Brachyura) and the
736 origin of freshwater crabs. *Mol Biol Evol* 31:1173–1187.
- 737 Valiela I, Babiec DF, Atherton W, Seitzinger S, Krebs C. 1974. Some consequences of
738 sexual dimorphism: feeding in male and female fiddler crabs, *Uca pugnax* (Smith).
739 *Biol Bull* 147:652–660.
- 740 Van de Kamp T, Vagovič P, Baumbach T, Riedel A. 2011. A biological screw in a
741 beetle's leg. *Science* 333:52.
- 742 Van der Meijden A, Herrel A, Summers A. 2010. Comparison of chela size and pincer
743 force in scorpions: getting a first grip. *J Zool, Lond* 280:319–325.
- 744 Van der Meijden A, Kleinteich T, Coelho P. 2012. Packing a pinch: functional
745 implications of chela shapes in scorpions using finite element analysis. *J Anat*
746 220:423–434.
- 747 Vermeij GJ. 1977. Patterns in crab claw size: the geography of crushing. *Syst Zool*
748 26:138–151.
- 749 Warner GF. 1977. *The Biology of Crabs*. New York: Van Nostrand Reinhold Company.
750 202p.
- 751 Warner GF, Jones AR. 1976. Leverage and muscle type in crab chelae (Crustacea:
752 Brachyura). *J Zool, Lond* 180:57–68.
- 753 Warner GF, Chapman D, Hawkey N, Waring DG. 1982. Structure and function of the
754 chela closer muscles of the shore crab *Carcinus maenas* (Crustacea: Brachyura). *J*

- 755 Zool Lond 196:431–438.
- 756 Weirauch C, Forero D, Jacobs DH. 2011. On the evolution of raptorial legs—an insect
757 example (Hemiptera: Reduviidae: Phymatinae). *Cladistics* 27:138–149.
- 758 Yamada SB, Boulding EG. 1998. Claw morphology, prey size selection and foraging
759 efficiency in generalist and specialist shell-breaking crabs. *J Exp Mar Biol Ecol*
760 220:191–211.
- 761 Zipser E, Vermeij GJ. 1978. Crushing behavior of tropical and temperate crabs. *J Exp*
762 *Mar Biol Ecol* 31:155–172.
- 763

Tables

TABLE 1. Results of Steel-Dwass tests of three indices related to chela—pinching efficiency (C_1/C_2) and passive disarticulation resistance (M_1/M_2)—among four different functional categories (C, G, P, and U). The tests were conducted for all the study specimens ($n = 259$: C, 34; G, 159; P, 45; U, 21). Asterisk indicates that the variables among two categories were not significantly different ($p < 0.05$). See boxplots in Fig. 3.

	C_1/C_2		M_1/M_2	
	t -score	p	t -score	p
C:G	6.34	1.36e-09*	5.64	1.01e-07*
C:P	7.11	7.03e-12*	6.93	2.51e-11*
C:U	5.94	1.69e-08*	6.18	3.73e-09*
G:P	3.94	4.67e-04*	5.82	3.37e-08*
G:U	2.61	4.49e-02*	7.08	7.73e-12*
P:U	0.0757	1.00	3.27	5.93e-03*

TABLE 2. Spearman's correlation test between mechanical advantages of pinching efficiency (C_1/C_2) and passive disarticulation resistance (M_1/M_2) ($n = 317$: C, 34; G, 159; P, 45; U, 21; X, 58). Spearman's ρ - and p -values, coefficient of determination (R^2), and regression line were indicated for each functional category (C, G, P, and U). See Fig. 3.

	n	ρ -value	p	R^2	regression line
total	317	0.789	<2.2e-16*	0.652	$y = 0.583x + 11.0$
C	34	0.744	1.10e-06*	0.529	$y = 0.474x + 15.7$
G	159	0.662	<2.2e-16*	0.481	$y = 0.441x + 15.9$
P	45	0.879	2.46e-15*	0.771	$y = 0.609x + 9.23$
U	21	0.584	1.68e-03*	0.413	$y = 0.527x + 5.60$

*Null-hypothesis that there is no association between the two variables was rejected ($p < 0.05$).

TABLE 3. Spearman's correlation test between moment arms of closing muscle contraction (C_1) and resistance force of the articular membrane (M_1) ($n = 317$: C, 34; G, 159; P, 45; U, 21; X, 58). Spearman's ρ - and p -values, coefficient of determination (R^2), and regression line were indicated for each functional category (C, G, P, and U). See Fig. 5.

	n	ρ -value	p	R^2	regression line
total	317	0.933	<2.2e-16*	0.875	$\log(M_1) = 0.908 \times \log(C_1) + 0.105$
C	34	0.971	<2.2e-16*	0.868	$\log(M_1) = 1.02 \times \log(C_1) - 0.0482$
G	159	0.912	<2.2e-16*	0.866	$\log(M_1) = 1.03 \times \log(C_1) + 0.0452$
P	45	0.905	<2.2e-16*	0.883	$\log(M_1) = 0.858 \times \log(C_1) + 0.135$
U	21	0.932	2.87e-11*	0.907	$\log(M_1) = 1.12 \times \log(C_1) - 0.184$

*Null-hypothesis that there is no association between the two variables was rejected ($p < 0.05$).

TABLE 4. Results of pair-wise analysis of covariance (ANCOVA) between pairs of regression lines of closing muscle contraction (C_1) and resistance force of the articular membrane (M_1) among the functional categories C ($n = 34$), G ($n = 159$), P ($n = 45$), and U ($n = 21$). Parallel line analysis (PLA) tests the null hypothesis that the slopes of the regression lines are parallel to each other. ANCOVA tests the null hypothesis that the adjusted means of the slopes are equal. Similarity of the two slope are supported if the p -values of the both tests exceed 0.05 ($p \geq 0.05$). See Table 3 and Fig. 5 for the regression lines.

test	PLA		ANCOVA	
	F -statistic	p -value	F -statistic	p -value
C : G	0.116	0.733	1.93	1.89e-05
C : P	7.78	6.70e-03	—	—
C : U	0.439	0.510	16.2	1.82e-04
G : P	8.29	4.42e-03	—	—
G : U	0.333	0.565	6.58	8.07e-14
P : U	2.96	0.0905	3.87	4.47e-08

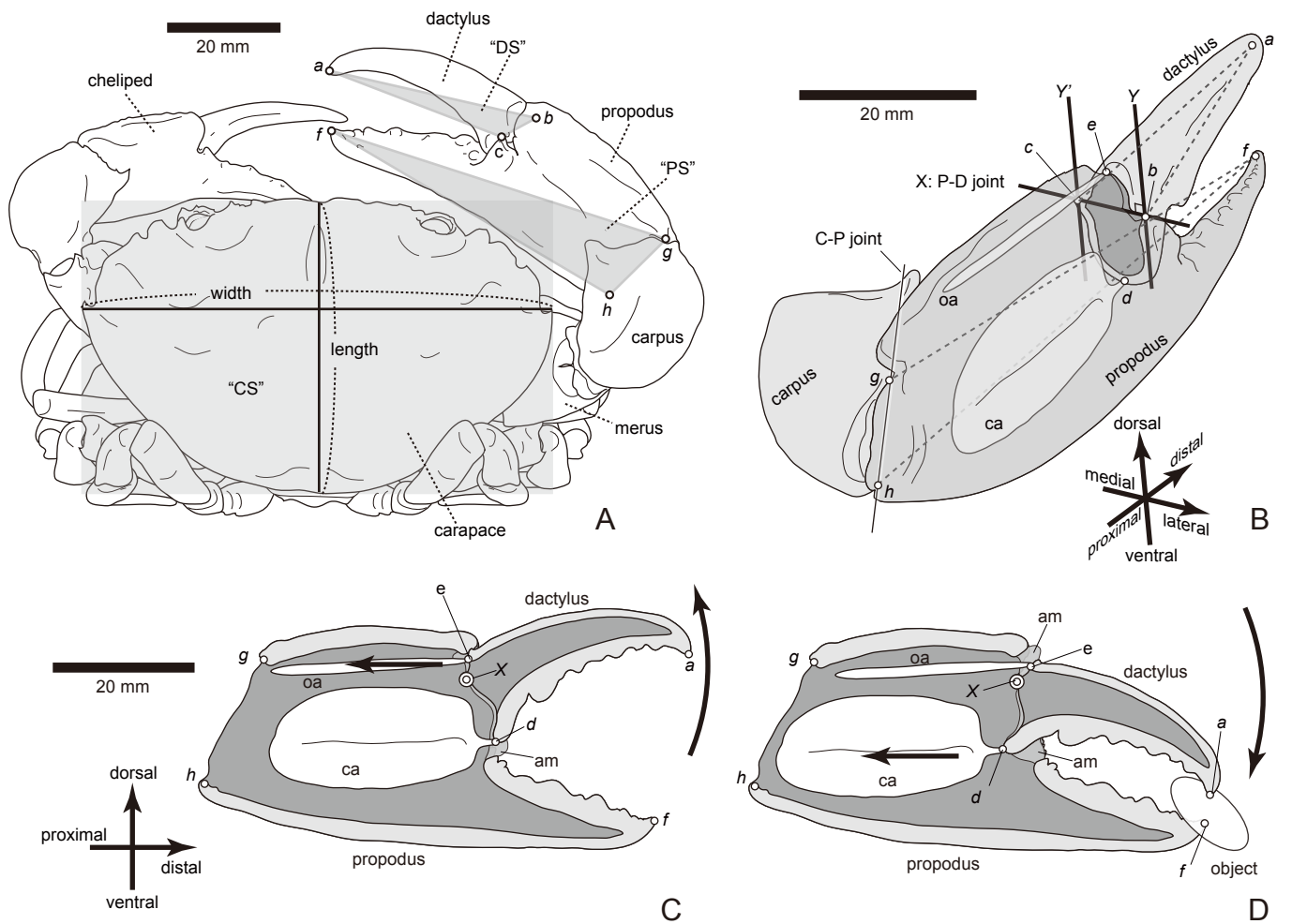


Fig. 1. Structures of decapod chela. **(A)** A scheme illustration of a decapod (*Baptozius vinosus*: KH66) with definition of carapace, dactylus, and propodus sizes in this study. **(B)** Connections of the distal three elements (carpus, propodus, and dactylus) of the right cheliped. These elements are connected via facet-fulcrum articulations and articular membranes (am). **(C)** Opening and **(D)** closing phases of the propodus-dactylus (P-D) joint. Abbreviations: (a) distal-most point on the dactylus; (b) medial and (c) lateral fulcrum of the P-D joint; (d) insertion of closer apodeme (ca), and (e) insertion of opener apodeme (oa) on the dactylus; (f) distal-most point on the propodus; (g) medial and (h) lateral fulcrum of the carpus-propodus (C-P) joint. Axis *X* (a line through points *b* and *c*) correspond to the P-D joint. Axes *Y* and *Y'* are lines through points *b* and *c*, which are perpendicular to the plane formed by points *a-c*, respectively. The axes *X*, *Y*, and *Y'* are determined to calculate moment arms (C_1 , C_2 , M_1 , M_{2L} , and M_{2M} ; see Fig. 2). In **(A)**, shaded area of rectangle represents the carapace size (CS), and shaded areas of triangles formed by points *a-c* and points *d-f*, respectively represent the propodus (PS) and dactylus (DS) sizes.

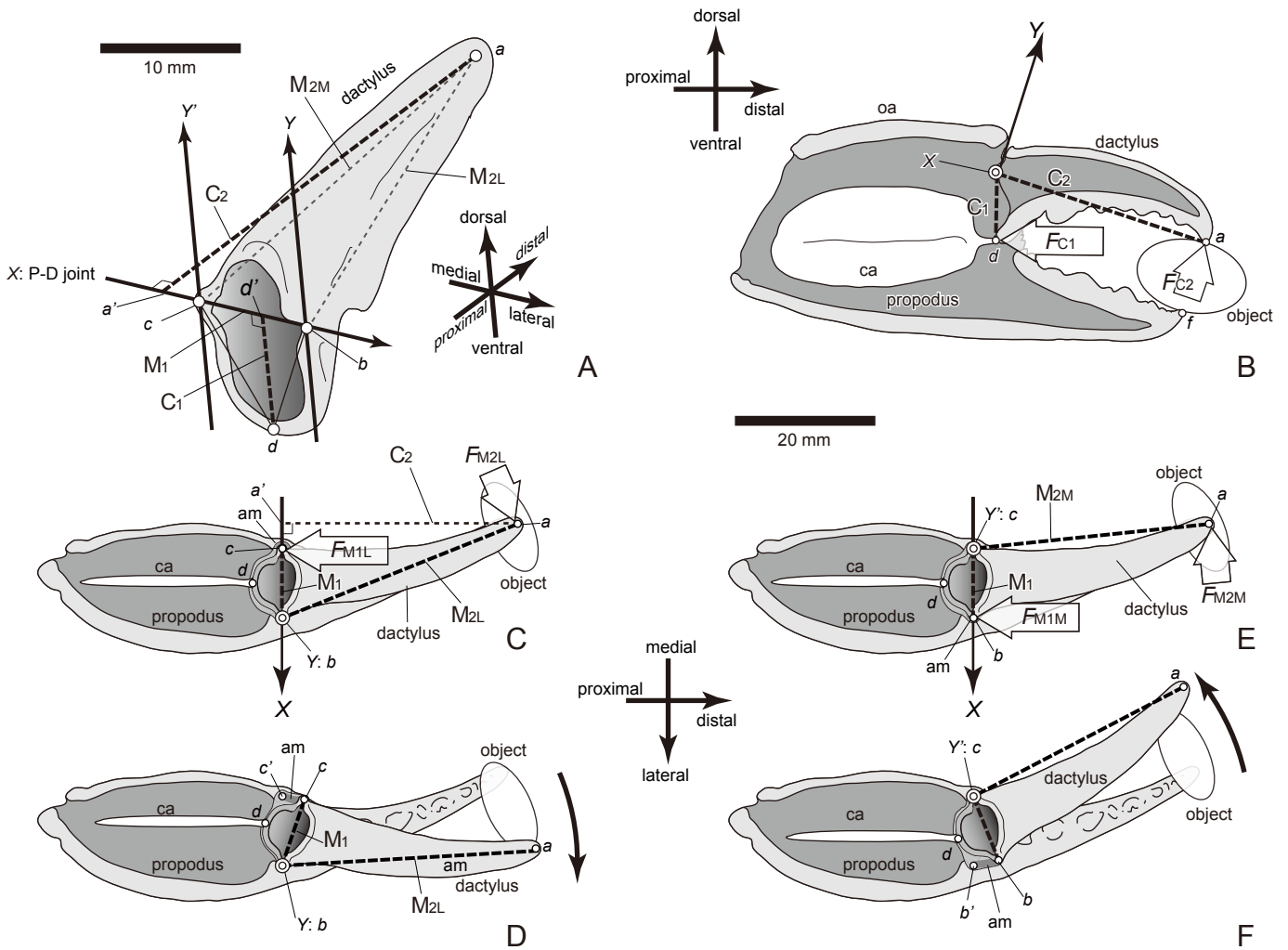


Fig. 2. (A) Measurement points on the dactylus, mechanical conditions of (B) pinching an object using the chela (in lateral view), and (C) and (E) resistance of the medial and lateral fulcra against lateral- and medial-ward thrusts on the chela tip that functions to dislocate the joint, respectively (in dorsal view). In (B), the dactylus rotate about axis X . A contractive force of closer muscle (F_{C1}) is applied to point d during the pinching phase. A product of F_{C1} and the in-lever moment arm C_1 is balanced by a product of a reaction force (F_{C2}) from the object to the tip of the dactylus (point a) and its moment arm C_2 . In (C), the dactylus rotates about an axis Y . An external force (F_{M2L}) on the tip of the dactylus (a) rotates the dactylus laterally about the point b , whereas the articular membrane functions in resisting the torque at the medial fulcrum (point c) at a certain force (F_{M1L}). A product of F_{M1L} and the in-lever moment arm M_1 is balanced by a product of the lateral force (F_{M2L}) from the object and its moment arm M_{2L} . (D) The medial fulcrum on the dactylus (c) is disarticulated with the medial facet on the propodus (c') under the following conditions: $|F_{M1L} \times M_1| > |F_{M2L} \times M_{2L}|$. Likewise, in (E), the dactylus rotates medially about an axis Y' by an external force (F_{M2M}) on the tip of the dactylus (a), while the articular membrane at the medial fulcrum (point c) produces resistant torque at a certain force (F_{M1M}): $|F_{M1M} \times M_1| = |F_{M2M} \times M_{2M}|$. (D) The lateral fulcrum on the dactylus (b) is disarticulated with the medial facet on the propodus (b') under the following conditions: $|F_{M1M} \times M_1| > |F_{M2M} \times M_{2M}|$. Abbreviations: (a) distal-most point on the dactylus; (a') a foot of perpendicular line through point a on axis X ; (b) medial and (c) lateral fulcra of the P-D joint; (b') medial and (c') lateral facets of the P-D joint; (d) insertion of closer apodeme (ca); (d') a foot of perpendicular line through point d on axis X ; X , a line through points b and c ; Y and Y' , lines through points b and c , which are perpendicular to the plane formed by points a - c .

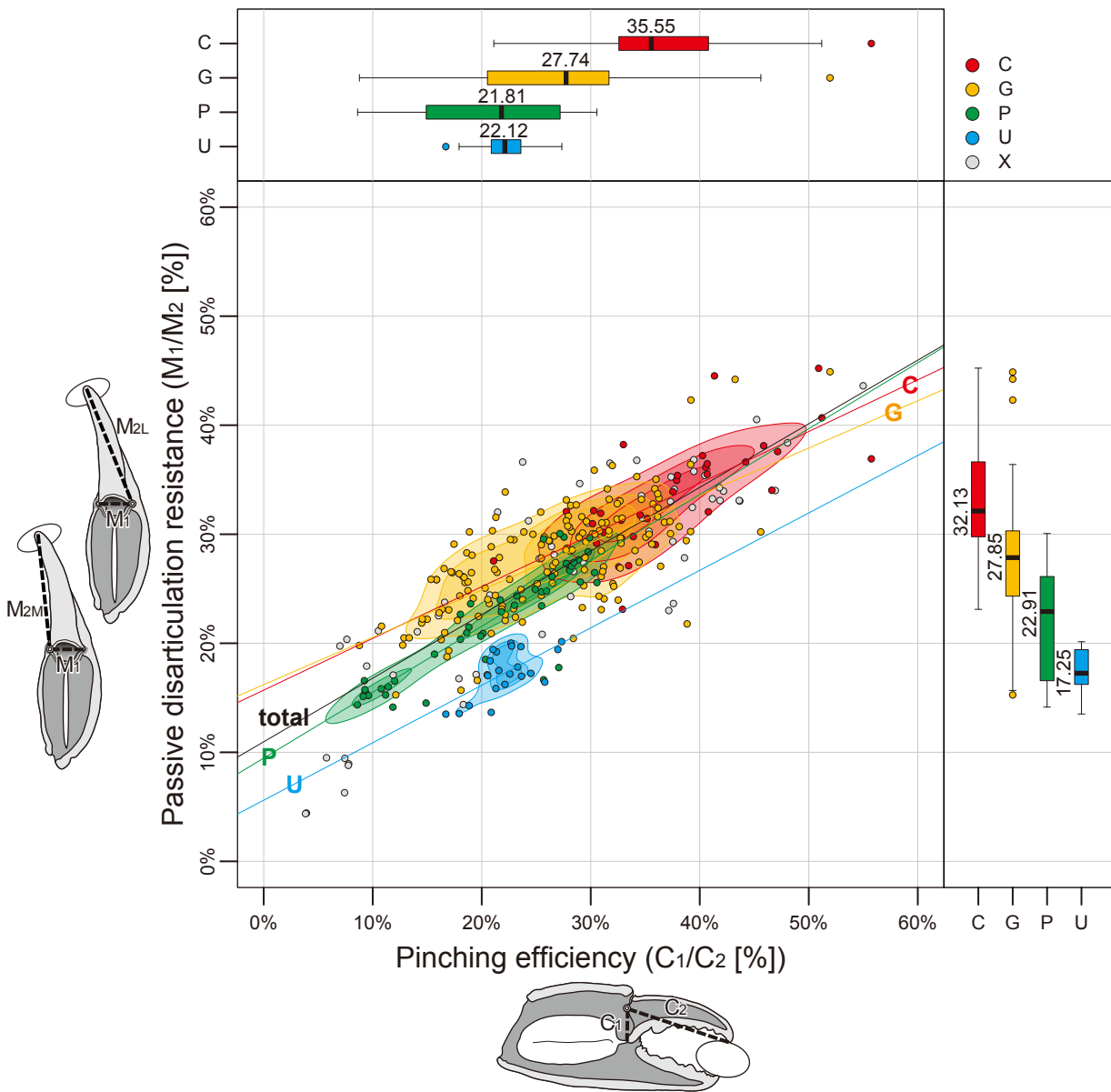


Fig. 3. Relationship between mechanical advantages of pinching efficiency (C_1/C_2) and passive disarticulation resistance (M_1/M_2). See main text for abbreviations. Each plot represents chela characteristics of the study specimens ($n = 317$ in total; C, crushing/chipping chela, $n = 34$; G, gripping chela, $n = 159$; P, pinching chela, $n = 45$; U, male ucine major chela, $n = 21$; X, uncategorized chela, $n = 58$). Bivariate kernel density distributions (densities: 25%, 50%, 75%) and box plots with median values are shown for each variable in the functional categories C, G, P, and U. See Table 1 for results of Steel-Dwass tests in the variables. Regression lines are drawn for total plots, in addition to the regression lines for plots of each functional category (C, G, P, and U). See Table 3 for slopes of the regression lines.

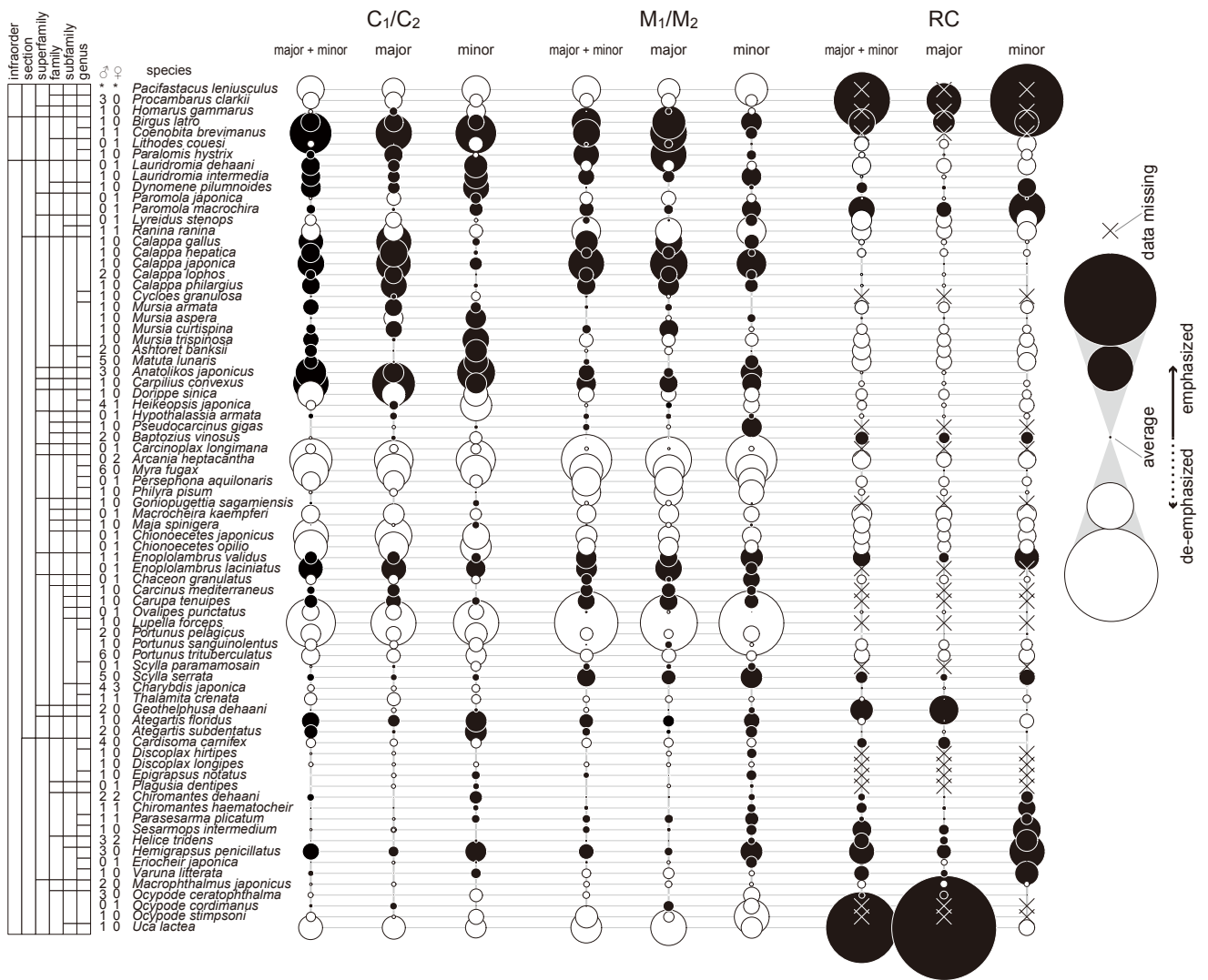


Fig. 4. Variations of three indices (C_1/C_2 , M_1/M_2 , and RC) among the studied species whose indices in both the major and minor chelae were available. The values of indices were estimated for the average of major and minor, major, and minor chelae. White and black symbols respectively correspond to values which are below and over the mean among the species. The values of indices were defined as the average of the studied chelae in the species. We followed Ng et al. (2008) for the ranks of classification (infraorder, section, superfamily, family, subfamily, and genus).

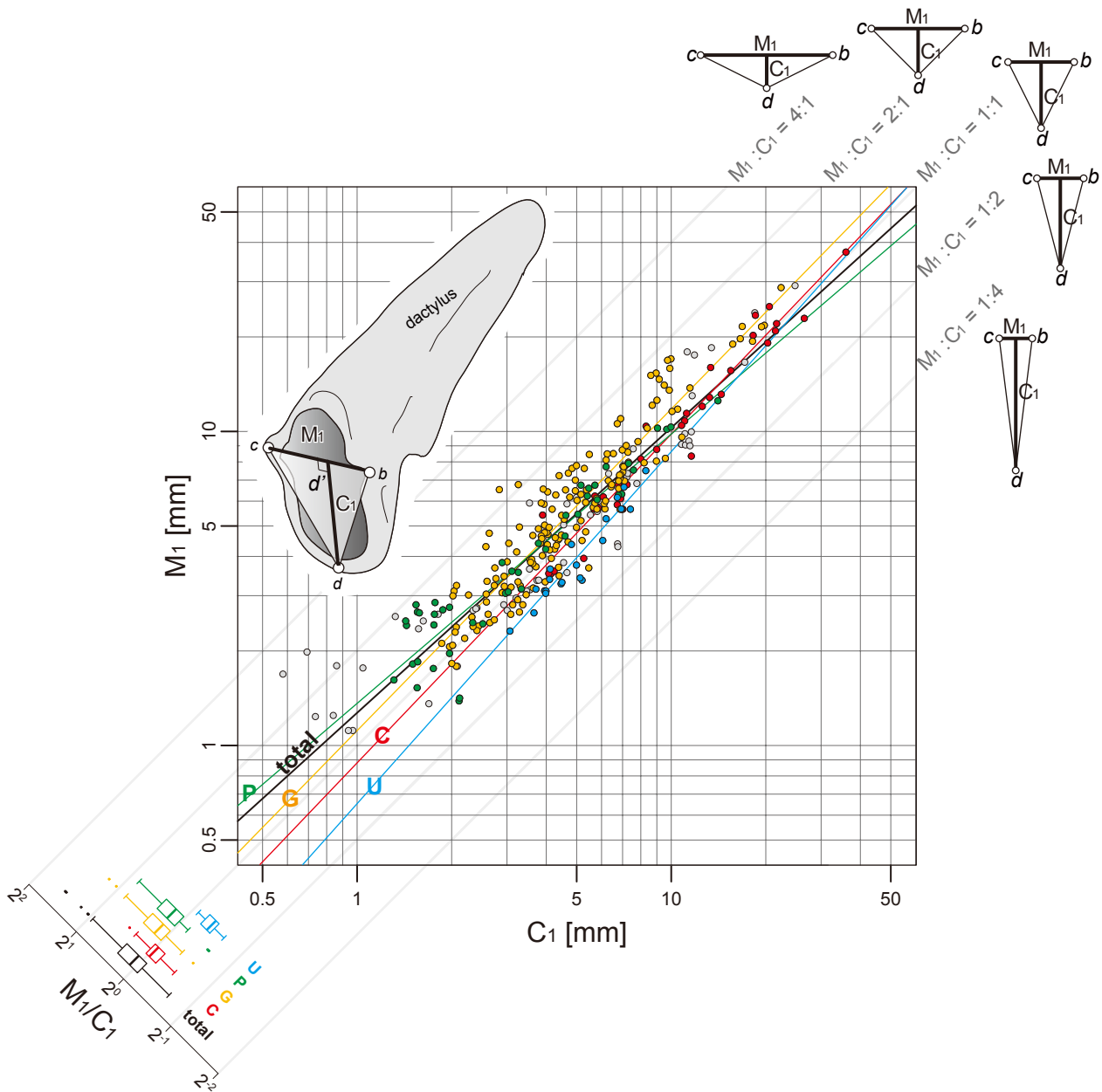


Fig. 5. Relationship between the moment arms of the closer muscle (C_1) and the articular membrane (M_1) of the proximal dactylus in the studied specimens. Regression lines are drawn for all the studied chelae (total) and each functional category (C, G, P, and U: see Table 3). The boxplots of the aspect ratio (C_1/M_1) are shown for the categories (total, C, G, P, and U) as well. See Figs. 1 and 2 for the abbreviations of the landmarks.

TABLE S1. A table of the studied specimens and measurement data of the claws. Family; species; specimen number; sex (♂, male; ♀, female); body mass (BM [g]); carapace size (CS [mm²]); side of the chela (L, major; S, minor); function of the chela (Fn: C, crushing/wedging; G, gripping; P, pinching; U, ucine; X, unknown); the dactylus size (DS [mm²]); the propodus size (PS [mm²]); the relative size of the chela (RC: (DS+PS)/CS[%]); moment arms of the closer muscle (C₁ [mm]) and the distal end of the dactylus (C₂ [mm]) about the propodus-dactylus joint, and the pinching efficiency (C₁/C₂[%]); moment arms of the articular membrane (M₁ [mm]) and the distal ends of the dactylus (M_{2L} and M_{2M} [mm]) about the lateral and medial facets of the propodus-dactylus joint, and the passive disarticulation resistance (M₁/M₂[%]); the ratio between C₁ and M₁ (M₁/C₁[%]); and the references for the chelae functions are listed. See the bottom for the abbreviations of the references. Classification of the species is based on Ng et al. (2008).

family	species	specimen	sex	BM	CS	chela	Fn	DS	PS	RC	C ₁	C ₂	C ₁ /C ₂	M ₁	M _{2L}	M _{2M}	M ₁ /M ₂	M ₁ /C ₁	Reference
AXIIDEA																			
Callianassidae	<i>Glypturus acanthochirus</i>	KH103	♂	—	351	L	G	29.9	99.2	36.8	3.63	12.8	28.4	4.68	22.9	20.0	20.4	1.29	D3; S3
						S	P	—	—	—	—	—	—	—	—	—	—	—	—
ASTACIDEA																			
ASTACOIDEA																			
Astacidae	<i>Pacifastacus leniusculus</i>	KPM-NH106516	—	130	2,280	L	G	304	—	—	7.28	42.9	17.0	8.62	44.4	44.6	19.3	1.18	G1, O1
						S	G	159	—	—	3.96	32.6	12.1	5.04	32.6	33.0	15.3	1.27	
Cambaridae	<i>Procambarus clarkii</i>	KPM-NH354	♂	26.2	1,040	L	G	97	172	25.9	6.44	29.1	22.1	6.67	29.7	30.2	22.1	1.04	O1, P2
						S	G	100	165	25.7	6.30	28.8	21.9	6.98	29.2	29.8	23.4	1.11	
	<i>P. clarkii</i>	KH99	♂	10.5	569	L	G	21.4	—	—	2.74	13.2	20.7	3.24	13.4	13.7	23.6	1.18	O1, P2
						S	G	19.9	—	—	2.58	13.1	19.7	3.04	13.3	13.5	22.5	1.18	
	<i>P. clarkii</i>	KH100	♂	10.8	521	L	G	37.4	—	—	3.22	18.1	17.8	4.14	18.4	18.7	22.1	1.29	O1, P2
						S	G	35.4	—	—	3.00	18.4	16.3	3.85	18.6	18.9	20.3	1.28	
NEPHOROIDEA																			
Nephropidae	<i>Homarus gammarus</i>	KH102	♂	—	—	L	C	627	—	—	20.3	57.7	35.2	19.2	58.5	61.0	31.4	0.945	S2; Y1
						S	X	553	—	—	11.8	71.4	16.6	17.6	72.0	73.8	23.8	1.48	
ANOMURA																			
Coenobitidae	<i>Birgus latro</i>	KH101	♂	620	4,270	L	G	381	896	29.9	15.7	40.1	39.2	19	44.5	45.0	42.3	1.21	R1; W1
						S	G	181	623	18.8	10.5	30.6	34.2	11.8	32.9	33.4	35.3	1.13	
	<i>B. latro</i>	KPM-NH141574	♀	173	4,760	L	G	135	363	10.5	10.1	23.3	43.3	11.6	26.0	26.3	44.2	1.15	R1; W1
						S	G	80.3	306	8.11	7.02	21.6	32.4	7.42	23.7	23.6	31.4	1.06	
	<i>Coenobita brevimanus</i>	NSMT-Cr.10289	♂	29.3	602	L	G	43.2	—	—	6.80	13.1	51.9	6.59	13.7	14.7	44.9	0.969	B1; H1
						S	G	12.7	—	—	3.63	7.97	45.6	3.18	10.5	9.60	30.2	0.875	
Lithodidae	<i>Lithodes couesi</i>	KPM-NH109042	♀	506	21,000	L	C	354	942	6.18	13.4	44.1	30.3	16	49.8	48.9	32.2	1.20	S2; V3
						S	G	206	461	3.18	6.89	37.3	18.5	11	43.1	41.7	25.6	1.60	
	<i>Paralomis hystrix</i>	KH105	♂	705	21,200	L	C	622	1,350	9.31	20.5	49.7	41.3	25	55.9	56.2	44.5	1.22	C3; S2
						S	G	292	762	4.97	9.86	43.0	22.9	13.6	45.5	46.0	29.5	1.38	
BRACHYURA																			
PROTOTREMATA																			
DROMIOIDEA																			
Dromiidae	<i>Lauridromia dehaani</i>	KPM-NH101140	♀	110	5,540	L	X	39.4	165	3.69	6.74	18.0	37.6	4.39	18.1	18.6	23.6	0.651	—
						S	X	39.1	145	3.32	6.76	18.2	37.2	4.3	18.2	18.7	23.0	0.636	
	<i>L. intermedia</i>	KPM-NH8	♂	40.4	2,210	L	X	46.2	139	8.36	5.90	15.7	37.7	5.9	17.3	17.2	34.1	1.00	—
						S	X	43.4	132	7.92	5.80	15.6	37.3	5.58	16.8	16.9	33.0	0.961	
Dynomenidae	<i>Dynomene pilumnoides</i>	KPM-NH101091	♂	2.65	572	L	X	23.2	47.4	12.3	4.54	12.1	37.5	3.83	13.0	13.1	29.3	0.843	—
						S	X	21.5	48.9	12.3	4.66	12.1	38.6	3.56	12.5	12.8	27.8	0.764	

TABLE S1 (cont.)

family	species	specimen	sex	BM	CS	chela	Fn	DS	PS	RC	C ₁	C ₂	C ₁ /C ₂	M ₁	M _{2L}	M _{2M}	M ₁ /M ₂	M ₁ /C ₁	Reference	
HOMOLOIDEA																				
Homolidae	<i>Paromola japonica</i>	KPM-NH0162161	♀	—	6,820	L	G	123	471	8.72	7.02	31.7	22.2	7.76	34.3	34.0	22.7	1.11	C2; S2	
						S	G	106	468	8.42	8.21	26.5	31.0	7.96	34.5	32.1	23.1	0.97		
	<i>P. macrochira</i>	NUM unnumbered	♀	827	14,900	L	G	662	1,900	17.2	19.8	60.6	32.7	21.9	65.9	66.2	33.0	1.10	C2; S2	
						S	G	646	1,850	16.7	19.4	59.8	32.4	21.6	65.9	65.6	32.8	1.11		
RANINOIDEA																				
Raninidae																				
(Lyreidinae)	<i>Lyreidus stenops</i>	KPM-NH140088	♀	13.3	1,060	L	G	15.1	20.7	3.36	2.03	9.69	21.0	3.11	9.93	10.3	30.3	1.53	S2	
(Ranininae)	<i>Ranina ranina</i>	KPM-NH102036	♂	10.6	1,520	L	G	9.45	41.9	3.39	2.07	10.6	19.6	1.79	10.7	10.8	16.6	0.864	B2; S2	
						S	G	8.93	37.3	3.04	2.00	9.76	20.5	1.83	10.7	10.5	17.1	0.915		
	<i>R. ranina</i>	KPM-NH186	♀	188	7,750	L	G	71.4	—	—	4.56	27.1	16.8	5.27	27.9	28.1	18.8	1.16	B2; S2	
						S	G	57.9	—	—	4.69	26.0	18.1	4.46	28.5	28.1	15.7	0.95		
EUBRACHYURA																				
HETEROTREMATA																				
CALAPPOIDEA																				
Calappidae																				
	<i>Calappa gallus</i>	KPM-NH103158	♂	16.3	1,770	L	C	41.2	97.6	7.83	6.90	13.5	51.2	6.12	14.9	15.0	40.7	0.887	S4	
						S	G	28.6	91.5	6.78	3.83	13.0	29.6	4.42	14.2	14.1	31.2	1.15		
	<i>Ca. hepatica</i>	KPM-NH103245	♂	17.1	2,390	L	C	42.6	120	6.81	7.01	15.0	46.6	5.67	16.7	16.6	34.0	0.809	S4	
						S	G	24.7	120	6.02	3.56	12.6	28.1	3.91	13.8	13.7	28.4	1.10		
	<i>Ca. japonica</i>	KPM-NH103159	♂	52.3	4,570	L	C	126	318	9.71	11.2	22.0	50.9	11.4	25.3	25.1	45.2	1.02	S4	
						S	G	95.7	290	8.43	6.98	21.8	32.0	8.76	24.1	24.1	36.3	1.25		
	<i>Ca. lophos</i>	KH33	♂	209	9,830	L	C	209	587	8.10	13.2	32.6	40.7	12.9	36.2	36.0	35.5	0.97	S4	
						S	G	169	572	7.54	8.38	32.9	25.5	10.3	35.2	35.4	29.0	1.23		
	<i>Ca. lophos</i>	KH34	♂	126	6,220	L	C	147	431	9.30	11.0	27.2	40.6	10.8	29.7	29.9	36.1	0.98	S4	
						S	G	113	391	8.09	6.54	26.5	24.7	8.52	28.0	28.4	30.0	1.30		
	<i>Ca. lophos</i>	KPM-NH103068	♂	—	8,240	X	X	127	430	6.75	7.57	28.7	26.4	8.83	30.2	30.6	28.9	1.17	S4	
	<i>Ca. philargius</i>	KPM-NH103611	♂	23.7	2,160	L	C	53.5	135	8.74	7.23	15.8	45.9	6.78	17.8	17.6	38.1	0.937	S4	
						S	G	36.1	128	7.58	4.09	14.6	28.1	4.96	16.2	16.0	30.7	1.21		
	<i>Cycloes granulosa</i>	KPM-NH130805	♂	114	1,130	L	C	20.2	—	—	4.15	12.4	33.5	3.54	12.8	13.1	27.1	0.852	V2	
						S	G	22.0	—	—	2.59	12.1	21.4	3.34	12.2	12.6	26.5	1.29		
	<i>Mursia armata</i>	KPM-NH103119	♂	9.32	1,310	L	C	18.7	51.8	5.40	4.24	10.4	40.8	3.6	11.1	11.2	32.1	0.849	V2	
						S	G	14.2	45.1	4.54	3.13	10.1	30.9	2.81	10.7	10.8	26.1	0.898		
	<i>M. aspera</i>	KPM-NH103460	♂	7.60	898	L	G	15.9	69.2	9.47	2.02	10.6	19.1	3	11.3	11.3	26.5	1.49	V2	
						S	C	20.1	46.7	7.44	4.08	11.4	35.9	3.54	12.1	12.2	29.0	0.868		
	<i>M. curtispina</i>	KPM-NH103320	♂	24.3	2,640	L	C	46.8	110	5.94	6.07	15.1	40.2	6.21	16.6	16.7	37.2	1.02	V2	
						S	G	30.8	117	5.61	3.89	15.3	25.5	4.03	16.5	16.4	24.4	1.04		
	<i>M. trispinosa</i>	KPM-NH103198	♂	32.4	2,980	L	C	31.6	93.3	4.18	5.26	16.0	32.9	3.95	17.1	17.1	23.1	0.751	V2	
						S	G	25.9	96.1	4.09	5.46	14.1	38.8	3.68	16.9	16.1	21.8	0.674		

TABLE S1 (cont.)

family	species	specimen	sex	BM	CS	chela	Fn	DS	PS	RC	C ₁	C ₂	C ₁ /C ₂	M ₁	M _{2L}	M _{2M}	M ₁ /M ₂	M ₁ /C ₁	Reference	
Matutidae	<i>Ashorea banksii</i>	KPM-NH103094	♂	12.9	2,050	L	G	20.7	63.7	4.12	3.97	12.4	32.0	3.33	12.9	13.1	25.4	0.838	S4	
						S	G	21.0	36.0	2.79	4.40	12.1	36.4	3.48	12.7	12.9	27.1	0.791		
	<i>A. miersii</i>	NSMT-Cr.10062	♂	7.17	1,040	L	G	10.7	—	—	2.32	8.35	27.8	2.57	8.87	8.95	28.7	1.11	P1	
						S	G	9.54	—	—	2.41	8.19	29.4	2.33	9.22	9.02	25.3	0.968		
	<i>Matuta lunaris</i>	KH80	♂	7.63	1,020	L	G	9.48	—	—	2.44	7.87	31.0	2.41	8.43	8.46	28.5	0.989	P1	
						S	G	6.18	—	—	2.20	5.62	39.2	2.2	5.67	6.04	36.4	1.00		
	<i>M. lunaris</i>	KPM-NH103244	♂	4.20	1,200	S	G	10.0	29.2	3.26	2.65	8.10	32.7	2.47	9.18	8.96	26.9	0.932	P1	
						L	G	11.1	28.9	3.32	2.73	8.77	31.2	2.52	9.22	9.33	27.0	0.922		
<i>M. lunaris</i>	KPM-NH130813	♂	53.0	3,900	L	G	49.6	—	—	5.64	17.2	32.7	5.75	19.4	19.0	29.7	1.02	P1		
					S	G	45.1	—	—	6.15	15.9	38.7	5.68	19.3	18.3	29.4	0.923			
<i>M. lunaris</i>	NSMT-Cr.3045	♂	40.7	3,840	L	G	48.2	—	—	5.80	17.0	34.0	5.66	19.9	19.2	28.5	0.976	P1		
					S	G	46.2	—	—	5.72	15.6	36.8	5.93	19.1	18.0	31.1	1.04			
<i>M. lunaris</i>	NSMT-Cr.3052	♂	15.5	1,750	L	G	27.7	—	—	4.02	12.8	31.4	4.33	13.9	13.9	31.1	1.08	P1		
					S	G	23.0	—	—	4.25	10.9	39.2	4.23	14.0	12.9	30.2	0.994			
CANCROIDEA																				
Cancridae	<i>Anatolikos japonicus</i>	KPM-NH105093	♂	83.2	5,910	L	X	117	382	8.44	10.8	25.8	41.9	9.11	26.4	27.5	33.1	0.845	—	
						S	X	116	347	7.83	11.1	25.4	43.7	9.09	27.0	27.5	33.0	0.819		
	<i>A. japonicus</i>	NSMT-Cr.7612	♂	132	6,920	L	X	141	—	—	11.6	28.2	41.1	10	28.8	30.1	33.3	0.863	—	
<i>A. japonicus</i>	NSMT-Cr.8239	♂	112	6,120	S	X	129	—	—	11.1	26.2	42.2	9.86	29.0	28.9	34.0	0.892	—		
					L	X	122	—	—	11.4	26.1	43.6	9.34	27.7	28.2	33.1	0.821	—		
						S	X	110	—	—	11.5	24.4	46.9	9.02	26.0	26.5	34.0	0.787		
CARPILIOIDEA																				
Carpiliidae	<i>Carpilius convexus</i>	KPM-NH107704	♂	112	4,410	L	C	86.9	285	8.45	11.6	20.8	55.7	8.36	21.8	22.6	36.9	0.721	L1; V2	
						S	G	69.3	201	6.14	7.10	19.9	35.7	6.97	20.6	21.3	32.8	0.982		
DORIPPOIDEA																				
Dorippidae	<i>Dorippe sinica</i>	KPM-NH103562	♂	6.50	824	L	X	14.8	31.1	5.56	1.81	11.3	16.0	2.62	11.4	11.6	22.5	1.45	—	
						S	X	14.4	30.5	5.45	1.62	11.5	14.1	2.5	11.7	11.9	21.1	1.54		
	<i>Heikeopsis japonica</i>	KH49	♂	10.3	596	L	X	16.2	40.7	9.56	3.79	9.63	39.3	3.37	10.2	10.4	32.5	0.89	—	
						S	X	9.01	17.5	4.45	0.69	9.06	7.65	1.99	9.77	9.69	20.4	2.87		
	<i>H. japonica</i>	KH50	♂	9.34	615	L	X	11.6	33.4	7.31	3.55	7.39	48.0	3.14	8.09	8.18	38.4	0.885	—	
						S	X	5.83	13.7	3.17	1.04	6.58	15.8	1.77	6.66	6.85	25.8	1.70		
	<i>H. japonica</i>	KH51	♂	9.80	600	L	X	12.9	39.6	8.75	3.47	8.30	41.8	3.11	8.99	9.07	34.3	0.896	—	
						S	X	7.35	12.7	3.34	0.86	8.16	10.5	1.8	8.43	8.51	21.2	2.09		
<i>H. japonica</i>	KH52	♂	10.9	610	L	X	13.0	31.4	7.28	3.33	8.23	40.5	3.15	8.58	8.90	35.4	0.946	—		
					S	X	7.02	19.3	4.32	0.58	8.30	6.99	1.69	8.44	8.55	19.8	2.91			
<i>H. japonica</i>	KH53	♀	23.4	1,240	L	X	18.1	—	—	1.33	14.1	9.43	2.58	14.2	14.4	17.9	1.95	—		
					S	X	15.6	48.3	5.15	1.57	13.2	11.9	2.36	13.8	13.8	17.1	1.50			

TABLE S1 (cont.)

family	species	specimen	sex	BM	CS	chela	Fn	DS	PS	RC	C ₁	C ₂	C ₁ /C ₂	M ₁	M _{2L}	M _{2M}	M ₁ /M ₂	M ₁ /C ₁	Reference
ERIPHIOIDEA																			
Hypothalassidae	<i>Hypothalassia armata</i>	KPM-NH106818	♀	568	14,400	L	X	410	876	8.94	17.1	49.3	34.7	16.6	51.7	52.9	31.5	0.971	—
						S	X	285	615	6.26	11.7	43.7	26.7	13	45.5	46.3	28.1	1.12	
Menippidae	<i>Pseudocarcinus gigas</i>	NSMT-Cr.15903	♂	3,070	45,800	L	C	2380	—	—	35.9	127	28.2	37.3	138	137	27.1	1.04	C5
						S	G	1160	—	—	22.3	80.5	27.7	28.8	85.0	86.9	33.1	1.29	
Oziidae	<i>Baptozius vinosus</i>	KH66	♂	119	3,530	L	C	167	436	17.1	10.8	31.8	33.9	10.5	35.2	34.8	29.8	0.971	V2
						S	G	102	276	10.7	5.00	26.2	19.1	7.79	27.2	27.7	28.1	1.56	
						L	C	231	317	13.5	12.6	38.3	32.8	12.1	39.8	40.7	29.6	0.959	
S	G	124	317	10.8	6.20	30.5	20.3	8.12	32.2	32.4	25.1	1.31							
GONEPLACOIDEA																			
Goneplacidae	<i>Carcinoplax longimana</i>	TMNH unnumbered	♀	68.0	2,530	L	X	—	—	—	6.32	25.0	25.3	7.35	26.0	26.5	27.8	1.16	—
						S	X	—	—	—	5.00	24.1	20.7	6.17	24.9	25.3	24.4	1.23	
LEUCOSIOIDEA																			
Leucosiidae	<i>Arcania heptacantha</i>	KH59	♀	2.85	672	L	X	7.04	11.1	2.70	0.84	11.3	7.44	1.25	13.2	12.9	9.45	1.49	—
						S	X	7.95	8.88	2.51	0.74	12.8	5.75	1.24	13.1	13.1	9.48	1.68	
	<i>A. heptacantha</i>	KH60	♀	3.22	747	L	X	6.95	26.5	4.48	0.97	12.4	7.80	1.12	12.5	12.5	8.94	1.16	—
						S	X	6.76	25.1	4.27	0.94	12.1	7.76	1.12	12.7	12.7	8.80	1.20	
	<i>Myra fugax</i>	KH54	♂	12.6	1,150	L	P	19.1	94.9	9.92	1.76	15.7	11.2	2.43	15.7	15.9	15.3	1.38	C4
						S	P	18.6	91.7	9.61	1.43	15.4	9.31	2.42	15.4	15.6	15.5	1.69	
	<i>M. fugax</i>	KH55	♂	16.0	1,280	L	P	26.3	114	10.9	1.77	18.4	9.61	2.86	18.7	18.8	15.2	1.62	C4
						S	P	24.1	111	10.5	1.56	18.1	8.61	2.67	18.6	18.6	14.3	1.72	
	<i>M. fugax</i>	KH56	♂	13.7	1,110	L	P	22.9	97.5	10.8	1.58	17.3	9.11	2.65	17.3	17.5	15.1	1.68	C4
						S	P	19.2	47.5	5.99	1.43	15.4	9.29	2.5	15.8	15.9	15.7	1.75	
	<i>M. fugax</i>	KH57	♂	7.18	811	L	P	11.5	43.2	6.75	1.50	12.7	11.9	1.82	12.8	12.9	14.1	1.21	C4
						S	P	7.96	33.7	5.14	1.55	10.4	14.9	1.53	10.5	10.5	14.5	0.986	
	<i>M. fugax</i>	KH58	♂	15.9	1,290	L	P	23.5	113	10.5	1.54	16.7	9.22	2.81	16.7	17.0	16.6	1.82	C4
						S	P	21.4	110	10.2	1.77	16.3	10.8	2.62	16.4	16.6	15.8	1.48	
	<i>M. fugax</i>	KPM-NH103565	♂	12.4	1,160	L	P	22.2	86.3	9.39	1.87	16.4	11.4	2.71	16.8	16.9	16.0	1.45	C4
						S	P	22.7	82.4	9.10	1.97	16.4	12.0	2.76	16.5	16.7	16.5	1.40	
	<i>Persephona aquilonaris</i>	KPM-NH103254	♀	2.15	1,760	L	X	23.0	77.2	5.69	2.93	16.3	17.9	2.81	16.6	16.8	16.8	0.959	—
S						X	24.3	71.4	5.43	3.20	16.4	19.5	2.95	17.2	17.2	17.1	0.921		
<i>Philyra pisum</i>	KH21	♂	3.66	374	L	P	5.72	21.1	7.18	2.11	8.24	25.7	1.39	8.24	8.35	16.6	0.658	K3	
					S	P	5.56	19.9	6.81	2.12	7.83	27.1	1.42	7.89	7.99	17.8	0.67		
MAJOIDEA																			
Epialtidae	<i>Goniopugettia sagamiensis</i>	TMNH unnumbered	♂	—	2,820	L	P	—	—	—	6.95	22.9	30.3	6.34	23.3	23.9	26.5	0.912	D2
						S	P	—	—	—	6.80	23.4	29.1	6.27	23.9	24.5	25.6	0.922	
Inachidae	<i>Macrocheira kaempferi</i>	KPM-NH104714	♀	182	12,600	L	P	69.2	317	3.05	4.61	25.6	18.1	5.42	26.4	26.6	20.4	1.18	U1
						S	P	68.4	309	2.98	5.04	25.0	20.1	5.46	25.9	26.1	20.9	1.08	

TABLE S1 (cont.)

family	species	specimen	sex	BM	CS	chela	Fn	DS	PS	RC	C ₁	C ₂	C ₁ /C ₂	M ₁	M _{2L}	M _{2M}	M ₁ /M ₂	M ₁ /C ₁	Reference	
Majidae	<i>Maja spinigera</i>	KPM-NH104423	♂	94.9	8,900	L	X	91.0	269	4.04	7.21	25.4	28.4	7.17	26.7	27.0	26.6	0.994	—	
						S	X	91.3	267	4.03	7.27	24.8	29.3	7.37	26.9	26.8	27.4	1.01	—	
Oregoniidae	<i>Chionoecetes japonicus</i>	KPM-NH1024172	♀	231	8,560	L	G	106	290	4.62	2.83	32.3	8.78	6.55	32.5	33.1	19.8	2.31	W2	
						S	G	102	185	3.36	4.04	31.7	12.8	6.44	32.0	32.5	19.8	1.59	—	
		<i>C. opilio</i>	KH75	—	—	—	X	G	434	—	—	8.95	56.5	15.8	15.4	58.6	59.5	25.8	1.72	W2
		<i>C. opilio</i>	KH76	—	—	—	X	G	516	—	—	9.98	60.3	16.5	17.1	62.4	63.6	26.9	1.71	W2
		<i>C. opilio</i>	KH77	—	—	—	X	G	362	—	—	9.17	49.2	18.6	14.7	50.6	51.9	28.3	1.60	W2
		<i>C. opilio</i>	KH78	—	—	—	X	G	373	780	—	8.60	49.3	17.5	15.1	50.4	52.0	29.1	1.76	W2
		<i>C. opilio</i>	KH79	—	—	—	X	G	456	—	—	9.91	57.2	17.3	15.9	58.9	60.2	26.5	1.61	W2
		<i>C. opilio</i>	KPM-NH104454	♀	106	7,560	L	G	99.8	237	4.45	3.91	30.4	12.9	6.56	31.9	32.0	20.5	1.68	W2
						S	G	102	204	4.05	3.26	30.2	10.8	6.79	31.2	31.5	21.6	2.08	—	
PARTHENOPOIDEA																				
Parthenopidae																				
(Daldophinae)	<i>Daldorfia horrida</i>	KPM-NH104909	♂	340	11,600	X	C	646	—	—	26.5	56.3	47.2	23	58.0	61.1	37.6	0.866	H3; V2	
						X	G	—	—	—	—	—	—	—	—	—	—	—	—	—
(Parthenopinae)	<i>D. investigatoris</i>	KPM-NH104896	♂	5.63	1,210	L	X	48.4	123	14.2	7.77	14.1	55.0	6.85	14.3	15.7	43.6	0.881	H3; V2	
						S	X	44.2	135	15.9	3.54	14.9	23.7	5.92	15.5	16.2	36.6	1.67	—	
	<i>Enoplolambrus validus</i>	KH48	♂	22.7	1,130	L	X	43.3	138	16.1	4.66	14.7	31.7	5.89	15.9	16.1	36.5	1.26	K4	
						S	X	44.2	135	15.9	3.54	14.9	23.7	5.92	15.5	16.2	36.6	1.67	—	
	<i>E. validus</i>	KPM-NH104431	♀	89.6	4,690	L	C	215	430	13.7	14.4	32.6	44.2	13.2	35.6	35.9	36.6	0.913	K4	
	<i>E. laciniatus</i>	NSMT-Cr.13118	♀	9.75	732	L	X	33.3	—	—	5.54	12.2	45.2	5.44	12.4	13.4	40.5	0.982	—	
						S	X	17.8	—	—	3.74	10.6	35.3	3.36	10.6	11.1	30.2	0.899	—	
PORTUNOIDEA																				
Geryonidae																				
	<i>Chaceon granulatus</i>	KPM-NH106820	♀	637	25,000	L	X	512	1,080	6.36	13.4	55.4	24.3	18.5	58.0	59.3	31.2	1.38	—	
						S	X	470	1,070	6.18	11.2	52.4	21.5	18	54.6	56.1	32.0	1.60	—	
Portunidae																				
(Carcininae)	<i>Carcinus aestuarii</i>	TMNH unnumbered	♂	44.0	2,550	L	C	—	—	—	6.78	17.9	37.9	6.77	18.8	19.4	34.9	0.999	E1; E2	
						S	G	—	—	—	4.48	17.1	26.2	5.41	18.3	18.4	29.4	1.21	—	
(Carupinae)	<i>Carupa tenuipes</i>	NSMT-Cr.3405	♂	15.0	1,000	L	X	45.9	—	—	5.93	15.0	39.5	6.12	16.6	16.6	36.9	1.03	—	
						S	X	38.7	—	—	4.55	15.3	29.7	5.06	15.9	16.3	31.0	1.11	—	
(Polybiinae)	<i>Ovalipes punctatus</i>	KPM-NH106360	♀	10.9	1,870	L	C	50.1	113	8.68	3.90	18.5	21.1	5.43	19.6	19.7	27.5	1.39	L1; P3	
						S	G	44.7	94.7	7.44	3.29	18.0	18.3	4.97	18.8	19.0	26.1	1.51	—	
(Portuninae)	<i>Lupella forceps</i>	NSMT-Cr.7144	♂	15.2	2,120	L	X	84.6	—	—	2.41	61.5	3.92	2.75	62.2	62.2	4.42	1.14	—	
						S	X	82.4	—	—	2.34	61.0	3.83	2.7	61.9	61.9	4.36	1.15	—	
	<i>L. forceps</i>	NSMT-Cr.7641	♂	12.6	1,950	X	X	44.1	—	—	2.39	32.3	7.40	2.73	43.3	42.2	6.30	1.14	—	
	<i>Portunus (Portunus) pelagicus</i>	KH23	♂	22.5	4,240	L	G	101	236	7.94	6.91	27.6	25.1	7.31	28.0	28.7	25.5	1.06	J1; W3	
						S	G	88.7	226	7.42	4.76	28.7	16.6	6.19	29.0	29.5	21.0	1.30	—	
	<i>P. (P.) pelagicus</i>	KH24	♂	52.6	8,320	L	G	294	730	12.3	8.70	48.4	18.0	12.2	48.6	50.0	24.3	1.40	J1; W3	
						S	G	268	527	9.56	6.74	50.5	13.4	10.6	50.8	51.8	20.5	1.57	—	

TABLE S1 (cont.)

family	species	specimen	sex	BM	CS	chela	Fn	DS	PS	RC	C ₁	C ₂	C ₁ /C ₂	M ₁	M _{2L}	M _{2M}	M ₁ /M ₂	M ₁ /C ₁	Reference
(Portuninae [cont.])	<i>Portunus (Portunus) pelagicus</i>	KH25	♀	—	4,700	L	G	—	218	—	5.17	—	—	6.41	—	—	—	1.24	J1; W3
						S	G	95.9	194	6.18	6.85	26.3	26.0	7.28	26.6	27.4	26.5	1.06	
	<i>P. (P.) pelagicus</i>	KH26	♂	—	1,080	X	G	15.8	—	—	2.07	9.74	21.3	3.24	9.74	10.3	31.6	1.56	J1; M1
						S	G	80.3	244	4.92	4.61	24.6	18.7	6.53	26.3	26.3	24.8	1.42	
	<i>P. (P.) sanguinolentus</i>	KPM-NH106908	♀	62.1	6,590	L	G	105	278	5.81	6.26	24.6	25.4	8.51	26.1	26.6	32.0	1.36	J1; M1
						S	G	80.3	244	4.92	4.61	24.6	18.7	6.53	26.3	26.3	24.8	1.42	
	<i>P. (P.) trituberculatus</i>	KH35	♂	62.8	5,570	L	G	76.0	196	4.88	6.12	25.8	23.7	5.9	26.6	26.9	21.9	0.965	J1; M1
						S	G	41.1	87.4	2.31	3.05	18.6	16.4	4.42	18.6	19.1	23.1	1.45	
	<i>P. (P.) trituberculatus</i>	KH36	♂	56.9	4,910	L	G	77.6	200	5.65	5.79	25.3	22.9	6.14	26.3	26.5	23.2	1.06	J1; M1
						S	G	76.2	119	3.96	3.86	25.7	15.0	5.93	26.3	26.7	22.2	1.54	
	<i>P. (P.) trituberculatus</i>	KH37	♂	62.6	5,310	L	G	92.1	193	5.37	6.45	27.2	23.7	6.78	27.7	28.3	24.0	1.05	J1; M1
						S	G	83.6	160	4.59	4.95	25.8	19.2	6.48	26.3	26.8	24.1	1.31	
	<i>P. (P.) trituberculatus</i>	KH38	♂	102	7,100	L	G	113	275	5.48	6.80	32.6	20.9	6.97	32.7	33.4	20.9	1.02	J1; M1
						S	G	120	165	4.02	4.71	32.5	14.5	7.38	33.3	33.8	21.9	1.57	
	<i>P. (P.) trituberculatus</i>	KH39	♂	84.4	7,740	L	G	125	171	3.83	7.06	32.3	21.9	7.75	32.9	33.5	23.1	1.10	J1; M1
						S	G	127	169	3.83	4.83	33.2	14.5	7.64	33.7	34.4	22.2	1.58	
	<i>P. (P.) trituberculatus</i>	KH40	♂	765	6,720	X	G	102	229	4.93	4.96	29.2	17.0	7.01	29.9	30.4	23.1	1.41	J1; M1
						S	G	124	311	6.03	7.31	31.0	23.6	7.99	31.1	32.0	24.9	1.09	
	<i>P. (P.) trituberculatus</i>	KH41	♂	45.8	7,220	X	G	124	311	6.03	7.31	31.0	23.6	7.99	31.1	32.0	24.9	1.09	J1; M1
						S	G	85.4	195	4.60	5.38	26.2	20.6	6.53	26.6	27.2	24.0	1.21	
<i>P. (P.) trituberculatus</i>	KH42	♂	65.1	6,090	L	G	85.4	195	4.60	5.38	26.2	20.6	6.53	26.6	27.2	24.0	1.21	J1; M1	
					S	G	84.0	180	4.34	4.30	26.7	16.1	6.29	27.0	27.6	22.8	1.46		
<i>Scylla paramamosain</i>	NSMT-Cr.19947	♀	720	19,400	L	C	370	—	—	15.5	47.2	32.8	15.7	48.1	50.0	31.3	1.01	L1	
					S	G	321	—	—	9.51	45.6	20.9	14.1	48.2	48.8	28.9	1.48		
<i>S. serrata</i>	KH65	♂	184	7,700	S	C	156	386	7.04	8.31	30.0	27.7	10.4	32.1	32.4	32.1	1.25	L1	
					L	X	760	2,400	14.3	18.4	63.5	29.0	23.9	67.5	69.0	34.7	1.30		
<i>S. serrata</i>	KH83	♂	1,900	22,200	S	X	1060	1,500	11.6	24.8	72.5	34.2	29.2	77.5	79.3	36.8	1.18	L1	
					L	C	631	1,500	12.9	21.7	57.1	37.9	22.1	61.5	62.4	35.4	1.02		
<i>S. serrata</i>	KPM-NH107270	♂	581	16,600	S	G	567	1,370	11.7	18.1	58.5	31.0	19.4	61.1	62.5	31.0	1.07	L1	
					L	C	613	—	—	18.2	60.5	30.2	20.3	65.0	65.4	31.0	1.11		
<i>S. serrata</i>	KPM-NH98	♂	573	15,400	L	C	613	—	—	9.73	51.6	18.9	16.9	55.8	55.9	30.2	1.74	L1	
					S	G	435	—	—	18.5	56.2	33.0	23.5	59.4	61.5	38.2	1.27		
<i>S. serrata</i>	NSMT-Cr.14835	♂	593	15,500	L	C	660	—	—	16.8	55.5	30.3	21.6	58.5	60.3	35.9	1.29	L1	
					S	G	600	—	—	21.5	52.8	40.7	20.9	55.3	57.4	36.5	0.973		
<i>S. serrata</i>	NSMT-Cr.16848	♂	650	16,000	L	C	553	—	—	16.6	52.6	31.5	19.8	57.8	57.8	34.2	1.19	L1	
					S	G	520	—	—	16.6	52.6	31.5	19.8	57.8	57.8	34.2	1.19		
(Thalamitinae)	<i>Charybdis japonica</i>	KH43	♂	79.3	3,760	L	G	115	262	10.0	7.18	25.5	28.2	9.05	27.5	27.7	32.6	1.26	J1
						S	G	108	238	9.20	5.28	28.2	18.7	7.65	29.6	29.9	25.6	1.45	
	<i>Ch. japonica</i>	KH44	♂	74.1	4,130	L	G	130	119	6.01	5.48	30.6	17.9	8.48	31.5	32.2	26.4	1.55	J1
						S	G	92.8	101	4.68	4.40	25.6	17.2	7.25	27.1	27.3	26.6	1.65	
	<i>Ch. japonica</i>	KH45	♀	33.2	2,170	L	G	47.7	101	6.86	5.16	18.3	28.2	5.21	18.4	19.1	27.3	1.01	J1
						S	G	40.8	95.7	6.28	2.63	17.2	15.3	4.75	18.3	18.4	25.9	1.8	

TABLE S1 (cont.)

family	species	specimen	sex	BM	CS	chela	Fn	DS	PS	RC	C ₁	C ₂	C ₁ /C ₂	M ₁	M _{2L}	M _{2M}	M ₁ /M ₂	M ₁ /C ₁	Reference	
(Thalamitinae [cont.])	<i>Charybdis japonica</i>	KH46	♀	82.8	4,920	X	G	139	247	7.86	7.83	29.9	26.2	9.31	30.8	31.7	29.4	1.19	J1	
						X	G	44.6	—	—	—	—	—	—	—	—	—	—	—	—
	<i>C. japonica</i>	KH47	♀	40.2	—	X	G	62.9	137	—	3.93	21.4	18.4	5.88	22.2	22.6	26.1	1.50	J1	
						X	G	—	—	—	—	—	—	—	—	—	—	—	—	—
	<i>C. japonica</i>	KH61	♂	33.9	813	L	G	16.2	52.6	8.47	3.37	11.5	29.2	2.81	11.9	12.1	23.3	0.833	J1	
						S	G	14.8	47.1	7.62	2.61	11.3	23.1	2.62	11.5	11.7	22.4	1.00	—	
	<i>C. japonica</i>	KH62	♀	24.5	2,900	X	G	41.2	135	6.06	5.34	17.2	31.1	4.8	17.7	18.1	26.6	0.898	J1	
						X	G	—	—	—	—	—	—	—	—	—	—	—	—	—
	<i>C. japonica</i>	KH63	♀	36.7	2,320	L	G	70.4	156	9.74	6.87	19.8	34.6	7.1	20.9	21.4	33.2	1.03	J1	
						S	G	54.7	138	8.30	4.18	19.3	21.6	5.66	19.7	20.3	27.9	1.35	—	
<i>C. japonica</i>	KH64	♀	14.9	1,050	L	G	23.9	59.9	8.00	2.74	13.0	21.2	3.69	13.7	13.8	26.8	1.34	J1		
					S	G	23.5	34.2	5.51	4.38	12.7	34.4	3.7	13.3	13.5	27.5	0.845	—		
<i>C. japonica</i>	KPM-NH107793	♂	13.5	5,140	L	G	250	496	14.5	11.5	36.2	31.7	13.8	41.5	40.5	33.2	1.20	J1		
					S	G	250	481	14.2	9.00	39.8	22.6	12.6	42.3	42.7	29.5	1.40	—		
<i>Thalmita crenata</i>	KPM-NH539	♀	34.3	2,460	L	G	67.2	158	9.17	5.01	22.2	22.6	6.05	23.0	23.4	25.9	1.21	C1		
					S	G	44.3	98.3	5.80	3.95	18.6	21.2	4.77	19.3	19.6	24.4	1.21	—		
POTAMOIDEA																				
Potamidae	<i>Geothelphusa dehaani</i>	KPM-NH106222	♂	5.61	503	L	G	33.8	83.9	23.4	4.05	14.3	28.3	4.72	15.6	15.6	30.3	1.16	K2	
						S	G	12.8	29.3	8.35	2.58	8.90	29.0	2.87	9.61	9.63	29.8	1.11	—	
	<i>G. dehaani</i>	TMNH unnumbered	♂	7.00	540	L	G	—	—	—	4.02	15.1	26.6	4.78	15.6	16.0	29.8	1.19	K2	
						S	G	—	—	—	2.07	7.80	26.5	2.39	8.82	8.62	27.1	1.15	—	
XANTHOIDEA																				
Xanthidae	<i>Atergatis floridus</i>	KPM-NH106520	♂	27.9	1,960	L	C	44.5	134	9.13	5.85	15.6	37.6	5.71	16.4	16.9	33.9	0.975	M4	
						S	G	22.7	61.4	4.29	4.15	11.5	36.1	3.95	12.5	12.5	31.6	0.952	—	
	<i>A. reticulatus</i>	KH28	♂	—	2,120	X	X	44.7	142	8.80	5.99	15.2	39.5	5.89	15.9	16.5	35.8	0.983	M4	
	<i>A. reticulatus</i>	KH29	♀	—	2,540	X	X	47.5	143	7.48	5.90	15.8	37.4	6.03	16.6	17.1	35.3	1.02	M4	
	<i>A. subdentatus</i>	KH31	♂	61.5	4,240	L	C	105	268	8.80	8.01	25.6	31.2	8.2	26.4	27.2	30.1	1.02	M4	
						S	G	103	261	8.60	9.57	25.1	38.1	8.22	26.1	26.8	30.7	0.859	—	
	<i>A. subdentatus</i>	KPM-NH106619	♂	56.6	4,220	L	C	114	258	8.83	8.99	26.0	34.6	8.78	26.6	27.7	31.8	0.977	M4	
						S	G	103	254	8.47	8.96	25.6	35.1	8.07	26.5	27.2	29.7	0.901	—	
THORACOTREMATA																				
GRAPSOIDEA																				
Gecarcinidae	<i>Cardisoma carnifex</i>	KH68	♂	163	4,170	L	P	198	497	16.7	9.68	38.9	24.9	10.2	40.1	40.8	24.9	1.05	M2	
						S	P	91.8	210	7.23	5.16	27.2	19.0	6.76	28.4	28.6	23.6	1.31	—	
	<i>C. carnifex</i>	KH69	♂	131	3,660	L	P	195	322	14.1	9.98	37.7	26.5	10.4	38.9	39.7	26.1	1.04	M2	
						S	P	77.8	226	8.30	5.41	24.9	21.7	6.24	25.6	26.0	24.0	1.15	—	
	<i>C. carnifex</i>	KPM-NH0161668	♂	—	5,260	L	P	289	565	16.2	14.1	46.0	30.6	12.6	49.0	49.1	25.6	0.892	M2	
						S	P	137	335	8.96	7.31	31.8	23.0	7.94	33.8	33.8	23.5	1.09	—	
	<i>C. carnifex</i>	KPM-NH106683	♂	116	4,360	L	P	213	508	16.5	9.04	41.4	21.8	10.3	44.8	44.5	22.9	1.14	M2	
						S	P	95.9	246	7.85	5.46	29.0	18.8	6.61	30.8	30.8	21.5	1.21	—	

TABLE S1 (cont.)

family	species	specimen	sex	BM	CS	chela	Fn	DS	PS	RC	C ₁	C ₂	C ₁ /C ₂	M ₁	M _{2L}	M _{2M}	M ₁ /M ₂	M ₁ /C ₁	Reference
Gecarcinidae (cont.)	<i>Discoplax hirtipes</i>	NSMT-Cr.21715	♂	69.9	2,590	L	P	102	—	—	7.59	27.0	28.1	7.54	27.5	28.2	26.7	0.994	N1
						S	P	93.5	—	—	6.21	24.2	25.7	7.73	26.1	26.2	29.6	1.24	
	<i>D. longipes</i>	NSMT-Cr.14238	♂	48.6	1,920	L	P	37.9	—	—	4.59	16.3	28.2	4.66	17.0	17.2	27.1	1.02	N1
	<i>Epigrapsus notatus</i>	NSMT-Cr.13151	♂	9.98	648	L	P	30.2	—	—	3.78	13.7	27.6	4.41	14.8	14.8	29.7	1.17	L2
						S	P	28.2	—	—	3.99	13.3	29.9	4.23	14.0	14.2	29.7	1.06	
Grapsidae	<i>Pachygrapsus crassipes</i>	KH27	—	—	—	X	G	56.7	162	—	6.18	18.8	32.8	6.02	20.6	20.5	29.2	0.974	B3
Plagusiidae	<i>Plagusia dentipes</i>	NSMT-Cr.14128	♀	39.9	1,900	L	P	16.4	—	—	2.97	10.7	27.8	3.06	10.9	11.2	27.3	1.03	S1
						S	P	16.2	—	—	3.03	10.5	28.9	3.09	11.1	11.2	27.6	1.02	
Sesarmidae	<i>Chiromantes dehaani</i>	KH13	♂	6.41	386	L	G	15.0	34.2	12.8	3.09	9.40	32.9	3.2	10.1	10.2	31.5	1.04	M3
						S	G	14.7	32.0	12.1	3.45	9.70	35.6	3.03	10.3	10.4	29.1	0.878	
	<i>C. dehaani</i>	KH14	♂	14.2	639	L	G	32.6	70.1	16.1	4.27	14.2	30.1	4.6	15.3	15.3	30.0	1.08	M3
						S	G	34.1	67.0	15.8	4.47	14.5	30.8	4.7	15.2	15.5	30.3	1.05	
	<i>C. dehaani</i>	KH15	♀	19.0	923	L	G	23.4	65.5	9.63	3.71	12.6	29.5	3.72	13.1	13.4	27.9	1.00	M3
						S	G	23.4	55.4	8.54	3.62	12.3	29.5	3.81	12.7	13.0	29.3	1.05	
	<i>C. dehaani</i>	KH16	♀	12.7	704	L	G	13.5	45.7	8.41	3.29	10.1	32.5	2.67	11.1	11.0	24.0	0.812	M3
						S	G	12.6	32.6	6.42	3.08	9.61	32.1	2.62	10.4	10.3	25.2	0.849	
	<i>C. haematocheir</i>	KH11	♂	5.85	377	L	G	17.1	30.7	12.7	3.25	10.3	31.7	3.33	10.8	11.0	30.3	1.02	M3
						S	G	15.7	31.3	12.5	2.90	10.2	28.3	3.07	10.4	10.8	28.5	1.06	
	<i>C. haematocheir</i>	KH12	♀	8.69	681	L	G	25.4	55.1	11.8	3.60	13.0	27.7	3.92	13.4	13.7	28.5	1.09	M3
						S	G	23.7	56.2	11.7	3.57	12.3	28.9	3.84	12.4	12.9	29.7	1.08	
	<i>Parasesarma plicatum</i>	KH09	♂	13.2	625	L	G	32.3	59.7	14.7	3.77	13.2	28.7	4.91	15.0	14.7	32.7	1.30	K5
						S	G	30.4	59.4	14.4	3.87	13.3	29.2	4.57	14.5	14.5	31.6	1.18	
	<i>Par. plicatum</i>	KH10	♀	5.83	410	L	G	7.74	19.8	6.70	1.86	7.30	25.5	2.12	7.36	7.62	27.8	1.14	K5
S						G	7.78	18.7	6.45	2.05	6.76	30.4	2.3	7.67	7.50	30.0	1.12		
<i>Sesarmops intermedius</i>	KH20	♂	5.28	355	L	G	18.3	34.7	14.9	2.94	10.5	27.9	3.47	11.1	11.3	30.7	1.18	M3	
					S	G	18.3	33.5	14.6	2.77	10.8	25.7	3.41	11.2	11.5	29.8	1.23		
<i>S. intermedius</i>	KH30	♂	—	816	X	G	—	—	—	2.57	11.6	22.1	4.3	12.6	12.7	33.9	1.67	M3	
Varunidae (Cyclograpsinae)	<i>Helice tridens</i>	KH01	♂	26.0	861	L	G	54.4	147	23.4	5.34	18.3	29.3	5.96	19.8	19.8	30.1	1.12	K5; T1
						S	G	58.3	134	22.3	5.16	18.5	27.9	6.32	19.8	20.0	31.6	1.22	
	<i>Hel. tridens</i>	KH02	♂	13.8	599	L	G	31.1	78.5	18.3	4.36	13.8	31.7	4.52	15.1	15.0	30.0	1.04	K5; T1
						S	G	32.4	65.4	16.3	3.86	13.9	27.8	4.66	14.6	14.9	31.2	1.21	
	<i>Hel. tridens</i>	KH03	♂	5.76	343	L	G	13.4	32.1	13.3	3.25	9.19	35.3	2.92	9.46	9.74	30.0	0.899	K5; T1
						S	G	10.6	28.5	11.4	2.34	8.83	26.5	2.4	9.36	9.4	25.5	1.03	
	<i>Hel. tridens</i>	KH04	♀	15.4	742	L	G	18.1	41.1	7.98	3.31	11.2	29.4	3.23	12.1	12.1	26.7	0.977	K5; T1
S						G	17.7	35.4	7.16	2.94	11.0	26.8	3.22	11.7	11.7	27.4	1.09		
<i>Hel. tridens</i>	KH05	♀	4.73	323	L	G	7.63	16.3	7.41	1.97	7.37	26.7	2.07	7.77	7.84	26.4	1.05	K5; T1	
					S	G	7.50	16.1	7.30	2.02	7.17	28.1	2.09	7.80	7.76	26.8	1.04		

TABLE S1 (cont.)

family	species	specimen	sex	BM	CS	chela	Fn	DS	PS	RC	C ₁	C ₂	C ₁ /C ₂	M ₁	M _{2L}	M _{2M}	M ₁ /M ₂	M ₁ /C ₁	Reference
(Varuninae)	<i>Eriocheir japonica</i>	KH22	♀	460	3,250	L	P	62.0	184	7.56	5.81	20.4	28.5	6.07	22.2	22.1	27.4	1.04	K1
						S	P	71.0	165	7.27	5.71	21.0	27.2	6.76	22.1	22.5	30.1	1.18	
	<i>Hemigrapsus penicillatus</i>	KH17	♂	7.34	524	L	G	25.8	55.4	15.5	4.30	11.9	36.2	4.34	13.4	13.2	32.4	1.01	M3
						S	G	28.1	49.9	14.9	4.40	12.3	35.9	4.57	13.2	13.4	34.2	1.04	
	<i>Hem. penicillatus</i>	KH18	♂	10.3	648	L	G	31.4	84.0	17.8	5.20	13.9	37.3	4.51	14.9	15.0	30.0	0.868	M3
						S	G	34.1	80.2	17.6	4.99	13.8	36.3	4.96	14.6	14.9	33.3	0.993	
	<i>Hem. penicillatus</i>	KH19	♂	6.03	432	L	G	24.5	49.4	17.1	4.04	11.2	36.0	4.37	12.5	12.4	35.0	1.08	M3
						S	G	23.8	48.4	16.7	4.10	11.4	36.1	4.2	12.5	12.5	33.7	1.02	
	<i>Varuna litterata</i>	KPM-NH140739	♂	27.8	1,740	L	G	63.1	174	13.6	6.97	22.3	31.2	5.66	23.3	23.5	24.1	0.813	D1
						S	G	63.3	173	13.5	6.87	22.4	30.7	5.66	22.8	23.3	24.3	0.824	
OCYPODOIDEA																			
Macrophthalmidae	<i>Macrophthalmus japonicus</i>	KH06	♂	3.88	321	L	P	4.47	11.7	5.05	1.97	6.63	29.8	1.97	6.69	6.94	28.4	0.999	H2
						S	P	5.31	10.3	4.87	1.75	6.85	25.5	1.76	6.94	7.12	24.7	1.01	
	<i>M. japonicus</i>	KH07	♂	5.19	408	L	P	9.71	25.1	8.52	2.51	9.85	25.5	2.45	10.4	10.5	23.4	0.975	H2
						S	P	7.91	24.0	7.80	2.33	8.99	260	2.47	9.96	9.81	24.8	1.06	
Ocypodidae																			
(Ocypodinae)	<i>Ocyponde ceratophthalma</i>	KPM-NH106326	♂	25.9	1,300	L	C	52.7	142	15.0	5.67	18.6	30.5	5.68	18.7	19.5	29.2	1.00	R2; V2
						S	P	28.1	71.6	7.66	3.11	15.6	19.9	3.6	17.4	17.1	20.6	1.16	
	<i>O. ceratophthalmus</i>	KH81	♂	—	407	X	P	7.76	—	—	1.56	8.39	18.6	1.85	8.81	8.83	20.9	1.18	R2; V2
						X	X	—	—	—	—	—	—	—	—	—	—	—	
	<i>O. ceratophthalmus</i>	KH82	♂	32.8	1,430	L	C	57.6	119	12.3	5.71	18.5	30.9	6.24	18.7	19.6	31.9	1.09	R2; V2
						S	P	30.7	79.3	7.66	2.89	16.0	18.1	3.83	16.8	16.9	22.7	1.32	
	<i>O. ceratophthalmus</i>	NSMT-Cr.4578	♂	43.2	1,860	L	C	60.4	—	—	6.73	20.7	32.6	5.85	21.1	21.7	27.0	0.869	R2; V2
						S	P	25.9	—	—	3.33	16.4	20.4	3.16	17.0	17.1	18.5	0.948	
	<i>O. cordimanus</i>	NSMT-Cr.10745	♀	7.38	451	L	X	18.7	—	—	3.54	10.2	34.6	3.65	10.3	10.9	33.5	1.03	R2
						S	X	7.30	—	—	2.08	8.16	25.5	1.79	8.60	8.61	20.8	0.859	
	<i>O. stimpsoni</i>	KPM-NH106516	♂	5.50	441	L	X	14.4	—	—	3.01	10.7	28.2	2.7	10.9	11.1	24.3	0.898	R2
						S	X	6.28	—	—	1.69	9.24	18.3	1.36	9.41	9.46	14.4	0.804	
(Ucinae)	<i>Uca (Austruca) lactea</i>	KPM-NH140616	♂	19.1	204	L	U	34.0	60.7	46.4	5.21	20.2	25.8	3.37	20.2	20.5	16.4	0.647	V1
	<i>U. (A.) lactea</i>	KH106	♂	14.9	680	L	U	118	267	56.6	6.93	41.5	16.7	5.68	41.7	42.0	13.5	0.820	V1
						S	P	6.78	19.0	3.79	1.31	8.36	15.7	1.62	8.39	8.53	19.0	1.24	
	<i>U. (Gelasimus) vocans</i>	KH70	♂	2.5	224	L	U	28.5	42.0	31.5	3.71	18.1	20.5	3.15	18.3	18.5	17.0	0.849	V1
	<i>U. (G.) vocans</i>	KH71	♂	2.54	221	L	U	27.3	48.5	34.4	3.96	17.5	22.6	3.12	18.1	18.2	17.2	0.789	V1
	<i>U. (G.) vocans</i>	KH72	♂	2.29	196	L	U	30.9	51.1	41.9	4.46	18.8	23.7	3.28	19.1	19.3	17.0	0.735	V1
	<i>U. (G.) vocans</i>	KH73	♂	2.71	235	L	U	32.2	51.5	35.7	4.10	19.0	21.6	3.39	19.1	19.3	17.5	0.827	V1
	<i>U. (G.) vocans</i>	KH74	♂	2.33	223	L	U	26.7	39.8	29.8	3.99	17.1	23.3	3.11	17.2	17.5	17.8	0.779	V1
	<i>U. (G.) vocans</i>	KPM-NH106380	♂	1.65	244	L	U	19.8	35.5	22.7	3.66	14.9	24.5	2.65	15.2	15.4	17.3	0.724	V1
	<i>U. (G.) vocans</i>	KPM-NH140654	♂	2.55	309	L	U	42.0	70.2	36.3	5.13	24.6	20.9	3.42	24.9	25.0	13.7	0.667	V1
	<i>U. (Paraleptuca) chlorophthalmus</i>	KPM-NH106482	♂	0.930	141	L	U	16.7	33.0	35.3	3.07	14.4	21.3	2.32	14.5	14.6	15.9	0.756	V1

TABLE S1 (cont.)

family	species	specimen	sex	BM	CS	chela	Fn	DS	PS	RC	C ₁	C ₂	C ₁ /C ₂	M ₁	M _{2L}	M _{2M}	M ₁ /M ₂	M ₁ /C ₁	Reference		
(Ucinidae [cont.])	<i>Uca (Tubuca) arcuata</i>	KPM-NH107735	♂	3.36	470	L	U	46.4	85.5	28.0	4.81	21.2	22.7	4.38	21.6	21.9	20.0	0.91	V1		
	<i>U. (T.) arcuata</i>	NSMT-Cr.3205	♂	14.7	698	L	U	97.5	—	—	6.73	31.5	21.3	6.18	31.6	32.1	19.2	0.918	V1		
	<i>U. (T.) arcuata</i>	NSMT-Cr.3905	♂	11.2	609	L	U	61.8	—	—	6.06	27.4	22.1	4.51	27.4	27.8	16.2	0.744	V1		
						S	P	—	—	—	—	—	—	—	—	—	—	—	—		
	<i>U. (T.) arcuata</i>	NSMT-Cr.7277	♂	14.5	706	L	U	112	—	—	7.08	33.6	21.0	6.66	33.7	34.3	19.4	0.941	V1		
						S	P	—	—	—	—	—	—	—	—	—	—	—	—	—	
	<i>U. (T.) arcuata</i>	NSMT-Cr.7577	♂	10.1	637	L	U	69.7	—	—	6.21	26.3	23.6	5.29	26.4	26.9	19.7	0.851	V1		
						S	P	—	—	—	—	—	—	—	—	—	—	—	—	—	
	<i>U. (T.) coarctata</i>	KPM-NH140347	♂	16.0	—	L	U	150	212	—	8.31	40.0	20.8	7.52	40.3	40.9	18.4	0.905	V1		
	<i>U. (T.) dussumieri</i>	NSMT-Cr.1172	♂	4.20	334	L	U	34.3	—	—	5.00	18.3	27.3	3.76	18.3	18.7	20.1	0.752	V1		
						S	P	—	—	—	—	—	—	—	—	—	—	—	—	—	
	<i>U. (T.) arcuata</i>	NSMT-Cr.13131	♂	4.22	387	L	U	33.0	—	—	4.12	18.1	22.7	3.65	18.1	18.5	19.8	0.887	V1		
						S	P	—	—	—	—	—	—	—	—	—	—	—	—	—	
	<i>U. (Tubuca) forcipata</i>	NSMT-Cr.14131	♂	4.44	369	L	U	27.5	—	—	4.49	16.6	27.0	3.31	16.8	17.0	19.4	0.738	V1		
<i>U. sp.</i>	KH32	♂	15.3	791	L	U	117	265	48.2	7.41	41.4	17.9	5.66	41.4	41.7	13.6	0.763	V1			
<i>U. sp.</i>	KPM-NH140867	♂	1.53	188	L	U	32.4	62.7	50.6	3.99	21.2	18.8	3.06	21.2	21.4	14.3	0.768	V1			

Abbreviations of institution:

KH, personal collections of Hiroki Kawai, Nagoya University Museum, Nagoya, Japan; KPM, Kanagawa Prefectural Museum, Odawara, Japan; NSMT, National Museum of Nature and Science, Tokyo (formerly, National Science Museum, Tokyo), Japan; NUM, Nagoya University Museum, Nagoya, Japan; TMNH, Toyohashi Museum of Natural History, Toyohashi, Japan.

Abbreviations of reference:

- B1: Barnes DKA. 1997. Ecology of tropical hermit crabs at Quirimba Island, Mozambique: a novel and locally important food source. *Mar Ecol Prog Ser* 161:299–302.
- B2: Baylon JC, Tito OD. 2012. Natural diet and feeding habits of the red frog crab (*Ranina ranina*) from Southwestern Mindanao, Philippines. *Philipp Agric Scientist* 95:370–377.
- B3: Bovbjerg RV. 1960. Behavioral ecology of the crab, *Pachygrapsus crassipes*. *Ecology* 41:668–672.
- C1: Cannicci S, Dahdouh-Guebas F, Anyona D, Vannini M. 1996. Natural diet and feeding habits of *Thalamita crenata* (Decapoda: Portunidae). *J Crustac Biol* 16:678–683.
- C2: Cartes JE. 1993. Diets of deep-sea brachyuran crabs in the Western Mediterranean Sea. *Mar Biol* 117:449–457.
- C3: Comoglio LI, Amin OA. 1999. Feeding habits of the false southern king crab *Paralomis granulosa* (Lithodidae) in the Beagle Channel, Tierra del Fuego, Argentina. *Sci Mar* 63:361–366.
- C4: Corsini M, Kondilatos G. 2006. On the occurrence of two brachyurans, *Myra subgranulata* and *Herbstia condyliata*, on Rhodes Island (Se Aegean Sea). *Crustaceana* 79:167–174.
- C5: Currie DR, Ward TM. 2009. South Australian giant crab (*Pseudocarcinus gigas*) fishery. Fishery Assessment Report for PIRSA, South Australian Research and Development Institute (Aquatic Sciences), Adelaide. SARDI Publication No. F2007/00698-2. South Australian Research and Development Institute Research Report Series 345.
- D1: Devi PL, Nair DG, Joseph A. 2013. Habitat ecology and food and feeding of the herring bow crab *Varuna litterata* (Fabricius, 1798) of Cochin backwaters, Kerala, India. *Arthropods* 2:172–188.
- D2: Dickinson PS, Stemmler EA, Christie AE. 2008. The pyloric neural circuit of the herbivorous crab *Pugettia producta* shows limited sensitivity to several neuromodulators that elicit robust effects in more opportunistically feeding decapods. *J Exp Biol* 211:1434–1447.
- D3: Dworschak PC. 2003. Biology of Mediterranean and Caribbean Thalassinidea (Decapoda). In: Tamaki A, editor. Proceedings of the Symposium on Ecology of Large Bioturbators in Tidal Flats and Shallow Sublittoral Sediments—From Individual Behavior to Their Role As Ecosystem Engineers. Nagasaki: Nagasaki University. p 15–22.
- E1: Edgell TC, Brazeau C, Grahame JW, Rochette R. 2008. Simultaneous defense against shell entry and shell crushing in a snail faced with the predatory shore crab *Carcinus maenas*. *Mar Ecol Prog Ser* 371:191–198.
- E2: Elnor RW. 1978. The mechanics of predation by the shore crab, *Carcinus maenas* (L.), on the edible mussel, *Mytilus edulis* L. *Oecologia* 36:333–344.
- G1: Guan R-Z, Wiles PR. 1998. Feeding ecology of the signal crayfish *Pacifastacus leniusculus* in a British lowland river. *Aquaculture* 169:177–193.
- H1: Hazlett BA. 1966. Observations on the social behavior of the land hermit crab, *Coenobita clypeatus* (Herbst). *Ecology* 47:316–317.
- H2: Henmi Y. 1992. Annual fluctuation of life-history traits in the mud crab *Macrophthalmus japonicus*. *Mar Biol* 113:569–577.
- H3: Hill BJ. 1979. Aspects of the feeding strategy of the predatory crab *Scylla serrata*. *Mar Biol* 55:209–214.

TABLE S1 (cont.)

Abbreviations of reference (cont.):

- J1: Jiang W-M, Meng T-X, Chen R-S, Wei S. 1998. Diet of *Charybdis japonica* (A. Milne-Edwards) and *Portunus trituberculatus* (Miers) in the Bohai Sea. Mar Fisheries Res, Haiyan Suichan Yanjiu 19:53–59.
- K1: Kobayashi S. 2009. Dietary preference of the Japanese mitten crab *Eriocheir japonica* in a river and adjacent seacoast in north Kyushu, Japan. Plankton Benthos Res 4:77–87.
- K2: Kobayashi S. 2012. Dietary preference of the potamid crab *Geothelphusa dehaani* in a mountain stream in Fukuoka, northern Kyushu, Japan. Plankton Benthos Res 7:159–166.
- K3: Kobayashi S. 2013. Feeding habits of the leucosiid crab *Pyrhila pisum* (De Haan) observed on a sandy tidal flat in Hakata Bay, Fukuoka, Japan. Japan J Benthol 68:37–41.
- K4: Kobayashi Y. 2010. Umibe no Ikimono: Shin-Yamakei Pocket Guide (Field Guide of Coast Animals). Tokyo: Yamato Keikoku. 281p [In Japanese].
- K5: Kuroda M, Wada K, Kamada M. 2005. Factors influencing coexistence of two brachyuran crabs, *Helice tridens* and *Parasesarma plicatum*, in an estuarine salt marsh, Japan. J Crustac Biol 25:146–153.
- L1: Lau CJ. 1987. Feeding behavior of the Hawaiian slipper lobster *Scyllarides squammosus*, with a review of decapod crustacean feeding tactics on molluscan prey. Bull Mar Sci 41:378–391.
- L2: Liu H-C, Jeng M-S. 2005. Reproduction of *Epigrapsus notatus* (Brachyura: Gecarcinidae) in Taiwan. J Crustac Biol 25:135–140.
- M1: Matsui S, Hagiwara Y, Tou H, Tsukahara H. 1986. Study on the feeding habit of the Japanese blue crab, *Portunus trituberculatus* (Miers). Sci Bull Facul Agric, Kyushu Univ 40:175–181.
- M2: Micheli F, Gherardi F, Vannini M. 1991. Feeding and burrowing ecology of two East African mangrove crabs. Mar Biol 111:247–254.
- M3: Miura T. 2008. Higata no Ikimono Zukan: Hikari Afureru Seimei no Rakuen (Field Guide of Tidal Animals). Tokyo: Nanpo Shinsha. 197p [In Japanese].
- M4: Muraoka K, Odawara T. 1995. *The Visual Guide to Crabs*. Tokyo: Seibido. 159p [In Japanese].
- N1: Ng PKL, Guinot D. 2001. On the land crabs of the genus *Discoplax* A. Milne Edwards, 1867 (Crustacea: Decapoda: Brachyura: Gecarcinidae), with description of a new cavernicolous species from the Philippines. Raffles Bull Zool 49:311–338.
- O1: Olden JD, Larson ER, Mims MC. 2009. Home field advantage: native signal crayfish (*Pacifastacus leniusculus*) out consume newly introduced crayfishes for invasive Chinese mystery snail (*Bellamya chinensis*). Aquat Ecol 43:1073–1084.
- P1: Perez OS, Bellwood DR. 1988. Ontogenetic changes in the natural diet of the sandy shore crab, *Matuta lunaris* (Forskål) (Brachyura: Calappidae). Aust J Mar Freshwater Res 39:193–199.
- P2: Pérez-Bote JL. 2005. Feeding ecology of the exotic red swamp crayfish, *Procambarus clarkii* (Girard, 1852) in the Guadiana River (SW Iberian Peninsula). Crustaceana 77:1375–1387.
- P3: du Preez HH. 1984. Molluscan predation by *Ovalipes punctatus* (de Haan) (Crustacea: Brachyura: Portunidae). J Exp Mar Biol Ecol 84:55–71.
- R1: Reyne A. 1939. On the food habits of the coconut crab (*Birgus latro* L.), with notes on its distribution. Arch Neerl Zool 3:283–320.
- R2: Robertson JR, Pfeiffer WJ. 1982. Deposit-feeding by the ghost crab *Ocyropsis quadrata* (Fabricius). J Exp Mar Biol Ecol 56:165–177.
- S1: Samson SA, Yokota M, Strüssmann CA, Watanabe S. 2007. Natural diet of grapsoid crab *Plagusia dentipes* de Haan (Decapoda: Brachyura: Plagusiidae) in Tateyama Bay, Japan. Fisheries Sci 73:171–177.
- S2: Schweitzer CE, Feldmann RM. 2009. The Decapoda (Crustacea) as predators on mollusca through geologic time. Palaios 25:167–182.
- S3: Shimoda K, Wardiatno Y, Kubo K, Tamaki A. 2005. Intraspecific behaviors and major cheliped sexual dimorphism in three congeneric callinassid shrimp. Mar Biol 146:543–557.
- S4: Štević Z. 1983. Revision of the Calappidae. Australian Museum Memoir 18:165–171.
- T1: Takeda S, Kurihara Y. 1987. The distribution and abundance of *Helice tridens* (De Haan) burrows and substratum conditions in a northeastern Japan salt marsh (Crustacea: Brachyura). J Exp Mar Biol Ecol 107:9–
- U1: Ueda R, Yasuhara T, Sugita H, Deguchi Y. 1989. Gut microflora of the Japanese giant crab *Macrocheira kaempferi*. Bull Japan Soc Sci Fish 55:181.
- V1: Valiela I, Babiec DF, Atherton W, Seitzinger S, Krebs C. 1974. Some consequences of sexual dimorphism: feeding in male and female fiddler crabs, *Uca pugnax* (Smith). Biol Bull 147:652–660.
- V2: Vermeij GJ. 1977. Patterns in crab claw size: the geography of crushing. Syst Zool 26:138–151.
- V3: Vinuesa JH, Varisco M, Balzi P. 2013. Feeding strategy of early juvenile stages of the southern king crab *Lithodes santolla* in the San Jorge Gulf, Argentina. Rev Biol Mar Oceanogr 48:353–353.
- W1: Wegmann A. 2008. Land Crab Interference with Eradication Projects: Phase I—Compendium of Available Information. Auckland: Pacific Invasives Initiative, The University of Auckland. 30p.
- W2: Wieczorek SK, Hooper RG. 1995. Relationship between diet and food availability in the snow crab *Chionoecetes opilio* (O. Fabricius) in Bonne Bay, Newfoundland. J Crustac Biol 15:236–247.
- W3: Williams MJ. 1982. Natural food and feeding in the commercial sand crab *Portunus pelagicus* Linnaeus, 1766 (Crustacea: Decapoda: Portunidae) in Moreton Bay, Queensland. J Exp Mar Biol Ecol 59:165–176.
- Y1: Yamada SB, Boulding EG. 1998. Claw morphology, prey size selection and foraging efficiency in generalist and specialist shell-breaking crabs. J Exp Mar Biol Ecol 220:191–211.

Appendix S1: Phylogenetic signals of the indices used in this study

INTRODUCTION

The relationship between a trait and its function cannot be strongly supported if a diversification of the traits were related to the phylogeny (Harvey and Pagel, 1991; Abouheif, 1999; Münkemüller et al., 2012; Pavione and Ricotta, 2012; Hallmann and Griebeler, 2015). Therefore, it is important to test whether a trait is autocorrelated with a phylogeny. Phylogenetic autocorrelation of a trait can be tested by determining a phylogenetic signal, which is defined by Blomberg and Garland (2002) as a tendency for related species to resemble each other more than they resemble species drawn at random evolution from the phylogenetic tree.

Three indices were used in this study, including mechanical advantages of pinching efficiency (C_1/C_2), passive disarticulation resistance (M_1/M_2), and relative size of chela (RC). We determined the phylogenetic signals for these indices to test whether they were autocorrelated with the phylogeny, though they seem to be diversified independently from the classification in Ng et al. (2008: Fig. 7).

MATERIALS AND METHODS

Phylogenetic signals can be determined from the value of each index and the phylogenetic relationships among the studied taxa (Münkemüller et al., 2012). Phylogenetic signals were determined for three different indices in this study (C_1/C_2 , M_1/M_2 , and RC). Many decapods show a left-right asymmetry in their chela (Palmer, 2004), so the autocorrelation of the indices to the phylogenetic tree may vary between major and minor chelae. Therefore, we used specimens for which index values were estimated for both major and minor chelae (Table S1), and the major, minor, and average of the major and minor chelae were estimated for each index. Sexual dimorphism of chelae was not accounted for in this analysis because there was an inadequate number of samples to determine the phylogenetic signals for males and females.

Phylogenetic trees containing all studied species were not available in the literature. Furthermore, a consensus on the phylogenetic relationships among decapods has yet to be obtained (e.g., Ahyong et al., 2007; Tsang et al., 2008; Bracken et al., 2009; Tsang et al., 2014). Therefore, we used six phylogenetic trees from published literature that were comprised of more than seven species or genera of our studied taxa (Fig. S1: Schubart et al., 2006; Ahyong et al., 2007; Tsang et al., 2008; Bracken et al., 2009; Spiridonov et al., 2014; Tsang et al., 2014). We used species in these trees that corresponded with species used in our study (Table S1) for estimating the phylogenetic signals (see species in Fig. S1). By following the method of Batalha et al. (2011), the average value of each index for all specimens within a species was defined as the representing index value for the species. For a genus in a tree that corresponded to one used in our study, but with a different species, we first confirmed that the monophyly of the clade containing the genus was well-supported in the literature (maximum likelihood bootstrap [BP] ≥ 70 ; or Bayesian inference posterior probability [PP] ≥ 0.95). Then, we averaged the value of each index for all specimens of all the species within the genus and defined it as the representing index value of the genus (see genera with asterisks in Fig. S1). Synonymy of the taxonomic names among the literatures were checked carefully based on Ng et al. (2008).

The topologies of the phylogenetic trees are shown in Fig. S1. We followed the nodes which were well-supported (BP ≥ 70 ; or PP ≥ 0.95). If the phylogenetic relationships among the lineages within the node were not well-supported (BP < 70 ; or PP < 0.95), the node was dealt as ptytomy. Members of the studied taxa in each tree depended on the taxa used in the original trees in the literature. The trees from Bracken et al. (2009) and Tsang et al. (2008) comprised species of astacideans, anomurans, and brachyurans: the former comprised 11 taxa (four species and seven other genera) and the latter comprised 11 taxa (eight species and three other genera). The tree from Tsang et al. (2014) and Ahyong et al. (2007) comprised species of anomurans and three sections (Prototremata, Heterotremata, and Thoracotremata) of brachyurans (30 taxa: 16 species and 14 other genera). The tree from Ahyong et al. (2007) comprised seven taxa (four species and three other genera) of the three sections of brachyurans. The tree in Spiridonov et al. (2014) comprised seven portunoid taxa and two other taxa (seven species and two other genera) of heterotremate brachyurans. The tree in Schubart et al. (2006) comprised 11 taxa (five species and six other genera) in ten thoracotremate and one heterotremate brachyurans. Although the topologies for the relationships among the studied taxa were available in these trees, the branch lengths were absent from the literature.

Among the several phylogenetic signals, we determined Abouheif's mean C -statistics (Abouheif, 1999) for each index, which was estimated using the topology of the phylogenetic tree, but was not related to branch length in the analysis (Münkemüller et al., 2012). Abouheif's mean C -statistics were used to determine the autocorrelation of values of neighboring taxa in the phylogenetic tree, and the null hypothesis (there is no phylogenetic autocorrelation) is rejected if the p -value does not exceed 0.05 (Abouheif, 1999).

We used packages “adephylo” and “ape” (Paradis et al., 2003; Jombart et al., 2010) in R 3.2.2 (R Core Team, 2015) for the Abouheif's tests—the package “ape” depends on R ($\geq 3.0.0$). We constructed phylogenetic trees among the taxonomic groups of studied taxa using package “ape” (Jombart and Dray, 2010). Abouheif's mean C -statistics were then estimated for each index using the function “abouheif.moran” of package “adephylo” in R (Jombart and Dray, 2010; Jombart et al., 2010).

Appendix S1 (cont.)

RESULT

According to the Abouheif's test, the indices C_1/C_2 , M_1/M_2 , and RC were not phylogenetically autocorrelated ($p \geq 0.05$) in the major (L), minor (S), or the average of major and minor (L+S) chelae in most of the phylogenetic trees (Table S2). However, the M_1/M_2 of minor chelae (S) and the RC of chelae (L, S, and L+S) were phylogenetically autocorrelated in the trees of Bracken et al. (2009) and Tsang et al. (2008), which comprised only a single taxon within each brachyuran superfamily, or only a few taxa within each brachyuran section (Table S2; Fig. S1).

DISCUSSION

Overall, in Abouheif's test conducted on a tree comprised of major lineages of brachyuran superfamilies (e.g., the tree in Tsang et al. [2014]) or on relatively detailed trees of a brachyuran section/superfamily (e.g., the trees in Spiridonov et al. [2014] and Schubart et al. [2006]), the indices used in this study (C_1/C_2 , M_1/M_2 , and RC) were not autocorrelated with the phylogeny (Table S2). However, some indices were not phylogenetically independent on trees of decapod infraorders (e.g., Bracken et al.

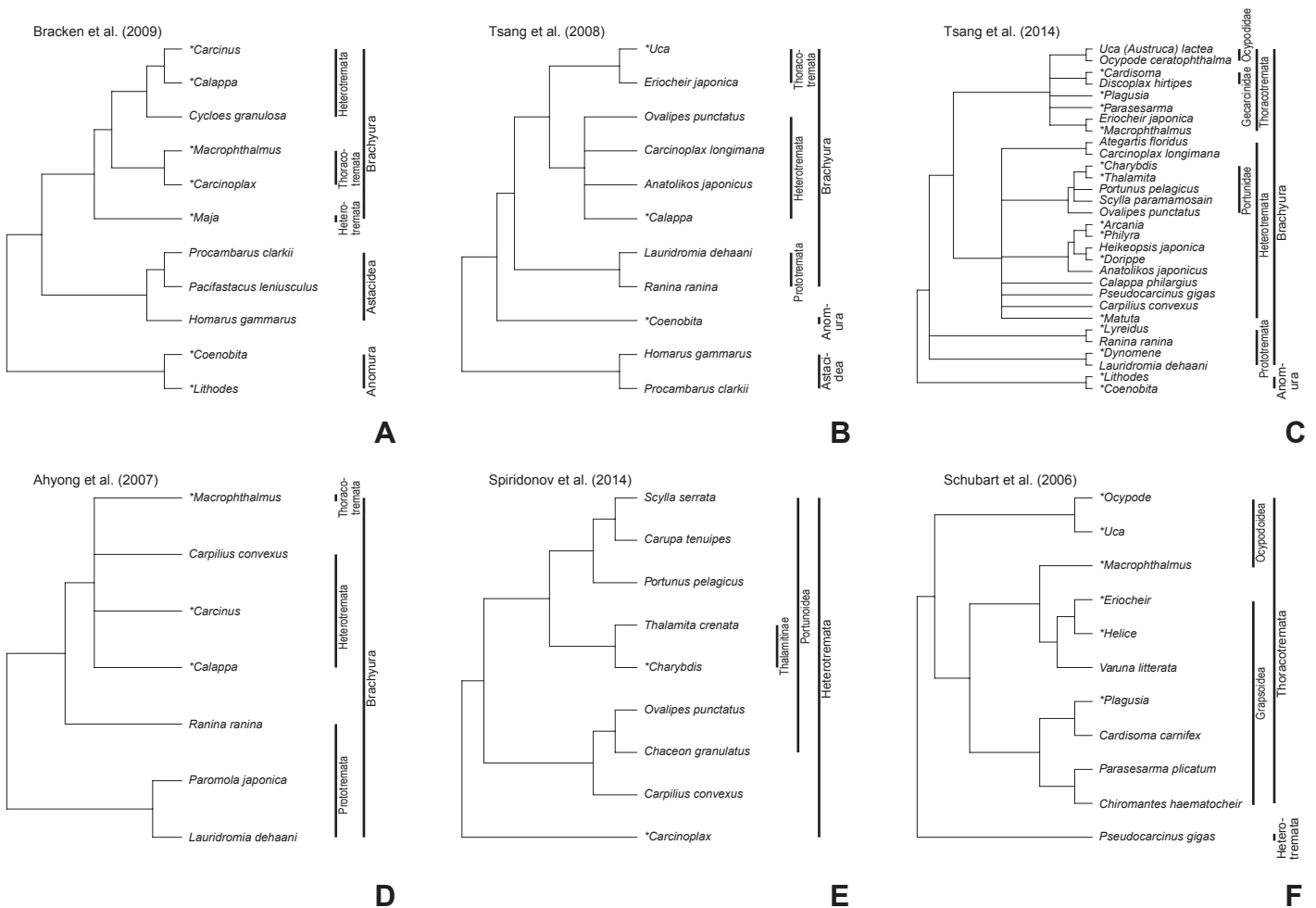


Fig. S1. Topologies of phylogenetic relationships among the studied taxa based on literatures supported by maximum likelihood boot strap values (>70) or by Bayesian inference posterior probabilities (>0.95): phylogenetic trees (A, B) among astacideans, anomurans, and brachyurans (A: Bracken et al., 2009; B: Tsang et al., 2008); (C) among anomurans and major lineages of brachyuran superfamilies (Tsang et al., 2014); (D) among prototremates, heterotremates, and thoracotremates (Ahyong et al., 2007); among portunoid brachyurans (Spiridonov et al., 2014); and among thoracotremate brachyurans (Schubart et al., 2006). Classification shown on the right side of each tree is based on Ng et al. (2008). The trees were constructed using species from this study that were also found in the available literature, and with studied taxa whose genera were the same, but whose species did not correspond with the one used in the literature. The names of genera whose species did not match the species in the literature are indicated with asterisks. Note that the branch lengths are not reflected in these topologies.

Appendix S1 (cont.)

[2009] and Tsang et al. [2008]).

There are some limitations in the method utilized in this study. The first limitation is that the phylogenetic relationships among decapods are yet to be fully understood. In particular, the debates on relationships among decapod infraorders, and among brachyuran superfamilies/families remain unresolved (e.g., Ahyong et al., 2007; Tsang et al., 2008; Bracken et al., 2009; Tsang et al., 2014). The tests on the phylogenetic signals delicately rely on the topologies of the trees, and therefore, as far as the consensus on phylogenetic relationships among decapods is unavailable, it is difficult to strongly argue that the indices used in this study are not phylogenetically autocorrelated. Note that the results in this appendix are case studies of Abouheif's test on six available decapod phylogenetic trees.

The second limitation concerns the use of phylogenetic tree whose species on the tip did not necessarily correspond to our study taxa for the estimation of phylogenetic significance (Fig. S1). Different topologies of phylogenetic trees could be proposed if a new phylogenetic analysis was conducted using all the taxa used in this study (Tables S1 and S2), which may affect the results of Abouheif's test. Additional analyses using a phylogenetic tree constructed from all the species included in our study may solve this problem.

The third limitation concerns the sexual differences of chelae within a species. The result of the phylogenetic autocorrelation of the indices would change if the phylogenetic signals were determined based solely on the either sex. Many brachyuran taxa, including *Uca* and *Hemigrapsus*, are known to show a pronounced sexual dimorphism in the size and shape of chelae (RC: e.g.,

TABLE S2. Results of Abouheif's tests for mechanical advantages of pinching efficiency (C_1/C_2), passive disarticulation resistance (M_1/M_2), and relative size of chela (RC), in the studied specimens whose indices in both the major and the minor chelae were available. The tests were conducted for major (L), minor (S), and the average of major and minor (L+S) chelae. The average of the indices within each taxon was used for the tests. See Fig. S1 for the phylogenetic tree and the taxa used to estimate Abouheif's mean C -statistics. The observed value of Abouheif's mean C -statistics (Obs), the standard deviation of Abouheif's mean C -statistics (Std.Obs.), and the p -value of the null hypothesis are listed.

chela	C_1/C_2			M_1/M_2			RC		
	Obs	Std.Obs	p	Obs	Std.Obs	p	Obs	Std.Obs	p
<Bracken et al. (2009)>									
L	0.302	1.50	0.088	0.262	0.986	0.181	0.618	2.55	0.032*
S	0.176	0.0669	0.382	0.368	2.51	0.017*	0.603	2.50	0.054
L+S	0.259	0.871	0.196	0.311	1.59	0.093	0.611	2.41	0.042*
<Tsang et al. (2008)>									
L	0.0601	-1.49	0.988	0.0811	-1.33	0.937	0.227	-0.253	0.488
S	0.153	-0.350	0.569	0.0936	-1.08	0.873	0.411	5.13	0.001*
L+S	0.0954	-1.04	0.875	0.0841	-1.25	0.926	0.293	0.774	0.226
<Tsang et al. (2014)> L									
L	0.132	1.86	0.053	0.122	1.47	0.076	0.0737	-0.623	0.736
S	0.0490	-0.897	0.835	0.106	0.887	0.179	0.0949	-0.000265	0.431
L+S	0.859	0.322	0.307	0.123	1.46	0.09	0.0665	-0.945	0.851
<Ahyong et al. (2007)>									
L	0.294	-0.0834	0.338	0.426	0.866	0.267	0.222	-0.519	0.642
S	0.394	0.786	0.187	0.372	0.539	0.303	0.180	-0.754	0.778
L+S	0.237	-0.538	0.538	0.404	0.739	0.296	0.199	-0.617	0.75
<Spiridonov et al. (2014)>									
L	0.300	0.115	0.621	0.238	0.147	0.322	0.276	0.154	0.463
S	0.221	-0.456	0.754	0.230	0.153	0.323	0.166	-0.910	0.824
L+S	0.276	0.447	0.619	0.241	0.223	0.295	0.219	-0.377	0.579
<Schubart et al. (2006)>									
L	0.126	-0.774	0.752	0.158	-0.230	0.519	0.419	2.08	0.07
S	0.332	1.88	0.065	0.321	1.82	0.069	0.239	0.00124	0.395
L+S	0.256	1.01	0.191	0.279	1.34	0.119	0.390	1.69	0.096

*Null-hypothesis that the index is not phylogenetically autocorrelated is rejected ($p < 0.05$).

Appendix S1 (cont.)

Valiela et al., 1974; Ng et al., 2008; Miyajima et al., 2012). However, we could not determine whether there were differences in the mechanical indices of chela (C_1/C_2 and M_1/M_2) between sexes due to inadequate samples of both sexes (Table S1). In a case study of a shrimp crab (*Neotrypaea*), whose chelae are sexually dimorphic in size, the C_1/C_2 in master and minor chelae did not differ significantly between the sexes (Labadie and Palmer, 1996), though the taxa were not used in this study. It would be worthwhile to test the differences of both mechanical indices of chelae (C_1/C_2 and M_1/M_2) for our studied species in the future.

CONCLUSION

According to Abouheif's tests conducted on published decapod phylogenetic trees, comprised of the major lineages of brachyurans, the three indices (C_1/C_2 , M_1/M_2 , and RC) were not autocorrelated with the phylogeny.

LITERATURE CITED

- Abouheif E. 1999. A method for testing the assumption of phylogenetic independence in comparative data. *Evol Ecol Res* 1:895–909.
- Ahyong ST, Lai JCY, Sharkey D, Colgan DJ, Ng PKL. 2007. Phylogenetics of the brachyuran crabs (Crustacea: Decapoda): the status of Podotremata based on small subunit nuclear ribosomal RNA. *Mol Phylogenet Evol* 45:576–586.
- Batalha MA, Silva IA, Cianciaruso MV, de Carvalho GH. 2011. Trait diversity on the phylogeny of cerrado woody species. *Oikos* 120: 1741–1751.
- Blomberg SP, Garland T. 2002. Tempo and mode in evolution: phylogenetic inertia, adaptation and comparative methods. *J Evol Biol* 15:899–910.
- Bracken HD, Toon A, Felder DL, Martin JW, Finley M, Rasmussen J, Palero F, Crandall KA. 2009. The decapod tree of life: compiling the data and moving toward a consensus of decapod evolution. *Arthropod Syst Phyl* 67:99–116.
- Hallmann K, Griebeler EM. 2015. Eggshell types and their evolutionary correlation with life-history strategies in squamates. *PLoS ONE* 10:e0138785.
- Harvey PH, Pagel MD. 1991. *The Comparative Method in Evolutionary Biology*. Oxford: Oxford University Press. 239p.
- Jombart T, Dray S. 2010. adephylo: exploratory analyses for the phylogenetic comparative method. *Bioinformatics* 26:1–21.
- Jombart T, Balloux F, Dray S. 2010. adephylo: new tools for investigating the phylogenetic signal in biological traits. *Bioinformatics* 26:1907–1909.
- Labadie LV, Palmer AR. 1996. Pronounced heterochely in the ghost shrimp, *Neotrypaea californiensis* (Decapoda: Thalassinidea: Callinassidae): allometry, inferred function and development. *J Zool, Lond* 240:659–675.
- Miyajima A, Fukui Y, Wada K. 2012. Agonistic and mating behavior in relation to chela features in *Hemigrapsus takanoi* and *H. sinensis* (Brachyura, Varunidae). *Crustacean Res* 41:47–58.
- Münkemüller T, Lavergne S, Bzeznik B, Dray S, Jombart T, Schifffers K, Thuiller W. 2012. How to measure and test phylogenetic signal. *Methods Ecol Evol* 3:743–756.
- Ng PKL, Guinot DG, Davie PJF. 2008. Systema brachyurum: Part I. An annotated checklist of extant brachyuran crabs of the world. *Raffles Bull Zool* 17:1–286.
- Paradis E, Claude J, Strimmer K. 2003. ape: Analyses of phylogenetics and evolution in R language. *Bioinformatics* 20:289–290.
- Pavione S, Ricotta C. 2012. Testing for phylogenetic signal in biological traits: the ubiquity of cross-product statistics. *Evolution* 67:828–840.
- R Core Team. 2015. *R: A Language and Environment for Statistical Computing*. Vienna: R Foundation for Statistical Computing. URL <http://www.R-project.org/>.
- Schubart CD, Cannicci S, Vannini M, Fratini S. 2006. Molecular phylogeny of grapsoid crabs (Decapoda, Brachyura) and allies based on two mitochondrial genes and a proposal for refraining from current superfamily classification. *J Zool Syst Evol Res* 44:193–199.
- Spiridonov VA, Neretina TV, Schepetov D. 2014. Morphological characterization and molecular phylogeny of Portunoidea Rafinesque, 1815 (Crustacea Brachyura): implications for understanding evolution of swimming capacity and revision of the family-level classification. *Zool Anz* 253:404–429.
- Tsang LM, Ma KY, Ahyong ST, Chan T-Y, Chu KH. 2008. Phylogeny of Decapoda using two nuclear protein-coding genes: origin and evolution of the Reptantia. *Mol Phylogenet Evol* 48:359–368.
- Tsang LM, Schubart CD, Ahyong ST, Lai JCY, Au E, Chan T-Y, Ng PKL, Chu KH. 2014. Evolutionary history of true crabs (Crustacea: Decapoda: Brachyura) and the origin of freshwater crabs. *Mol Biol Evol* 31:1173–1187.
- Valiela I, Babiec DF, Atherton W, Seitzinger S, Krebs C. 1974. Some consequences of sexual dimorphism: feeding in male and female fiddler crabs, *Uca pugnax* (Smith). *Biol Bull* 147:652–660.

Appendix S2: Relationships between relative size of chela (RC) and mechanical indices for pinching efficiency (C_1/C_2) and passive disarticulation resistance (M_1/M_2)

TABLE S2. Results of Steel-Dwass tests of three indices related to chela—pinching efficiency (C_1/C_2), passive disarticulation resistance (M_1/M_2), and relative size of chela (RC)—among four different functional categories (C, G, P, and U) (p. 1).

TABLE S3. Spearman’s correlation test between relative size of chela (RC) and mechanical advantage of pinching efficiency (C_1/C_2) (p. 1).

TABLE S4. Spearman’s correlation test between relative size of chela (RC) and mechanical advantage of passive disarticulation resistance (M_1/M_2) (p. 1).

Fig. S2. Relationship between relative size of chela ($RC = (DS + PS)/CS$) and mechanical advantage of pinching efficiency (C_1/C_2) (p. 2).

Fig. S3. Relationship between relative size of chela ($RC = (DS + PS)/CS$) and mechanical advantage of passive disarticulation resistance (M_1/M_2) (p. 3).

TABLE S2. Results of Steel-Dwass tests of three indices related to chela—pinching efficiency (C_1/C_2), passive disarticulation resistance (M_1/M_2), and relative size of chela (RC)—among four different functional categories (C, G, P, and U). The tests were conducted for the study specimens whose carapace sizes were able to be measured ($n = 191$: C, 24, G, 121; P, 33; U, 13). Asterisk indicates that the variables among two categories were not significantly different ($p < 0.05$). See boxplots in Figs. S2 and S3.

	C_1/C_2		M_1/M_2		RC	
	<i>t</i> -score	<i>p</i>	<i>t</i> -score	<i>p</i>	<i>t</i> -score	<i>p</i>
C : G	5.54	1.78e-07*	5.11	1.85e-06*	0.883	8.14e-01
C : P	6.09	6.63e-09*	6.11	5.99e-09*	0.760	8.73e-01
C : U	4.71	1.48e-05*	4.96	4.14e-06*	4.96	4.14e-06*
G : P	4.82	8.57e-06*	6.22	3.07e-09*	0.112	9.99e-01
G : U	2.78	2.80e-02*	5.81	3.81e-08*	5.80	3.98e-08*
P : U	0.915	7.97e-01	2.45	6.77e-02	5.23	9.98e-07*

TABLE S3. Spearman’s correlation test between relative size of chela (RC) and mechanical advantage of pinching efficiency (C_1/C_2) ($n = 230$: C, 24; G, 121; P, 33; U, 13; X, 39). Spearman’s ρ - and *p*-values, coefficient of determination (R^2), and regression line were indicated for each functional category (C, G, P, and U). See Fig. S2.

	<i>n</i>	ρ -value	<i>p</i>	R^2	regression line
total	230	0.269	0.445	2.56e-03	$y = 0.0565x + 25.9$
C	24	-0.0635	0.570	1.49e-02	$y = -0.315x + 41.1$
G	121	0.440	2.26e-05*	1.41e-01	$y = 0.437x + 22.4$
P	33	-0.182	0.835	1.43e-03	$y = 0.0783x + 18.1$
U	13	-0.527	3.23e-02*	0.353	$y = -0.158x + 27.6$

*Null-hypothesis that there is no association between the two variables was rejected ($p < 0.05$).

TABLE S4. Spearman’s correlation test between relative size of chela (RC) and mechanical advantage of passive disarticulation resistance (M_1/M_2) ($n = 230$: C, 24; G, 121; P, 33; U, 13; X, 39). Spearman’s ρ - and *p*-values, coefficient of determination (R^2), and regression line were indicated for each functional category (C, G, P, and U). See Fig. S3.

	<i>n</i>	ρ -value	<i>p</i>	R^2	regression line
total	230	0.235	7.56e-02	1.38e-06	$y = -0.0934x + 27.5$
C	24	0.0183	0.991	6.53e-06	$y = -0.00414x + 33.9$
G	121	0.527	5.50e-06*	0.160	$y = 0.301x + 24.6$
P	33	-0.0491	0.648	6.81e-03	$y = 0.112x + 19.5$
U	13	-0.830	4.66e-03*	0.532	$y = -0.146x + 21.8$

*Null-hypothesis that there is no association between the two variables was rejected ($p < 0.05$).

Appendix S2 (cont.)

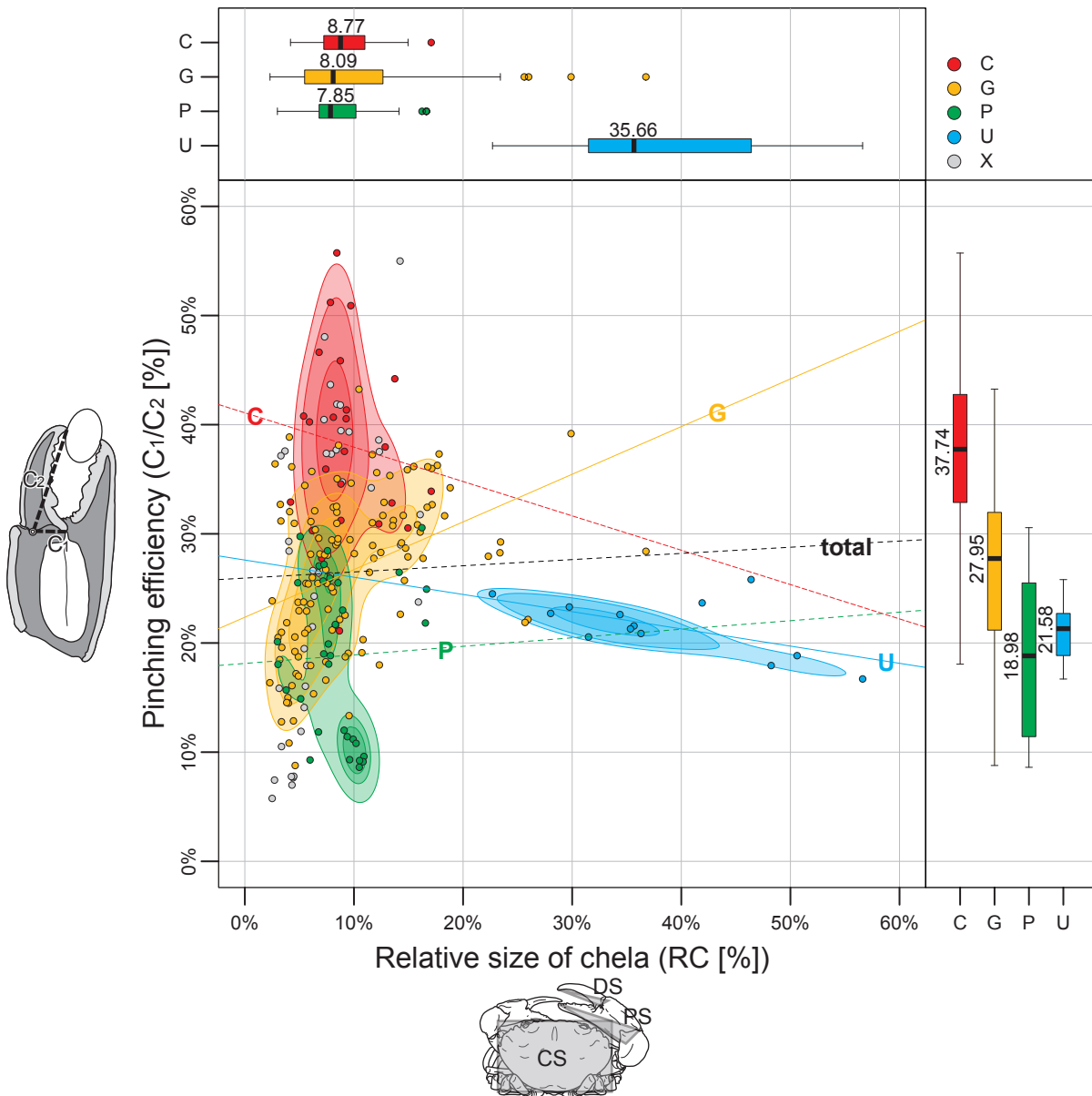


Fig. S2. Relationship between relative size of chela ($RC = (DS + PS)/CS$) and mechanical advantage of pinching efficiency (C_1/C_2). See main text for abbreviations. Each plot represents chela characteristics of the study specimens ($n = 230$ in total; C, crushing/chipping chela, $n = 24$; G, gripping chela, $n = 121$; P, pinching chela, $n = 33$; U, male ucine major chela, $n = 13$; X, uncategorized chela, $n = 39$). Bivariate kernel density distributions (densities: 25%, 50%, 75%) and box plots with median values are shown for each variable in the functional categories C, G, P, and U. See Table S2 for results of Steel-Dwass tests in the variables. Regression lines are drawn for total plots, in addition to the regression lines for plots of each functional category (C, G, P, and U). Absence of correlation between the variables is represented using dotted lines ($p < 0.05$: Table S3). See Table S3 for slopes of the regression lines.

Appendix S2 (cont.)

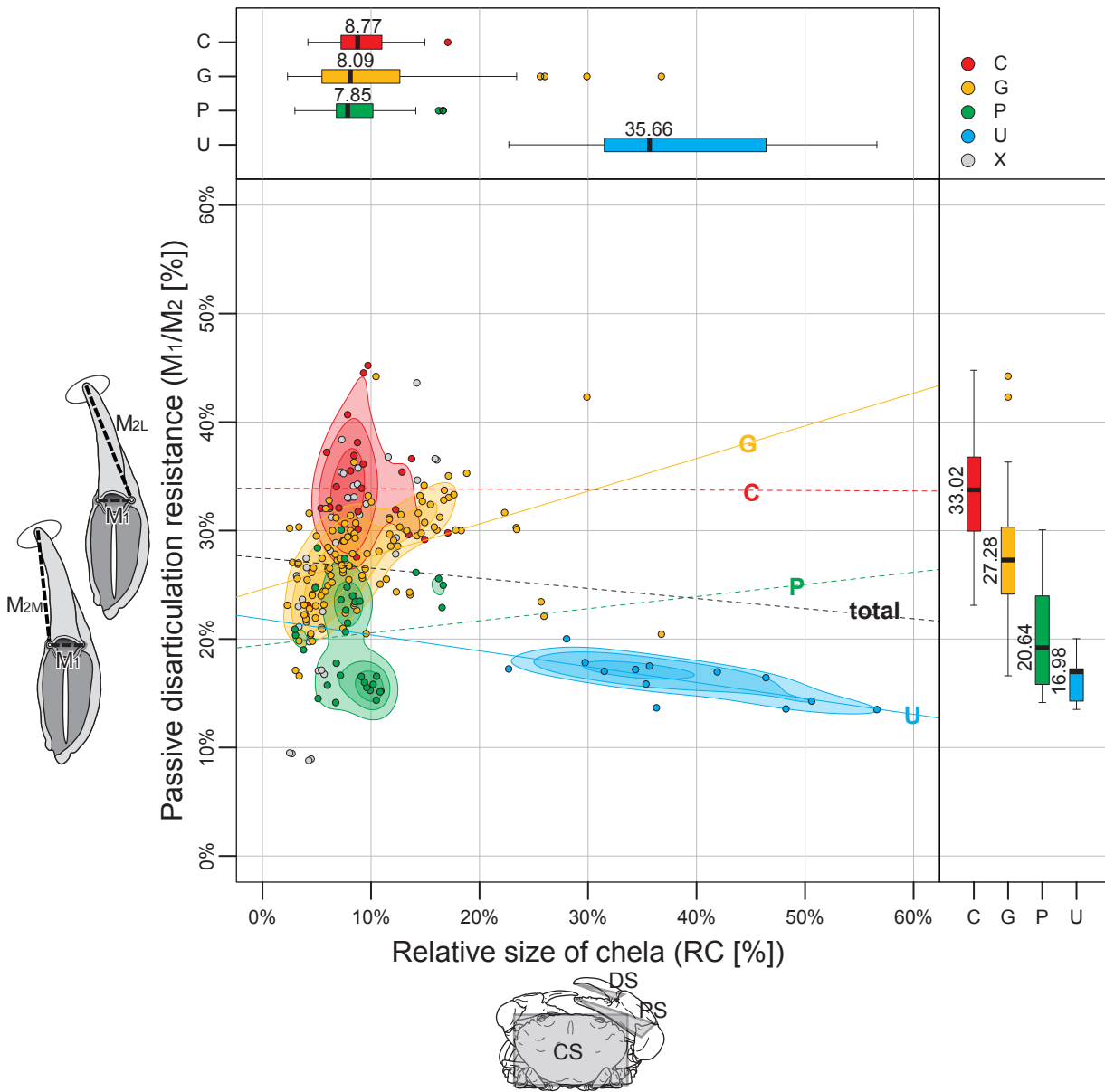


Fig. S3. Relationship between relative size of chela ($RC = (DS + PS)/CS$) and mechanical advantage of passive disarticulation resistance (M_1/M_2). See main text for abbreviations. Each plot represents chela characteristics of the study specimens ($n = 230$ in total; C, crushing/chipping chela, $n = 24$; G, gripping chela, $n = 121$; P, pinching chela, $n = 33$; U, male ucine major chela, $n = 13$; X, uncategorized chela, $n = 39$). Bivariate kernel density distributions (densities: 25%, 50%, 75%) and box plots with median values are shown for each variable in the functional categories C, G, P, and U. See Table S2 for results of Steel-Dwass tests in the variables. Regression lines are drawn for total plots, in addition to the regression lines for plots of each functional category (C, G, P, and U). Absence of correlation between the variables is represented using dotted lines ($p < 0.05$: Table S4). See Table S4 for slopes of the regression lines.

Appendix S3: Mechanical advantages of pinching efficiency (C_1/C_2) and passive disarticulation resistance (M_1/M_2) in chelae of the major group of the studied taxa

Fig. S4. Mechanical advantages of pinching efficiency (C_1/C_2) and passive disarticulation resistance (M_1/M_2) in chelae of the major group of the studied taxa (p. 2).

Fig. S5. Mechanical advantages of pinching efficiency (C_1/C_2) and passive disarticulation resistance (M_1/M_2) in major and minor chelae of non-brachyuran decapods (Axiidea [Callinassidae], Astacoidea [Astacidae, Cambaridae, and Nephropidae], and Anomura [Coenobitidae and Lithodidae]) (p. 2).

Fig. S6. Mechanical advantages of pinching efficiency (C_1/C_2) and passive disarticulation resistance (M_1/M_2) in major and minor chelae of “podotramate” brachyurans (Dromiacea [Dromiidae, Dynomenidae, and Homolidae] and Raninidae [Lyreidinae and Ranininae]) (p. 3).

Fig. S7. Mechanical advantages of pinching efficiency (C_1/C_2) and passive disarticulation resistance (M_1/M_2) in major and minor chelae of majoids (Oregoniidae, Majidae, Inachidae, and Epialtidae) (p. 3).

Fig. S8. Mechanical advantages of pinching efficiency (C_1/C_2) and passive disarticulation resistance (M_1/M_2) in major and minor chelae of Calappidae, Matutidae, Potamidae, Carpiliidae, and Parthenopidae (Daldolphinae and Parthenopinae) (p. 4).

Fig. S9. Mechanical advantages of pinching efficiency (C_1/C_2) and passive disarticulation resistance (M_1/M_2) in major and minor chelae of a monophyletic heterotremate clade composed of Cancridae, Dorippidae, and Leucosiidae (p. 4).

Fig. S10. Mechanical advantages of pinching efficiency (C_1/C_2) and passive disarticulation resistance (M_1/M_2) in major and minor chelae of portunoids (Geryonidae and Portunidae [Carcininae, Polybiinae, Carupinae, Thalamitinae, and Portuninae]) (p. 5).

Fig. S11. Mechanical advantages of pinching efficiency (C_1/C_2) and passive disarticulation resistance (M_1/M_2) in major and minor chelae of xanthoids (Hypothalassiidae, Oziidae, Goneplacidae, and Xanthidae) and Pseudocarcinus (Menippidae) (p. 5).

Fig. S12. Mechanical advantages of pinching efficiency (C_1/C_2) and passive disarticulation resistance (M_1/M_2) in major and minor chelae of grapsoid thoracotremates (Gecarcinidae, Grapsidae, Plagusidae, Sesarmidae, and Varunidae [Cyclograpsinae and Varuninae]) (p. 6).

Fig. S13. Mechanical advantages of pinching efficiency (C_1/C_2) and passive disarticulation resistance (M_1/M_2) in major and minor chelae of ocypodoid thoracotremates (Macrophthalmidae and Ocypodidae [Ocypodinae and Ucininae]) (p. 6).

Appendix S3 (cont.)

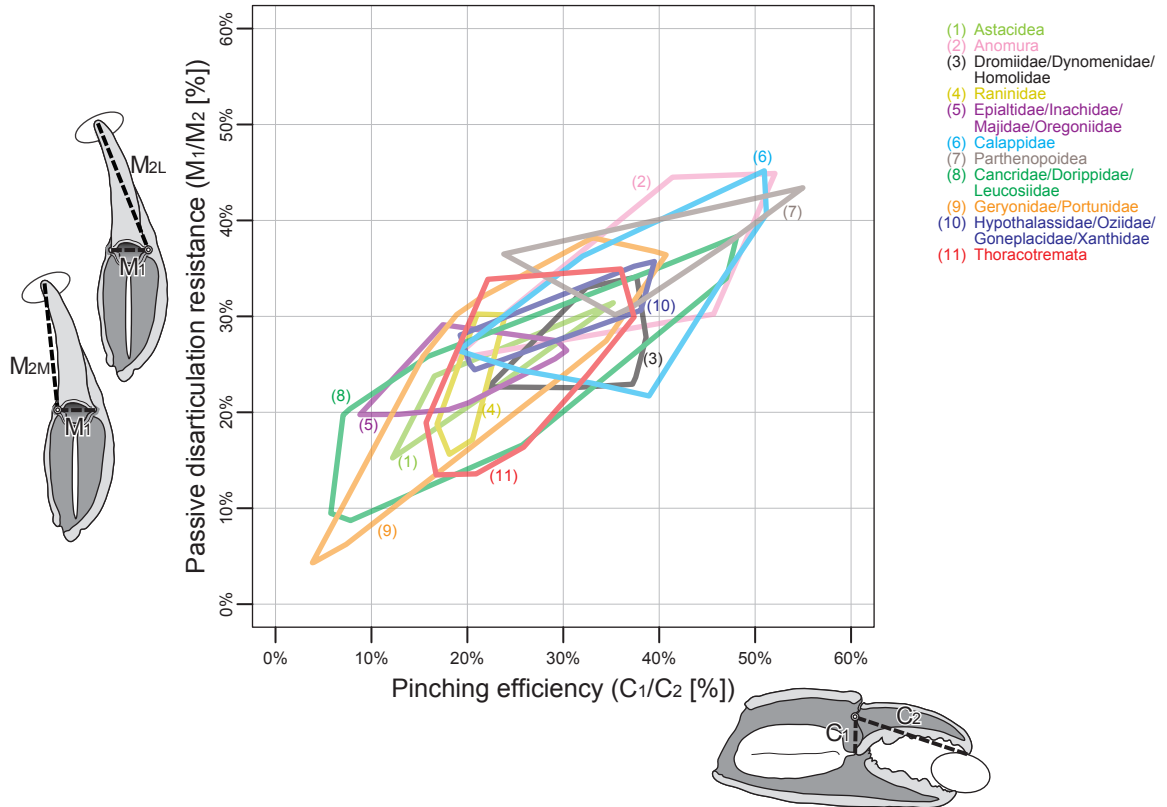


Fig. S4. Mechanical advantages of pinching efficiency (C_1/C_2) and passive disarticulation resistance (M_1/M_2) in major group of the studied specimens. Range of the plots of each group is shown in convex hull. (1) Astacidea (Fig. S5); (2) Anomura (Fig. S5); (3) Dromiidae + Dynomenidae + Homolidae (Fig. S6); (4) Raninidae (Fig. S6); (5) Epialtidae + Inachidae + Majidae + Oregoniidae (Fig. S7); (6) Calappidae (Fig. S8); (7) Parthenopoidea (Fig. S8); (8) Cancridae + Dorippidae + Leucosiidae (Fig. S9); (9) Geryonidae + Portunidae (Fig. S10); (10) Hypothalassidae + Oziidae + Goneplacidae + Xanthidae (Fig. S11); (10) Thoracotremata (Figs. S12, S13). Monophylies of the groups (1)–(10) are well supported in Tsang et al. (2014). See Table S1 for the data.

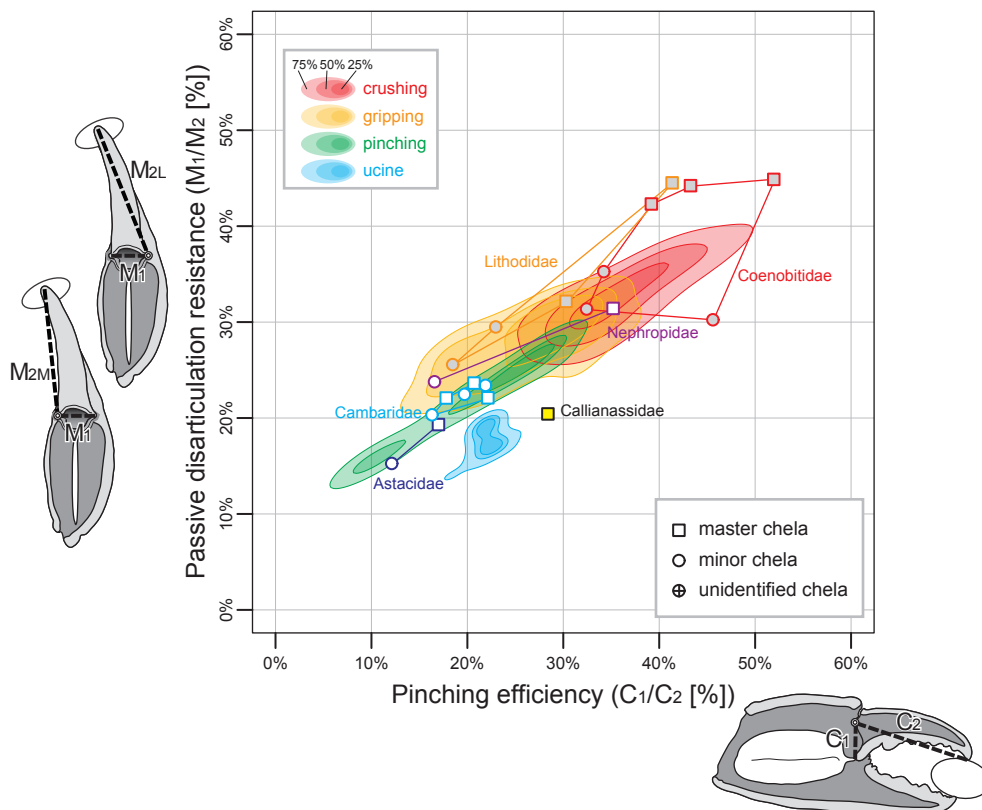


Fig. S5. Mechanical advantages of pinching efficiency (C_1/C_2) and passive disarticulation resistance (M_1/M_2) in major and minor chelae of non-brachyuran decapods (Axiidea [Callianassidae], Astacidea [Astacidae, Cambaridae, and Nephropidae], and Anomura [Coenobitidae and Lithodidae]). Colour gradations in the background are kernel densities (25%, 50%, and 75%) of chelae in the studied specimens for four different categories (crushing, gripping, pinching, and ucine). Range of the plots of each group is shown in convex hull. See Table S1 for the data.

Appendix S3 (cont.)

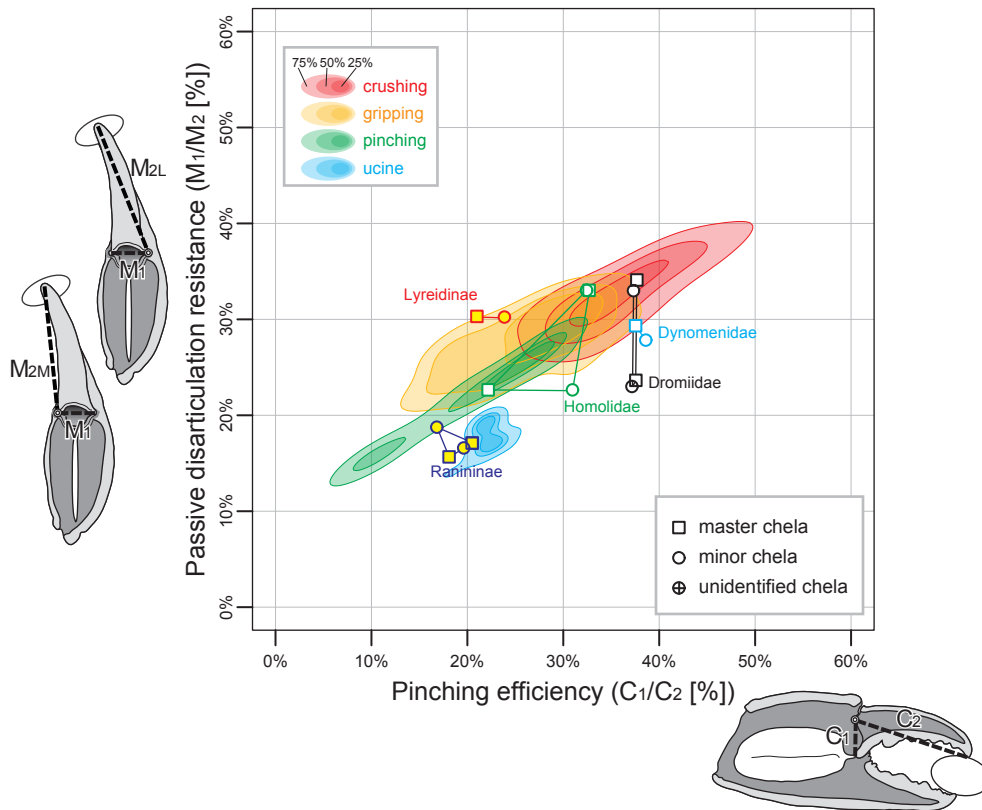


Fig. S6. Mechanical advantages of pinching efficiency (C_1/C_2) and passive disarticulation resistance (M_1/M_2) in major and minor chelae of “podotremate” brachyurans (Dromiacea [Dromiidae, Dynomenidae, and Homolidae] and Raninidae [Lyreidinae and Ranininae]). Colour gradations in the background are kernel densities (25%, 50%, and 75%) of chelae in the studied specimens for four different categories (crushing, gripping, pinching, and ucine). Range of the plots of each group is shown in convex hull. See Table S1 for the data.

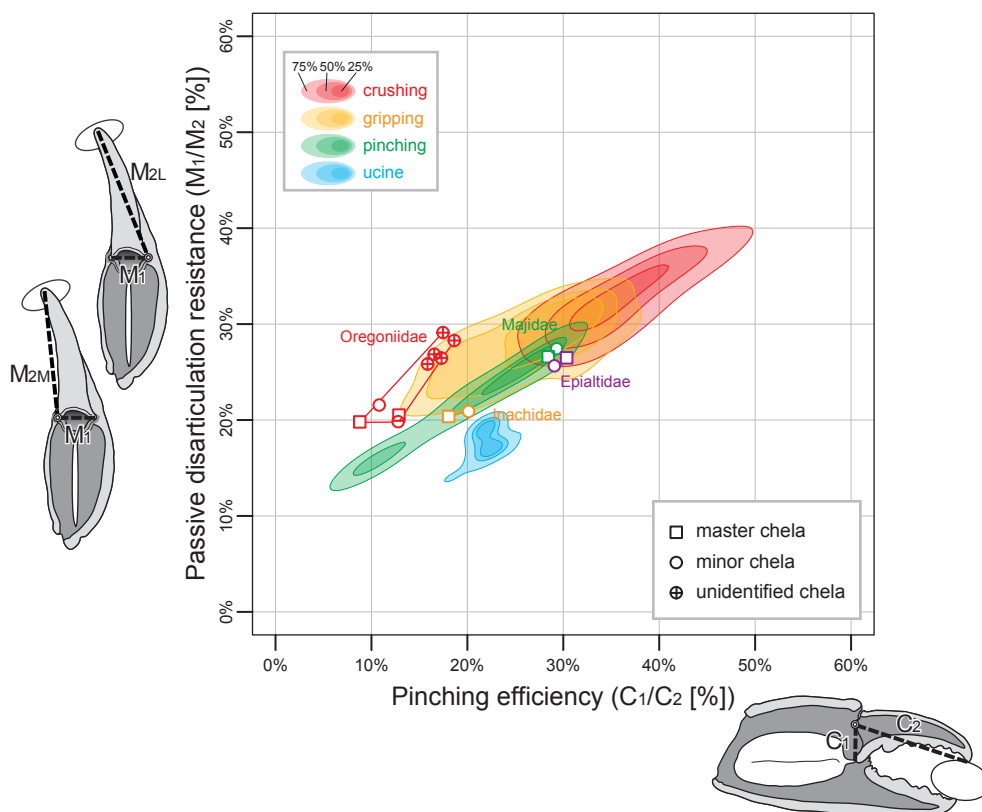


Fig. S7. Mechanical advantages of pinching efficiency (C_1/C_2) and passive disarticulation resistance (M_1/M_2) in major and minor chelae of majoid brachyurans (Oregoniidae, Majidae, Inachidae, and Epialtidae). Colour gradations in the background are kernel densities (25%, 50%, and 75%) of chelae in the studied specimens for four different categories (crushing, gripping, pinching, and ucine). Range of the plots of each group is shown in convex hull. See Table S1 for the data.

Appendix S3 (cont.)

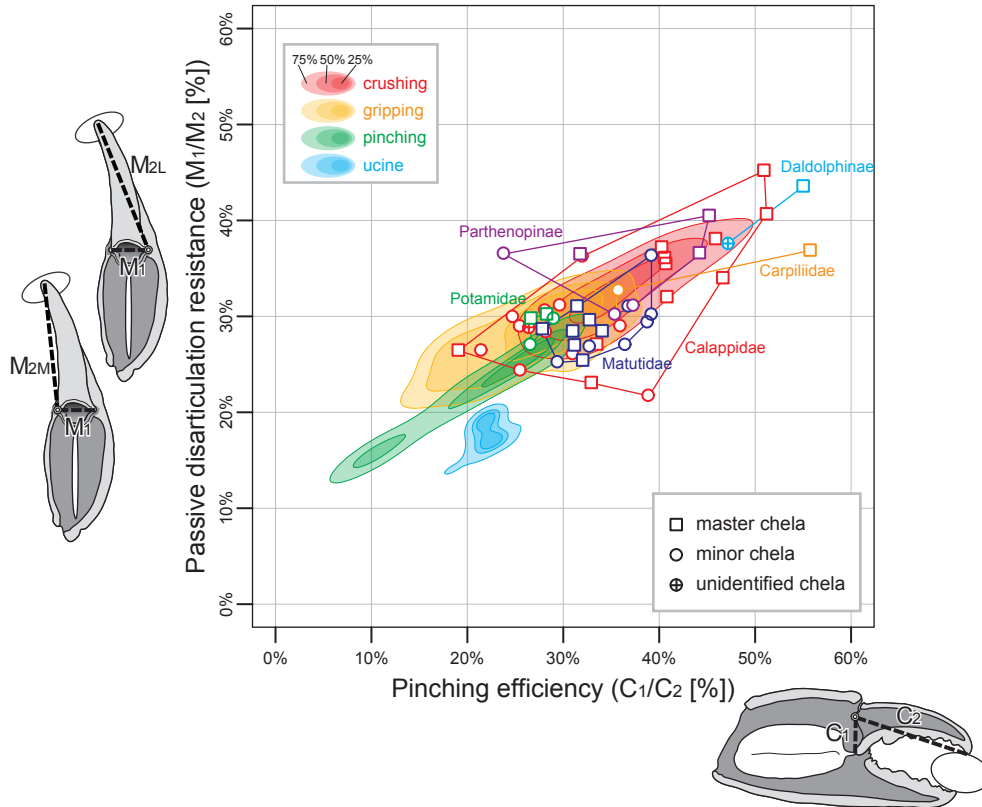


Fig. S8. Mechanical advantages of pinching efficiency (C_1/C_2) and passive disarticulation resistance (M_1/M_2) in major and minor chelae of Calappidae, Matutidae, Potamidae, Carpiliidae, and Parthenopidae (Daldolphinae and Parthenopinae). Colour gradations in the background are kernel densities (25%, 50%, and 75%) of chelae in the studied specimens for four different categories (crushing, gripping, pinching, and ucine). Range of the plots of each group is shown in convex hull. See Table S1 for the data.

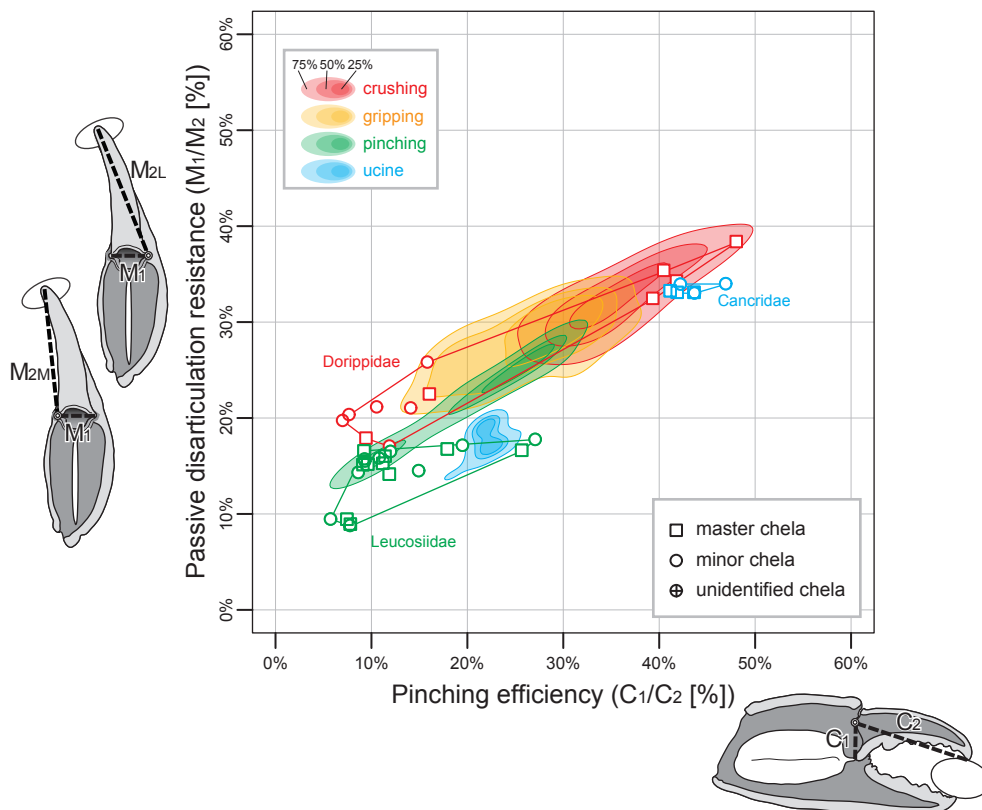


Fig. S9. Mechanical advantages of pinching efficiency (C_1/C_2) and passive disarticulation resistance (M_1/M_2) in major and minor chelae of a monophyletic brachyuran group which comprises Cancroidea, Dorippidae, and Leucosiidae. Colour gradations in the background are kernel densities (25%, 50%, and 75%) of chelae in the studied specimens for four different categories (crushing, gripping, pinching, and ucine). Range of the plots of each group is shown in convex hull. See Table S1 for the data.

Appendix S3 (cont.)

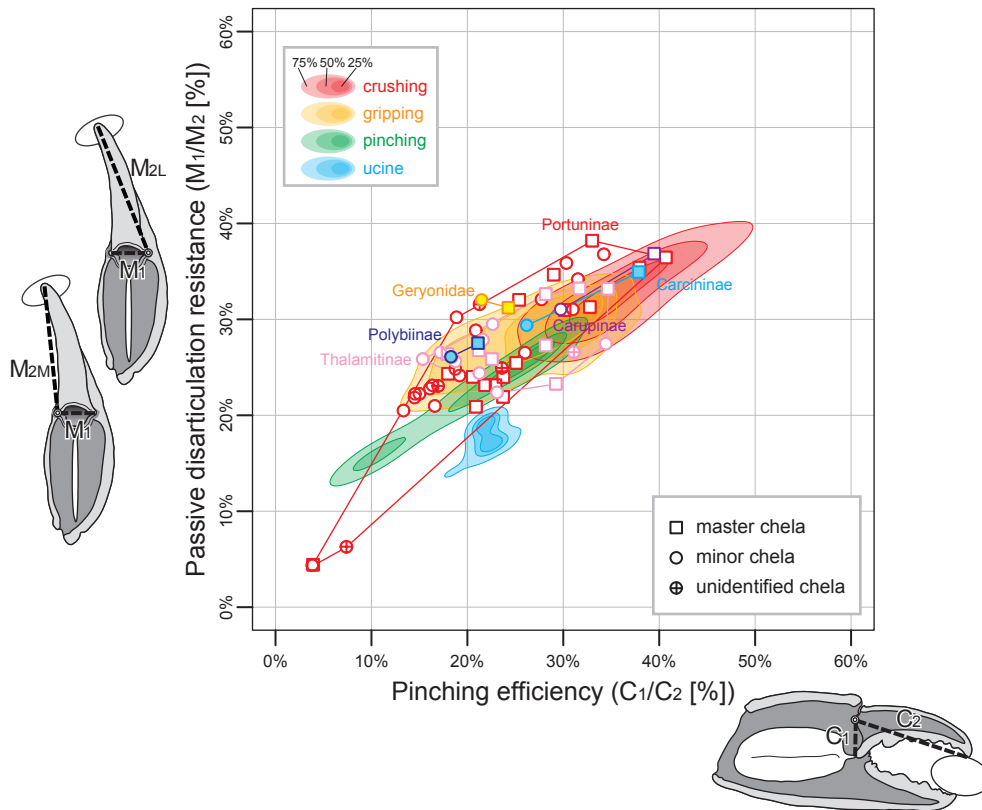


Fig. S10. Mechanical advantages of pinching efficiency (C_1/C_2) and passive disarticulation resistance (M_1/M_2) in major and minor chelae of portunoids (Geryonidae and Portunidae [Carcininae, Polybiinae, Carupinae, Thalamitinae, and Portuninae]). Colour gradations in the background are kernel densities (25%, 50%, and 75%) of chelae in the studied specimens for four different categories (crushing, gripping, pinching, and ucine). Range of the plots of each group is shown in convex hull. See Table S1 for the data.

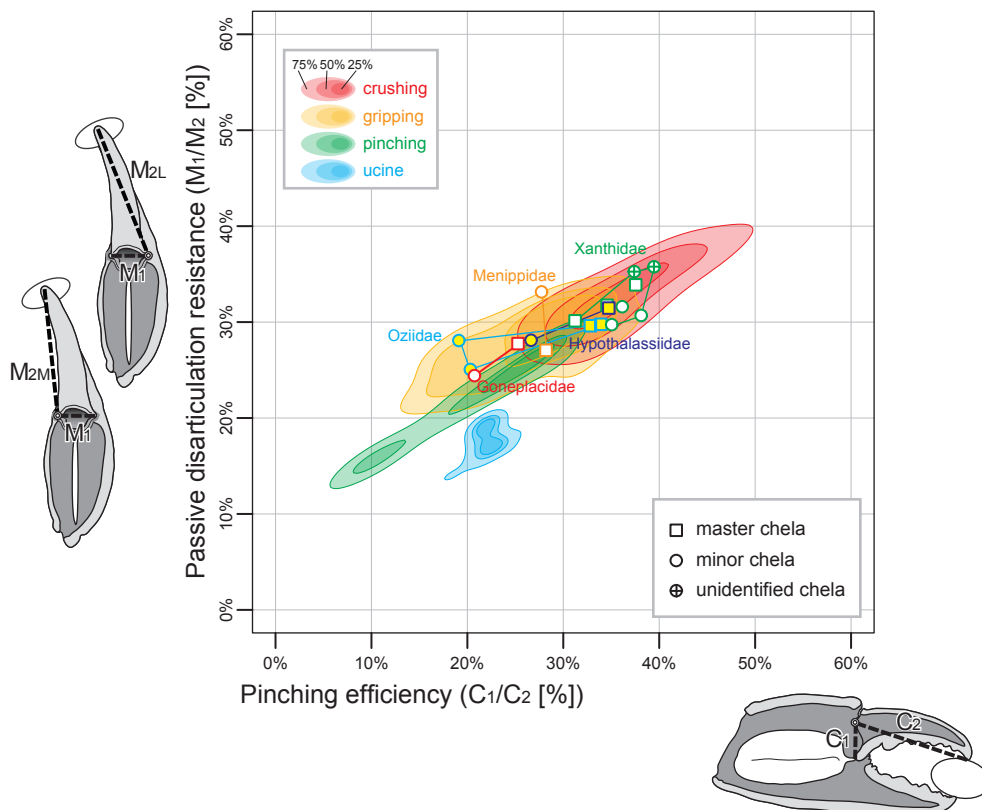


Fig. S11. Mechanical advantages of pinching efficiency (C_1/C_2) and passive disarticulation resistance (M_1/M_2) in major and minor chelae of eriphioid (Hypothalassiidae, Menippidae, and Oziidae), goneplacoid (Goneplacidae), and xanthoid (Xanthidae) brachyurans. Colour gradations in the background are kernel densities (25%, 50%, and 75%) of chelae in the studied specimens for four different categories (crushing, gripping, pinching, and ucine). Range of the plots of each group is shown in convex hull. See Table S1 for the data.

Appendix S3 (cont.)

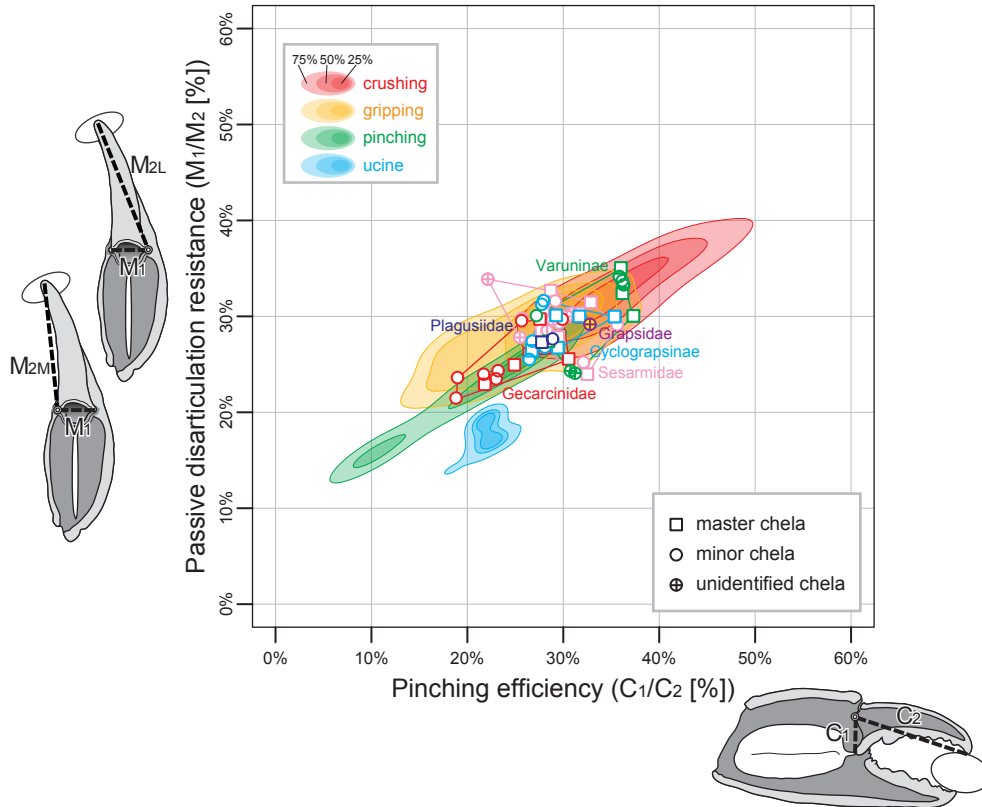


Fig. S12. Mechanical advantages of pinching efficiency (C_1/C_2) and passive disarticulation resistance (M_1/M_2) in major and minor chelae of grapsoid thorecotremates (Gecarcinidae, Grapsidae, Plagusiidae, Sesarmidae, and Varunidae [Cyclograpsinae and Varuninae]). Colour gradations in the background are kernel densities (25%, 50%, and 75%) of chelae in the studied specimens for four different categories (crushing, gripping, pinching, and ucine). Range of the plots of each group is shown in convex hull. See Table S1 for the data.

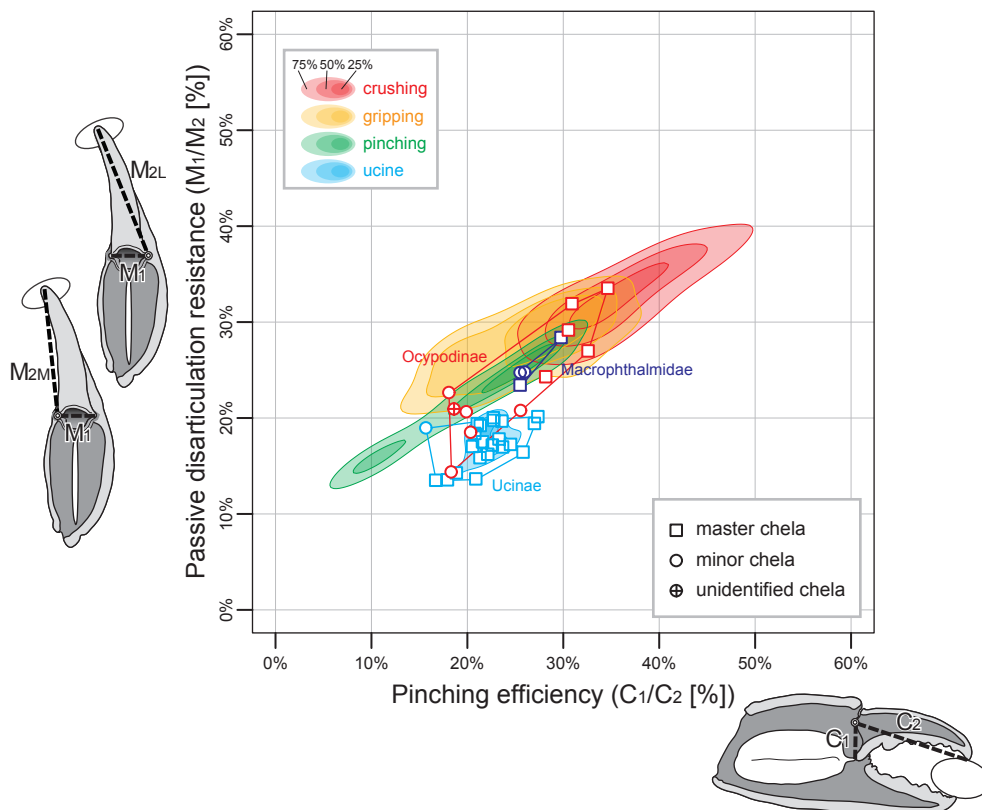


Fig. S13. Mechanical advantages of pinching efficiency (C_1/C_2) and passive disarticulation resistance (M_1/M_2) in major and minor chelae of ocypodoid thoracotremates (Macrophthalmidae and Ocypodidae [Ocypodinae and Ucinidae]). Colour gradations in the background are kernel densities (25%, 50%, and 75%) of chelae in the studied specimens for four different categories (crushing, gripping, pinching, and ucine). Range of the plots of each group is shown in convex hull. See Table S1 for the data.

Appendix S4: Use of triangle area as a proxy for the chela size

We assumed the chela as a triangle, and defined the area of the triangle as the size of the chela (see Fig. 1 and main text), while a distance from the proximal to the distal ends of the propodus has been used as a proxy for the chela size in many other studies (e.g., Savage and Sullivan, 1978; Abele et al., 1981; Brock and Smith, 1998). Therefore, the use of the triangular area (mm²) as the proxy for the chela size need to be validated.

To answer the abovementioned concern, we tested the relationship between the chela sizes employed in previous studies (PL: propodus length which was defined as the distance between points *f* and *h* in Fig. 1 [mm]) and in this study (PS + CS: the triangle areas formed by points *a-c* and points *f-h* in Fig. 1) in the studied specimens (Table S1). Spearman's correlation test was conducted between "PL" and "PS + DS" by using a statistical software R 3.1.0 (R Foundation for Statistical Company). Null-hypothesis that there is no association between the two variables was rejected if *p*-value did not exceed 0.05.

According to the correlation test, "PL" and "PS + DS" were proved to be correlated ($p < 0.05$), and the coefficient of determination (R^2) was 0.875 (Fig. S14). Therefore, we consider that the use of "PS + DS" as a proxy of the chela size is valid.

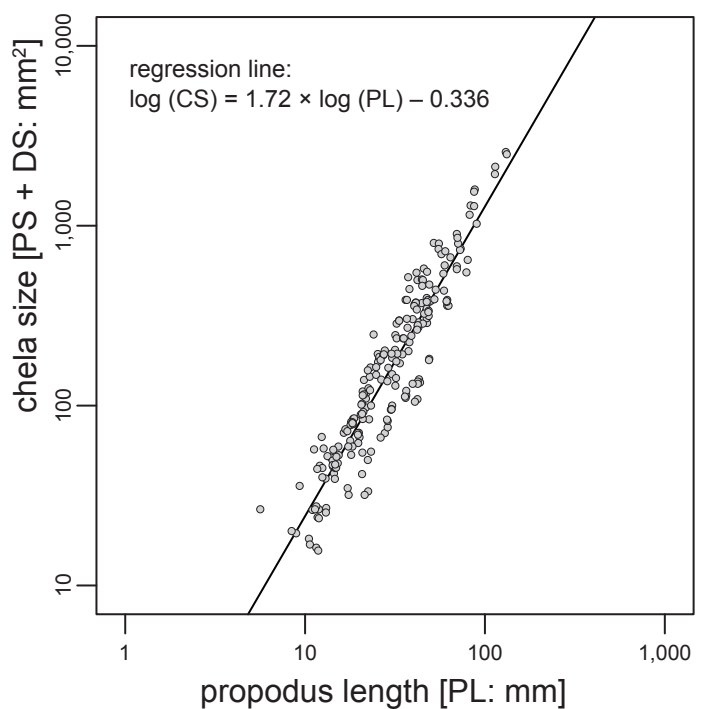


Fig. S14. Relationship between propodus length (PL: mm) and chela size (PS + DS: mm²). An equation of the regression line is shown in the figure. Correlation between these two variables was supported by Spearman's correlation test: Spearman's ρ -value = 0.931; p -value < 2.2e-16; coefficient of determination (R^2) = 0.875.

LITERATURE CITED

- Abele LG, Heck KL, Simberloff DS, Vermeij GJ. 1981. Biogeography of crab claw size: assumptions and a null hypothesis. *Syst Zool* 30:406-424.
- Brock RE, Smith LD. 1998. Recovery of claw size and function following autotomy in *Cancer productus* (Decapoda: Brachyura). *Biol Bull* 194:53-62.
- Savage T, Sullivan JR. 1978. Growth and claw regeneration of the stone crab, *Menippe mercenaria*. Florida Marine Research Publication 32:1-27.